PHOTOGRAPH THIS SHEET

AD A951404

DTIC ACCESSION NUMBER

LEVEL

INVENTORY

Massachusetts Inst of Tech
Cambridge

Equilibrium Relationships in the Iron-Nitrogen System. [1949]

DOCUMENT IDENTIFICATION

Contract W-19-020-ORD-6474 WAL-334/14-23a

DISTRIBUTION STATEMENT A
Approved for public release;
Distribution Unlimited

DISTRIBUTION STATEMENT

ACCESSION FOR
NTIS GRA&I ☒
DTIC TAB ☐
UNANNOUNCED ☐
JUSTIFICATION
([1949])
BY
DISTRIBUTION /
AVAILABILITY CODES
DIST | AVAIL AND/OR SPECIAL
A-1

DISTRIBUTION STAMP

Released

DTIC
ELECTE
OCT 22 1981
S D
D

DATE ACCESSIONED

UNANNOUNCED Sa. U10545

81 9 24 279

DATE RECEIVED IN DTIC

PHOTOGRAPH THIS SHEET AND RETURN TO DTIC-DDA-2

DTIC FORM OCT 79 70A

DOCUMENT PROCESSING SHEET

RESEARCH ON THE IRON-NITROGEN SYSTEM

Contract No. W-19-020-ORD-6474 New

O. O. Project No. TR3-3002D

WAL Project No. 10.42-5

R. A. D. No. 2-6587

[1949]

Technical Report

on

EQUILIBRIUM RELATIONSHIPS IN THE IRON-NITROGEN SYSTEM

Department of Metallurgy

Massachusetts Institute of Technology

Cambridge, Massachusetts

Submitted by Vijay G. Paranjpe

Approved by Morris Cohen

NOTE:-This form is to be executed to show proposed distribution, and forwarded in triplicate to the Chief of Ordnance for prior approval of all distributions. Proposed distribution to agencies or individuals whose official interest in the report is not obvious must be justified by explanatory statements on the back of this form.

BINDING AREA FORM NO. ORDBE-342 L. (Rev.) 2 Sept. 1947 *BINDING AREA*

COPIES PREPARED 2

WATERTOWN ARSENAL
TECHNICAL REPORT DISTRIBUTION

EXTRA COPIES REMAINING

REPORT NO. 334/14-23 a TITLE: MIT. Contract W19-020-ORD-6474 Tech. report

TO:	NO. OF COPIES	DATE OCO APPROVAL	DATE SENT
WATERTOWN ARSENAL-ORDBE			
Laboratory File	1		
~~Author:~~ Dr. Jaffe	1	#2	
OFFICE, CHIEF OF ORDNANCE			
ORDIR-Artillery			
ORDIM-Ammunition			
ORDIT-Automotive			
ORDIS-Small Arms			
ORDTB-Res . & Materials			
ORDTM-Ammunition Dev.			
ORDTR-Artillery Dev.			
ORDTS-Small Arms Dev.			
ORDTT-Tank Automotive			
ORDTU-Rocket Dev.			
ORDTX-Executive			
ORDTX-AR - Executive Library	1		
ORDNANCE DEPARTMENT AGENCIES			
ORDBA-Frankford Arsenal			
ORDBB-Picatinny Arsenal			
ORDBC-Rock Island Arsenal			
ORDBD-Springfield Armory			
ORDBF-Watervliet Arsenal			
ORDBG-Aberdeen Prov. Ground			
ORDJR-Raritan Arsenal			
ORDMX-Detroit Arsenal			

TO:	NO. OF COPIES	DATE OCO APPROVAL	DATE SENT
OTHER:			

APPROVING AUTHORITY:
ltr.:
Date:
From:

TABLE OF CONTENTS

LIST OF ILLUSTRATIONS

LIST OF TABLES

ACKNOWLEDGMENTS

The author wishes to express his sincere appreciation to a number of people for their assistance in carrying out the work reported in this investigation.

To Professor Morris Cohen, the director of this work, without whose unfailing guidance, interest, and encouragement this work could not have been brought to a successful conclusion.

To Professors Carl F. Floe and Michael B. Bever, who acted as co-supervisors of this research program, for their suggestions and helpful assistance.

To Dr. Leonard Jaffe of the Watertown Arsenal Laboratories, for his help and suggestions.

To Mr. A. Sloan of the Watertown Arsenal Laboratories for his help in carrying out nitrogen determinations.

To Mr. Samuel K. Nash, coworker in this research work, for his help and suggestions.

To Miss Miriam Yoffa for her help in making a large number of nitrogenizing experiments.

To Mr. William R. Yankee for his help in the x-ray work involved in this investigation.

To members of the staff of the Department of Metallurgy at the Massachusetts Institute of Technology for their help and assistance.

This research was sponsored by the United States Army Ordnance Department under Contract Nos. W-19-066-ORD-1093 and W-19-020-ORD-6474.

I. INTRODUCTION

The development of the nitriding process was the first important step in the application of iron-nitrogen alloys. Prior to this, nitrogen was considered to have only a detrimental effect on the mechanical properties of irons and steels. Most of the early work, for example, by Warren[1], Braune[2,3,4] and Strauss[5,6] was thus concerned with the effect of nitrogen on physical properties. Fry's[7] work on the modern nitriding process, and the growing success of commercial nitriding, however, created renewed interest in the iron-nitrogen system. The development of the carbonitriding process by Cowan and Brice[8] following the original studies by Machlet[9], and the use of nitrogen as an alloying element in stainless steels[10], increased the importance of nitrogen as an alloying element in steels. Further, one finds suggestions in current literature that nitrogen plays a significant role in various phenomena like blue brittleness, strain aging and temper-brittleness. Nitrogen has also been recognized as a powerful austenite stabilizer[11]. In order to achieve a complete understanding of these effects of nitrogen, it is important to know the phase relationships in the binary iron-nitrogen system which forms the basis of the other complicated systems.

The literature on the iron-nitrogen system is abundant with proposed iron-nitrogen phase diagrams. The various phase diagrams suggested by Fry[12], Sawyer[13], Epstein and coworkers[14,15], Lehrer[16], Eisenhut and Kaupp[17], Hägg[18,19] and Palatnik[20] differ consid-

erably from one another. It was therefore necessary to redetermine the iron-nitrogen phase diagram. It was with this goal that this investigation was undertaken.

II. REVIEW OF PREVIOUS WORK

The early work on the iron-nitrogen phase diagram was mostly concerned with the nature of the various iron-nitrogen phases. No attempts were made at first to propose any definite phase diagram.

Remsen[21] appears to be the first to investigate the reaction between iron and nitrogen. He stated that a cyanide is formed when iron and certain non-nitrogenous organic compounds are heated together in nitrogen. This suggests the Bucher[22] process, in which iron catalyses, at red heat, the formation of cyanide from nitrogen, carbon and alkalies.

Fowler[23] studied the form in which nitrogen exists in steel, and stated his agreement with an earlier writer Stahlschmidt[24] that only one nitride of iron, Fe_2N, exists. About two years later, Harbord and Twynam[25] recognized that nitrogen may be both mechanically occluded and chemically combined in steel.

Braune[2,3,4] believed that nitrogen occurred in steel as the nitride Fe_5N_2 in solid solution in ferrite. He found a pearlitic structure in iron containing over 0.2 percent nitrogen. This eutectoid structure in the iron-nitrogen system is now named "Braunite" in his honor.

Andrew[11] reported that nitrogen lowered the critical points of iron, and he classified nitrogen as an austenite stabilizer.

Tschischewski[26] considered the needle-like constituent in nitrided iron to be the compound $Fe_{12}N$. He reported that the maximum

solubility of nitrogen in alpha iron was about 0.02 percent, since no evidence of nitride needles was found in iron containing nitrogen up to this limit. He also appears to be the first to suggest that iron-nitrogen alloys can be hardened by quenching from about 700° C, presumably by the formation of martensite. Comstock and Ruder[27] supported this suggestion, and showed that the eutectoid transformation can be suppressed by fast cooling from a high austenitizing temperature.

The first systematic attempts to set up a constitutional diagram for the iron-nitrogen system seem to have been made independently by Sawyer and Fry.

Sawyer[13] used thin discs to achieve homogeneous nitrogenizing throughout his samples, and then studied the phase relationships by microscopic examination and thermal analysis. The phase diagram proposed by Sawyer is shown in Figure 1(a). His heating curves indicated a thermal arrest point at 620° C corresponding to a eutectoid between the alpha phase and Fe_8N. The alpha iron at this temperature contained a maximum of 0.108 percent nitrogen. Sawyer also observed a second arrest point at 700° C corresponding to a eutectoid between Fe_8N and Fe_6N. He believed that the outermost layer of his nitrided samples was Fe_4N, and that Fe_6N and Fe_8N were the two intermediate layers.

Fry[7,12] based his diagram on the results of microscopic examination and magnetic measurements. This diagram, presented in Figure 1(b), indicates an increasing solubility of nitrogen in alpha

iron with increasing temperature, and shows the nitrogen content of the alpha phase to be 0.015, 0.2 and 0.5 percent nitrogen at room temperature, 550° and 580° (eutectoid temperature) respectively. Fry fixed the eutectoid composition at 1.5 percent nitrogen, and believed it to consist of the alpha solid solution and the compound Fe_4N. Fry observed two layers in his nitrided blocks, and called them Fe_4N and Fe_2N, Fe_2N being the outer one. He did not show any relation between these two phases. Fry's diagram, however, does not apply strictly to the iron-nitrogen binary system, since his samples contained about 0.13 percent carbon.

The third proposal on the phase diagram was advanced by Epstein and his coworkers[14,15]. The diagram is shown in Figure 1(c). This work was essentially a modification and extension of Sawyer's and Fry's investigations. Epstein employed microscopic and thermal methods, and reported x-ray data on some of the iron-nitrogen phases. In this thermal analyses, he found a double arrest at 578° and 604° C in a sample containing 0.19 percent nitrogen, but he neglected these points and maintained that 0.5 percent nitrogen is soluble in the alpha phase. Epstein observed two thermal arrests in high nitrogen samples, similar to those reported by Sawyer, but he did not see any indication of the second eutectoid (Figure 1(a)) and therefore proposed a peritectoid reaction in place of the second eutectoid of Sawyer. The x-ray investigation by Epstein was incomplete, but it indicated that the outermost layer had a hexagonal close packed structure. Epstein reported three nitrides: Fe_2N (hexagonal close packed), and Fe_4N and Fe_8N (based on metallographic work).

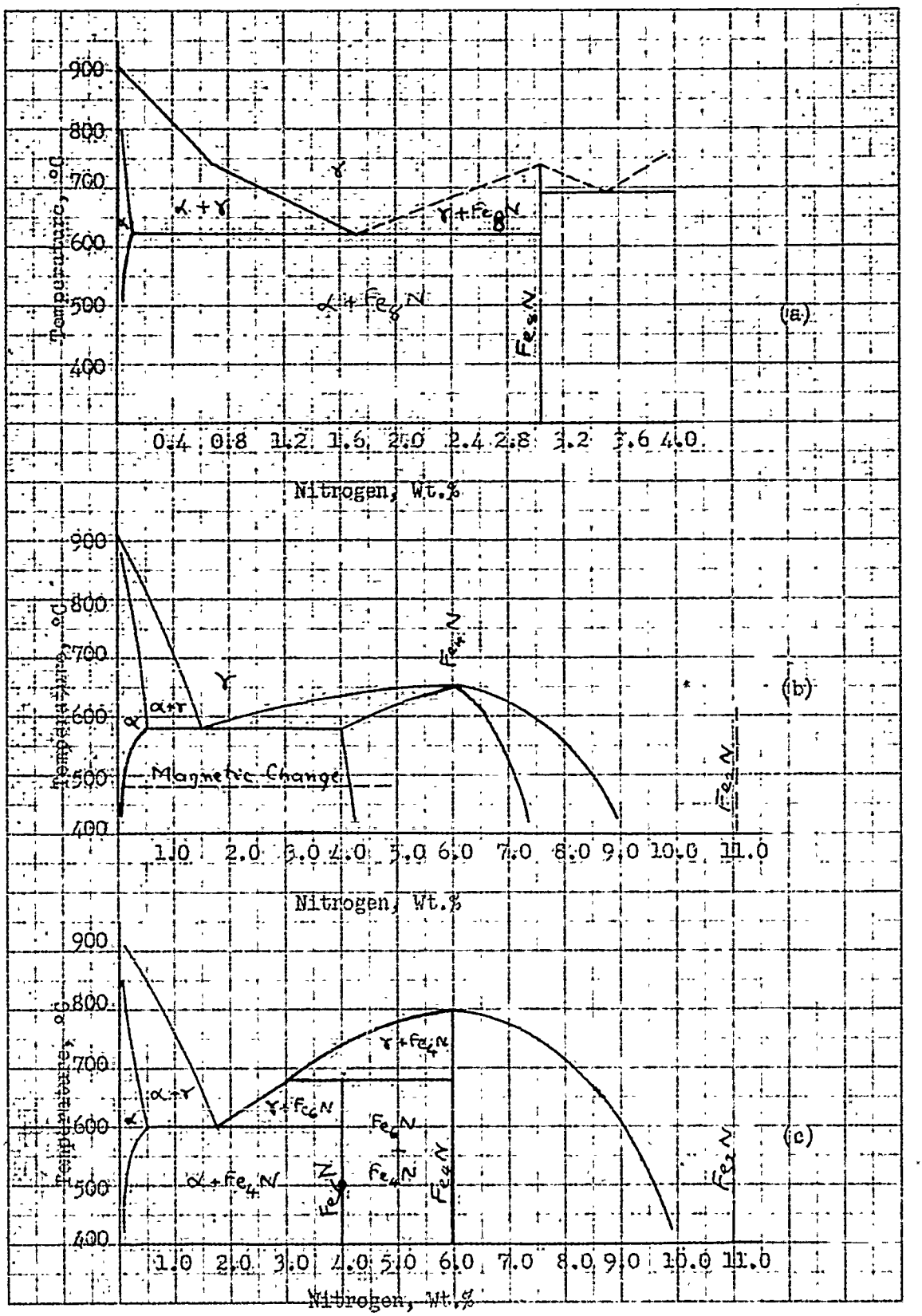

FIGURE 1. The Iron-Nitrogen Phase Diagrams Proposed by (a) Sawyer, (b) Fry, and by (c) Epstein.

Bramley and Haywood[28] determined the iron-iron nitride eutectoid temperature and composition as being 608° C, and 2.0 percent nitrogen respectively. This was based on metallographic work.

Hägg[18,19] investigated the iron-nitrogen system with particular emphasis on the crystal structure of the various iron nitrogen phases. This phase diagram is shown in Figure 2(a). He found four distinct phases in the iron-nitrogen system. These were alpha, gamma, epsilon and zeta, with progressively increasing nitrogen concentration. The alpha phase had a body-centered cubic structure and contained a small amount of nitrogen in solution. Hägg could not detect any measurable change in the unit cell dimensions of the alpha phase with increasing nitrogen content. The next phase, gamma, was a face-centered cubic phase resembling austenite in the iron-carbon system. The compound Fe_4N, occurring at about six percent nitrogen, was according to Hägg the same as the gamma phase, with the exception that the former had an ordered arrangement of the nitrogen atoms. The nitrogen atoms occupied the positions $(\frac{1}{2}, \frac{1}{2}, \frac{1}{2})$ or $(\frac{1}{4}, \frac{1}{4}, \frac{1}{4})$ in this ordered phase. The diagram in Figure 2(a) shows that this ordering takes place simultaneously with the restriction of the solubility limits of the gamma phase at about 600° C. The exact nature of the diagram above the eutectoid temperature was not determined by Hägg. The epsilon phase had a hexagonal close packed arrangement of iron atoms, and extended according to Hägg from 8 to 11 percent nitrogen. The lattice dimensions changed regularly with increasing

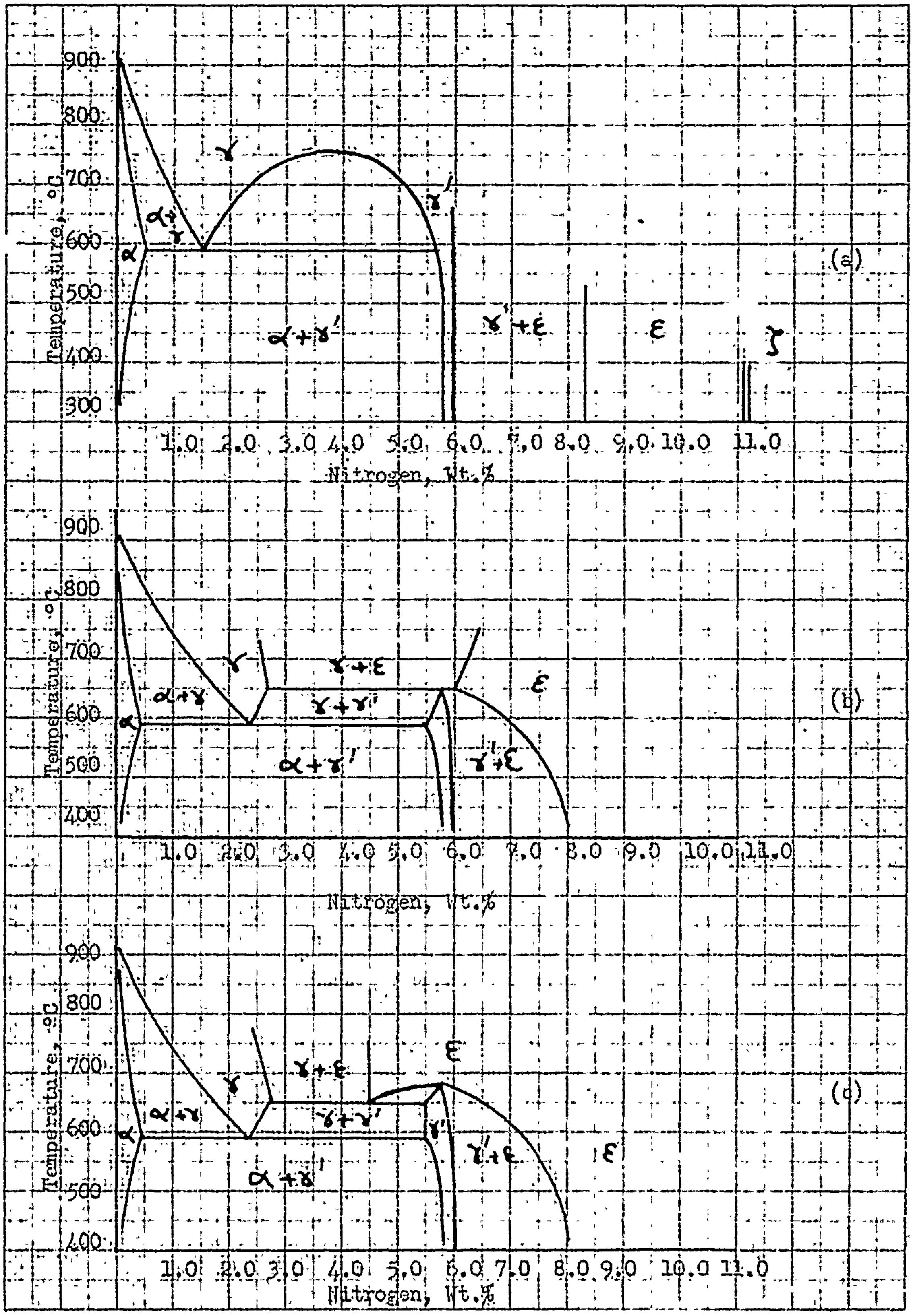

FIGURE 2. The Iron-Nitrogen Phase Diagrams Proposed by (a) Hägg, (b) Eisenhut and Kaupp, and by (c) Lehrer.

nitrogen content. Lastly Hägg detected a new phase, zeta, with an orthorhombic structure (a = 2.758, b = 4.819, and c = 4.419 Å) starting at about 11.2 percent nitrogen. The theoretical composition of Fe_2N corresponds closely to the low nitrogen end of the orthorhombic zeta phase. Hägg states in his paper that the structures he determined were dependent only on the nitrogen content, and not on the temperature or manner in which the alloys were formed. He therefore shows no change of the phase boundaries with changes in temperature.

The next two investigations of the diagram were carried out simultaneously by Lehrer and Eisenhut and Kaupp. The two diagrams proposed by these authors are however in some disagreement above the eutectoid temperature.

Eisenhut and Kaupp used carbonyl iron after thoroughly decarburizing and annealing under pure hydrogen. Their phase diagram was based on x-ray studies of nitrided powdered iron. Their diagram (Figure 2(b)) shows essentially the same phases as Hägg's diagram, with one significant difference. Eisenhut and Kaupp found that the gamma (austenite) and the gamma prime (Fe_4N) were two distinct phases, and that there was a two phase field (gamma plus gamma prime) between them. Eisenhut and Kaupp found an appreciable increase in the lattice parameter of the alpha phase with increasing nitrogen content. They employed this variation to determine the alpha solubility curve: 0.34, 0.39, 0.42, and 0.32 percent nitrogen at 700, 620, 591 and 450° C respectively. They determined the

eutectoid temperature and composition to be 591° C and 2.35 percent nitrogen respectively. The gamma phase occurred above the eutectoid temperature, and its limits were 1.1 and 2.0 percent nitrogen (lower limits) at 620 and 700° C, and 2.75 percent nitrogen (upper limit) at 650° C. These were again determined by x-ray lattice parameter measurements on the gamma phase. Eisenhut and Kaupp found a peritectoid reaction at 650° C, between the gamma phase (2.75 percent nitrogen) and the epsilon phase (5.8 to 5.9 percent nitrogen) yielding the gamma prime phase containing about 5.8 percent nitrogen. The gamma prime phase was found to have a face-centered cubic structure and restricted homogeneity limits. The epsilon phase was reported to have a close packed hexagonal structure and a wide range of homogeneity. The lower limit of the epsilon phase was 6.1, 5.8 (or 5.9), 6.85 and 8.1 percent nitrogen at 700, 650, 600 and 450° C respectively. No evidence of the zeta phase was obtained by Eisenhut and Kaupp. A careful examination of the data presented by these investigators for points above the peritectoid reaction at 650° C shows a discrepancy between their results and the phase diagram. Their specimens containing from 4.6 to 6.2 percent nitrogen, and quenched from above the peritectoid temperature contained epsilon and gamma prime phases. These data are inconsistent with the peritectoid reaction.

Lehrer's[16] phase diagram, shown in Figure 2(c), shows a eutectoid reaction at 650° C, whereby a epsilon phase containing 4.5 percent nitrogen decomposes on cooling into gamma and gamma prime phases. This eutectoid reaction is consistent with the results of

Eisenhut and Kaupp mentioned above. Lehrer based his phase diagram on thermodynamic and magnetic investigations, and his diagram agrees in all respects with the one proposed by Eisenhut and Kaupp with the exception of the region above 650° C.

Palatnik[20] did not do any extensive work on the phase boundary relationships, beyond confirming the x-ray data reported by Hägg on the structures of the gamma prime and the epsilon phases.

Norton[29] confirmed the existence of the phases reported by Hägg. He, however, put the upper limit of the epsilon phase at 10 percent nitrogen instead of 11 percent as obtained by Hägg, and corresponding lower limit of the zeta phase was set by Norton as 10.2 percent instead of Hägg's 11.2 percent nitrogen.

Following these phase-diagram investigations, there have been two separate investigations on the alpha solid solubility curve. The first was by Portevin and Seferian, and the other by Dijkstra.

Portevin and Seferian[30] used an entirely different technique in preparing their iron-nitrogen alloys. Recognizing the difficulty in obtaining thoroughly uniform samples by nitriding in ammonia, they introduced nitrogen by arc melting their iron in an atmosphere of nitrogen. They then obtained the transformation points of their alloys by a dilatometric technique. Portevin and Seferian demonstrated at first that no material change in composition of their alloys took place on alternately heating them to 900° C and cooling from that temperature in air. Thus having proved the applicability of the dilatometric method they found the critical points of several

iron-nitrogen alloys. The alpha solubility curve was thus plotted. The maximum solubility was, according to these investigators, about 0.13 percent nitrogen. This differs radically from the findings of Fry and Eisenhut and Kaupp.

Dijkstra[31] has recently used anelastic measurements to determine the alpha solubility line. His results also show a much lower solubility than that indicated by Fry and Eisenhut and Kaupp. Dijkstra's values of solubility are: 0.075, 0.050, 0.035, 0.025, 0.015, 0.010, 0.005, and 0.003 percent nitrogen at 575, 500, 450, 400, 350, 300, 250 and 200° C respectively.

In addition to the determination of the phase boundary relationships in the iron-nitrogen system, the structural characteristics of the various phases have been studied by several investigators.

Emmett and his coworkers[32] have reported on the variation of the lattice constants of the epsilon phase with changing nitrogen content. Osawa and Iwaizumi[33] have also studied the variation of lattice parameters of the alpha, gamma prime and the epsilon phases. They do not observe any significant changes in the cell dimensions of the alpha phase with increasing nitrogen content.

Brill[34], quite independently of Hägg, has shown that the gamma prime phase has an ordered structure, and Hendricks and Kostings[35] have postulated on the structural relationships between the epsilon and zeta phases. They have also suggested a way in which the epsilon phases change structurally with increasing nitrogen content.

The most recent investigation of the structure of the iron-nitrogen phases was carried out by Jack[36]. He has based his conclusions on a very careful study of superlattice reflections in the gamma prime and zeta phases. The gamma prime phase has, according to Jack, a face-centered arrangement of the iron atoms, and the nitrogen atom is the center of the unit cell. The true unit cell of the zeta phase (containing 11.3 percent nitrogen) is, according to Jack, made up of two base-centered orthorhombic structural units of the iron atom arrangement. This true unit cell has the dimensions: $a' = 2a = 5.512$, $b = 4.820$, and $c = 4.416$ kX. It contains eight iron atoms at 000, $\frac{1}{2}\,00$, $\frac{1}{4}\,\frac{1}{2}\,0$, $\frac{3}{4}\,\frac{1}{2}\,0$, $0\,\frac{1}{3}\,\frac{1}{2}$, $\frac{1}{2}\,\frac{1}{3}\,\frac{1}{2}$, $\frac{1}{4}\,\frac{5}{6}\,\frac{1}{2}$, $\frac{3}{4}\,\frac{5}{6}\,\frac{1}{2}$, and four nitrogen atoms at $\frac{1}{4}\,\frac{1}{6}\,\frac{1}{4}$, $\frac{1}{2}\,\frac{2}{3}\,\frac{1}{4}$, $\frac{3}{4}\,\frac{1}{6}\,\frac{3}{4}$ and $0\,\frac{2}{3}\,\frac{1}{4}$. The iron atoms are in approximately hexagonal close-packed array. In each layer plane of octahedral interstices one-half of their number is occupied in a manner that allows each nitrogen atom to have unoccupied holes above and below it in adjacent planes. Each nitrogen atom is surrounded by six iron atoms, two at distances of 1.949 kX, and four at 1.940 kX giving an average iron-nitrogen distance of 1.943 kX.

An attempt has been made in this review to present the highlights of previous work on the iron-nitrogen phases and the equilibrium relationships existing among them. Differences between various investigations have been pointed out, and in some cases discrepancies between the experimental results and the proposed phase diagrams have been emphasized, since these points will be referred to in the forth-

coming discussion of the results of this investigation. A review of the investigations on the effect of pressure on the phase diagram, and other essentially thermodynamic studies on the iron-nitrogen system is not included herein, since this in all propriety belongs to a later chapter dealing with the thermodynamic calculations on the iron-nitrogen system.

III. EXPERIMENTAL PROCEDURES

A large variety of experimental methods have been used by previous investigators in determining the rion-nitrogen diagram. These include microscopic examination, thermal analysis, magnetic and electrical resistance measurements, dilatometric measurements, x-ray diffraction and anelastic experiments.

It may be proper to discuss at this point some advantages and disadvantages of the methods used so far. The heating and cooling curves on iron-nitrogen alloys are not absolutely reliable in studying the iron-nitrogen system, since the composition of most alloys tends to change during heating or cooling unless extreme care is taken to use a proper neutral atmosphere. Further it is well known that thermal analysis is usually inaccurate in determining changes in the solid state with the possible exception of strong eutectoid reactions. Metallographic investigations are also complicated by possible changes during cooling. The dilatometric technique is also liable to have the same objections as the thermal analysis. X-ray lattice parameter measurements are usually quite satisfactory in determining phase boundaries if the cooling rates are fast enough to prevent structural changes.

With the above analysis of the various techniques in mind, two methods were utilized in this investigation of the iron-nitrogen diagram. These were:

1. A controlled atmosphere nitriding technique, and

2. X-ray diffraction studies on the iron-nitrogen alloys produced by the above.

The first method represents an addition to the methods used so far in studying this system, and is therefore described in some detail in the following pages. A brief description of the apparatus and raw materials used, and the x-ray method, is also included.

A. Raw Materials

Carbonyl iron powder was used in preparing all iron-nitrogen alloys. The powder was obtained from the General Aniline Works, a division of the General Aniline and Film Corporation, New York. Table I shows the chemical composition of this material as determined by the Watertown Arsenal Laboratories, Watertown, Massachusetts. The carbon content of this iron was reduced to 0.01 percent by a decarburizing treatment prior to nitriding. This was achieved by passing wet hydrogen over the carbonyl iron which was at the nitriding temperature.

The controlled atmosphere nitriding process required the use of hydrogen and ammonia. Ammonia was obtained in tanks from Armour and Company, Boston, Massachusetts. It contained not less than 99.98 percent ammonia by volume. Hydrogen was also obtained in tanks from the Air Reduction Company, Boston, Massachusetts and contained less than 0.5 percent oxygen.

Prepurified nitrogen was used for flushing the nitriding furnaces. This was obtained from the Air Reduction Company in tank

Table I

Chemical Analysis of Carbonyl Iron Powder

Constituent	Amount, Weight Percent
Carbon	0.030 (reduced to 0.010 - 0.015 by wet hydrogen treatment)
Copper	Nil
Chromium	"
Manganese	"
Molybdenum	"
Nickel	"
Nitrogen	0.003
Phosphorus	Nil
Silicon	0.001
Sulfur	Nil

FIGURE 3. Schematic Diagram of the Experimental Set-up Used in Nitrogenizing.

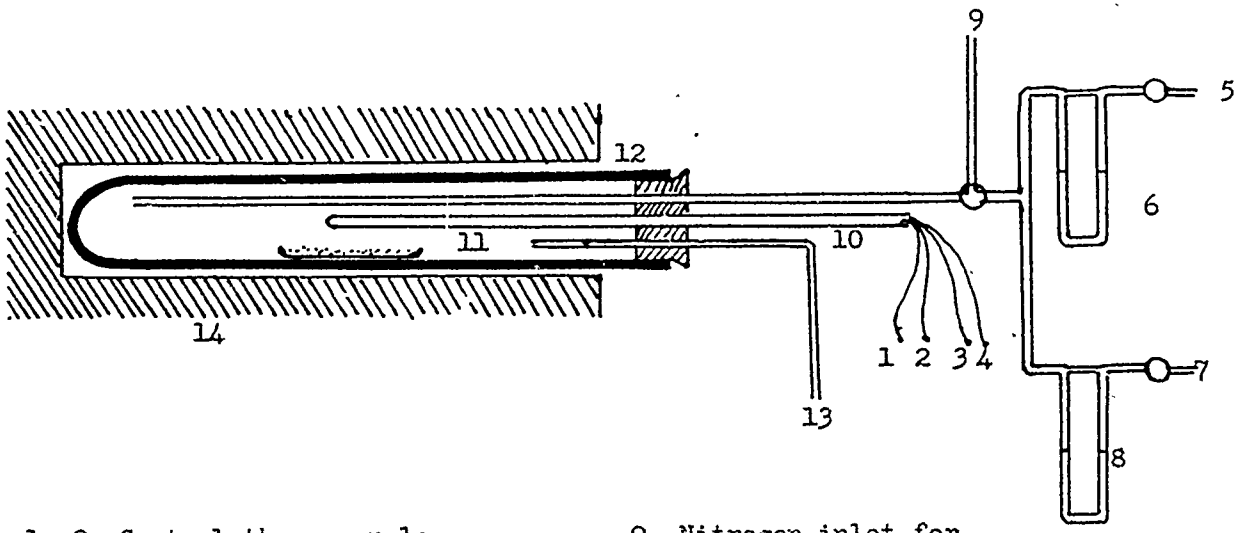

1, 2 Control thermocouple
3, 4 Measuring thermocouple
5 Hydrogen inlet from tank
6 Hydrogen monometer
7 Ammonia inlet from tank
8 Ammonia monometer
9 Nitrogen inlet for flushing
10 Pyrometer tube
11 Alundum boat
12 Quartz chamber
13 exhaust
14 Furnace

containers. The gas contained less than 0.001 percent each of hydrogen and oxygen (by volume).

B. Nitriding Apparatus

The experimental set-up used in all nitriding experiments is shown schematically in Figure 3. The nitriding was done in furnaces of the electric resistor type, using chromel windings. One furnace was made with Kanthal windings, for use at high temperatures. The furnace contained a quartz nitriding chamber. The sample of carbonyl iron powder was placed in an alundum boat at the center of the nitriding chamber. The nitriding chamber was sealed before any gas was led over the specimen. The thermocouple tube shown in Figure 3 contained two chromel-alumel thermocouples, one for regulating and the other for measuring the temperature. Temperature variation along the length of the specimen as studied by exploration was less than 0.5° C. The temperature was also checked periodically during the nitriding runs, and the maximum deviation from the desired temperature was less than 2.0° C. This variation includes all sudden changes in temperature.

The ammonia-hydrogen gas mixture which was used in any particular nitriding experiment was made up by mixing ammonia and hydrogen withdrawn from their tank-containers. The flow rate of each constituent was regulated and measured by accurately calibrated manometers, and a careful check was kept to minimize any errors due to possible fluctuations.

C. Experimental Procedure

The experimental procedure used for the controlled atmosphere nitriding technique was evolved after many trial runs. The procedure adopted was as follows.

A measured amount of carbonyl iron powder was spread uniformly in a new alundum boat. This was then inserted into the nitriding chamber which was maintained at the nitriding temperature. During this operation, prepurified nitrogen was passed through the chamber. The chamber was then appropriately sealed and the flow of prepurified nitrogen continued for about five minutes. After this, a stream of wet hydrogen was introduced through the inlet tube, and passed over the sample. This decarburizing process was continued for about six hours, after which the desired ammonia-hydrogen mixture was passed over the sample for a period long enough to attain equilibrium. The equilibration time was determined, as described later, to be about sixteen hours. At the end of the nitriding period, the ammonia-hydrogen mixture was shut off and the container was flushed for one minute with prepurified nitrogen. The seal was then broken, with nitrogen still flowing, and the sample was quickly withdrawn into a beaker of cold water. This last step was carried out in less than thirty seconds. The samples were then cleansed with alcohol and ether, dried and prepared for x-ray and chemical analysis.

D. Chemical Analysis of the Nitrided Alloys

The nitrogen content of the samples thus prepared was determined by the micro-Kjedahl method. These determinations were made by the Watertown Arsenal Laboratories, Watertown, Massachusetts. The analytical method* was tested for reproducibility and was found to be accurate within about 10 percent of the nitrogen content for low nitrogen samples (0.1 percent), and about 1 to 5 percent of the nitrogen content for high nitrogen samples (containing up to 11 percent nitrogen). The micro-Kjedahl method was also compared with the vacuum fusion technique of nitrogen determination, and a good agreement was found between the results obtained by the two methods.

E. X-Ray Examination of Iron-Nitrogen Alloys

The x-ray diffraction method was used for identification of the phases present in the alloys prepared in the nitriding experiments. The samples were always quenched from the nitrogenizing temperature, and thus information regarding the high temperature structures was obtained. The quenching rates employed were high enough to suppress any structural changes except the martensite transformation in samples containing low nitrogen austenite. The disappearing phase method and the lattice parameter variation technique were used to determine the phase boundaries. The results of the latter method were always preferred, since the x-ray method is not sensitive enough to detect small amounts of one phase present with another.

---

* A detailed description of the analytical method and test experiments is presented in Appendix I.

Powdered samples were used to ensure homogeneity of nitrogen content in the specimens, and the "powder method" of x-ray analysis was used. A Debye-Scherrer camera with a radius of 57.3 mm. was used. Phragmen No. 2 camera was also employed for some accurate lattice parameter measurements. The high angle lines in the photograms with the Phragmen type of focusing cameras were invariably diffuse, and thus no significant advantage was gained by the use of this type of apparatus.

In all of the photograms of this investigation, the characteristic radiation from a cobalt target was employed. This radiation was chosen because iron acts as a filter for the K_β radiation and also gave good superlattice reflections due to an increase in the relative influence of the nitrogen by depressing the atomic scattering factor of iron by the absorption-edge effect.

The structure and lattice constants of the various phases was determined from the Debye-Scherrer and Phragmen photograms in the conventional manner. The lattice parameters thus calculated are given to four significant figures. The fourth significant figure is, however, printed in small numerals since the technique employed was not precise enough to guarantee its accuracy.

F. Phase-Boundary Determination by the Controlled Atmosphere Nitriding Method

This method consists in principle of nitriding iron with a gas phase of controlled "nitriding power", and then correlating the nitriding power of the gas phase with the nitrogen content of the

iron-nitrogen alloy produced.

If a gas phase containing a known element is allowed to come into equilibrium with a solid, the element will so distribute itself between the gas and solid phases that its thermodynamic potential is the same in both. A definite relationship therefore exists between the concentration of the element, or its partial pressure, in the gas phase and its concentration in the solid. The controlled atmosphere nitriding method used in this investigation rests on this fundamental principle.

The logic of the method can be explained with reference to Figure 4. Figure 4(a) shows a hypothetical phase diagram for the iron-nitrogen system. The principal reaction in the nitriding process can be stated as follows:

$$NH_3 \text{ (gas)} = \underline{N} \text{ (Dissolved in an iron-nitrogen phase)} + \frac{3}{2} H_2 \text{ (gas)} \qquad (1)$$

The equilibrium constant K_T for reaction (1) at temperature T, is

$$K_T = a_N \times \frac{P_{H_2}^{3/2}}{P_{NH_3}} \qquad (2)$$

where a_N is the thermodynamic activity of nitrogen in the solid phase, and p_{H_2} and p_{NH_3} are the partial pressures of hydrogen and ammonia in the gas phase. Rewritting equation (2) as in (3) below

$$a_N = K_T \frac{P_{NH_3}}{P_{H_2}^{3/2}} \qquad (3)$$

it is evident that the activity of nitrogen in the solid is a function of the gas composition. The activity a_N is a function of the nitrogen content. Therefore the concentration of nitrogen can be expressed as follows:

$$N = f\left(\frac{p_{NH_3}}{p_{H_2}^{3/2}}\right) \qquad (4)$$

The equilibrium constant K_T is obviously constant at constant temperature.

It can be seen from equation (4) that the concentration of nitrogen in the solid phase will increase steadily with increasing ammonia content in an ammonia-hydrogen nitriding mixture. Such a behavior is shown schematically in Figure 4(b) for the alpha phase. When the ammonia concentration reaches the value A' and the nitrogen content of the solid is A, the gamma prime phase may exist together with the alpha phase. For this mixture therefore the nitrogen content of the solid may be anywhere between A and B (the lower limit of the gamma prime phase - see Figure 4(a)). Any further increase of ammonia concentration in the gas will only produce the gamma prime phase with an increased nitrogen content, until at an ammonia concentration C', the gamma prime phase with a nitrogen content C is capable of co-existence with an epsilon phase of composition D. A further increase of ammonia concentration will only serve to produce epsilon phases of progressively higher nitrogen contents as shown in Figure 4(b). A series of nitriding experiments made at temperature T, with progressively increasing ammonia

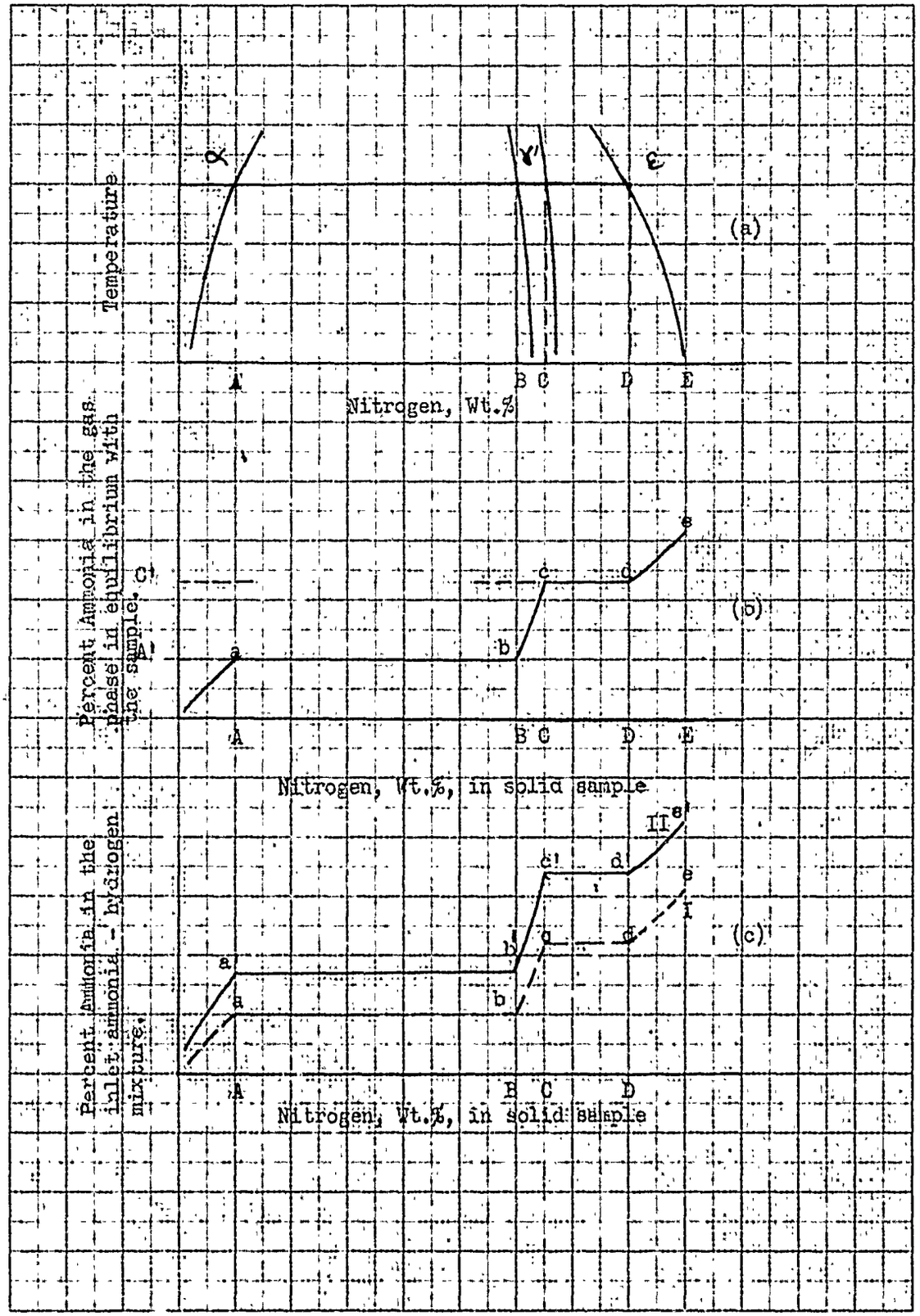

FIGURE 4. Schematic Diagrams Illustrating the Principle of Application and the Method of Plotting the Results Obtained by the Controlled Atmosphere Nitrogenizing Method.

concentrations in the gas mixture, can thus yield data to plot the curve abcde. The points a, b, c and d where discontinuities appear in this line represent the phase boundaries of the corresponding phases. The plotting of ammonia concentration along the ordinate of the diagram in Figure 4(b), instead of the true variable ($p_{NH_3}/p_{H_2}^{3/2}$), and a possible deviation from Raoult's or Henry's Laws can alter the curvature of the lines Oa, bc, and de. However, the nitrogen concentrations a, b, c and d at which the discontinuities appear are invariable at the temperature, since they are dictated by the equilibrium relationships embodied in the phase-diagram shown in Figure 4(a). Particular emphasis is laid on this fact because it forms the basis of determining phase boundaries by the technique used in this work.

Under actual experimental conditions it is difficult to obtain a plot like Figure 4(b), due to the presence of a side reaction represented by the following equation

$$NH_3\ (gas) = N_2\ (gas) + \frac{3}{2} H_2\ (gas) \qquad (5)$$

This reaction of ammonia dissociation proceeds simultaneously with reaction (1), and its extent depends upon temperature, flow rate of the gas mixture, and the catalytic conditions which prevail during a particular nitriding experiment. The composition of the nitriding mixture - ammonia and hydrogen - changes as it passes through the nitriding chamber due to a progressive dissociation of ammonia. Therefore the composition of the gas mixture that is in equilibrium with the solid phase cannot be measured accurately,

except at low temperatures where the dissociation reaction can be suppressed almost completely.

The method used to overcome the difficulty introduced by the catalytic dissociation is illustrated in Figure 4(c). The dashed line I in this plot is the same as the line oabcde in Figure 4(b), and represents the conditions where the ordinate is the ammonia content of the gas phase in equilibrium with the solid phase. This is equal to the composition of the inlet gas, as plotted in Figure 4(c), only when there is no catalytic dissociation. As is commonly the case, however, the gas phase in contact with the iron specimen contains less ammonia than the inlet mixture, due to catalytic dissociation. This decrement is proportional to the amount of catalytic dissociation, and can be held constant when the amount of the latter is constant. When such a constancy of catalytic dissociation is maintained, a curve like the full line II in Figure 4(c) can be obtained. This curve is similar to the dashed line I, except that the ammonia concentration in the inlet gas required to produce a certain nitrogen content in the solid is higher. The points a', b', c' and d' on this new line II still represent the phase boundaries, as these are independent of the amount of catalytic dissociation and are fixed by equilibrium relationships in the solid phases. It is important to mention here that the ammonia concentrations for this line II, like that corresponding to the point a' cannot be used in computing the thermodynamic functions for reaction (1). This investigation was, however, primarily concerned with phase boundary determinations, and thus the presence

of catalytic dissociation did not interfere as long as the amount of this dissociation was kept reasonably constant to obtain data to plot curves like the line II in Figure 4(c).

An increase in the amount of catalytic dissociation, if this higher value can be maintained reasonably constant throughout an isothermal series of nitriding experiments, can only raise the line II in Figure 4(c) vertically without changing the nitrogen contents at which the discontinuities in this line would appear. These nitrogen contents represent the phase boundaries, and are the intersections of the sloping single phase lines with the horizontal two phase lines.

The theory of the controlled atmosphere nitriding method is explained above. The application of this technique depends on the following conditions:

(a) The catalytic dissociation of ammonia should be held constant throughout an isothermal series of experiments.

(b) The iron-nitrogen alloy should be in equilibrium with the gas phase in contact with it.

(c) The nitrogen content of the alloy, characteristic of the gas phase and temperature of investigation should be determined.

A considerable amount of experimentation was necessary to determine the optimum operating condition satisfying the three conditions set forth above.

The temperature, gas flow rate and the catalytic conditions prevailing during a particular experiment have been mentioned

earlier as the variables governing the degree of ammonia dissociation by reaction (5). The first two variables were held constant without much difficulty. A careful check was kept over these, and if any irregularities were observed, the results of the experiments were discarded. The catalytic conditions in the nitriding chamber depend on the nature and amount of various surfaces that come into contact with the gas mixture. Quartz is known to be a relatively inert catalyst for the dissociation reaction, and therefore the nitriding chamber, inlet and outlet tubes for the gas mixture and the thermocouple tube were made of quartz. Iron is a good catalyst for the dissociation process, and thus special care was taken to use the same amount of powder and spreading it uniformly in the alundum boat. The boat got contaminated with iron and thus a new boat was used for every experiment. Having taken these precautions it was assumed that the catalytic conditions were held approximately constant, and the results of experiments conducted in this manner seem to justify this assumption.

Several experiments were conducted to determine the time necessary to attain equilibrium. In these experiments the time of nitrogenizing was varied, while holding the temperature of operation and the catalytic conditions constant. The results of a typical series of runs are presented in Table II. It was concluded from these data that a period of sixteen hours was more than sufficient to attain equilibrium.

Some trial runs were made to determine the best way of retaining the nitrogen content of the alloy when it was taken out of the

Table II

Determination of the Equilibration Time

Nitrogenizing Temperature - 550° C

Constant Composition and Flow Rate of the Inlet Gas.

Sample No.	Duration, hours	Nitrogen, weight percent in water quenched samples
7-H	1/2	0.74 - 0.77 (0.755)
8-H	1	4.35 - 4.39 (4.37)
9-H	2	5.56 - 5.62 (5.59)
10-H	4	5.51 - 5.55 (5.53)
11-H	8	5.60 - 5.58 (5.59)
12-H	16	5.56 - 5.49 (5.53)
13-H	24	5.55 - 5.58 (5.57)
14-H	32	5.50 - 5.50 (5.53)

nitrogenizing chamber for chemical analysis. The results of this preliminary work* showed that the nitrogen content was either increased or decreased during cooling depending upon whether the cooling conditions exerted a nitrogenizing or denitrogenizing influence. It was therefore necessary to adopt the procedure of water quenching with the assumption that this retained all the nitrogen existing in the sample under the nitrogenizing conditions of the experiment.

The principles and the experimental procedures used in the controlled atmosphere nitriding technique are described above. The method of interpreting the results obtained thereby is illustrated by Figure 5. This diagram summarizes the results** obtained in an isothermal series of nitrogenizing experiments at 500° C. The ammonia contents of the inlet ammonia-hydrogen gas mixtures, and the nitrogen contents of the solid samples are plotted along the ordinate and abscissa respectively. The experimental points are joined by a line similar to the line II in Figure 4(c). The phase boundaries are determined by the intersections of the horizontal two-phase lines with the sloping single phase lines. For example, the gamma prime line intersects the alpha-gamma prime line and the gamma prime-epsilon lines (Figure 5) at 5.45 and 5.75 percent nitrogen respectively. These two compositions therefore represent the

---

* The results of all preliminary investigations are presented in Appendix II.

** The results of all controlled atmosphere nitriding experiments are presented in Appendix III.

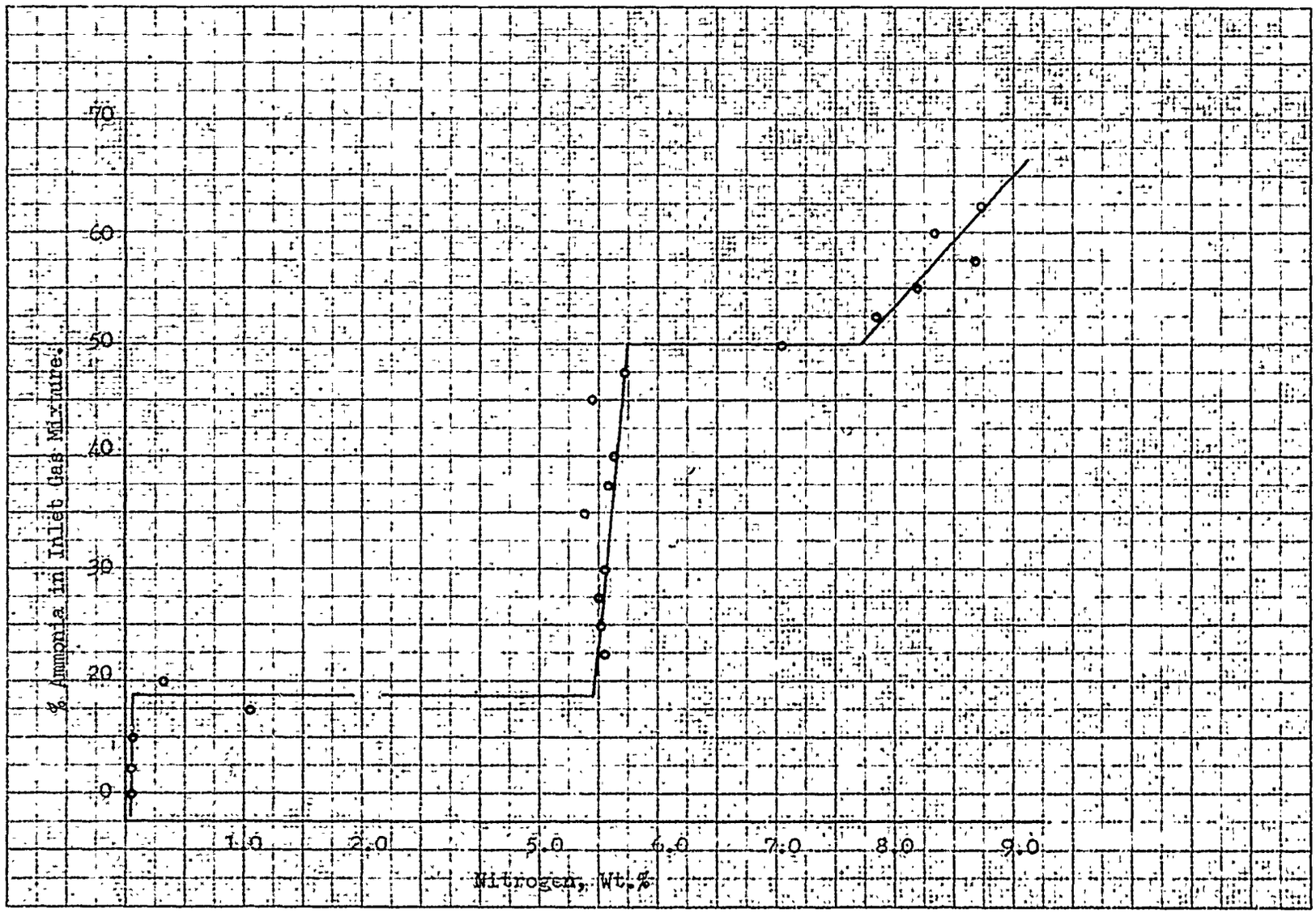

FIGURE 5.. Results of a Typical Series of Controlled Atmosphere Nitrogenizing Runs.

homogeneity limits of the gamma prime phase at 500° C. The maximum solubility in the alpha phase can be similarly read off from Figure 5 as being about 0.05 percent nitrogen. This is the nitrogen content at which the alpha-phase line intersects the horizontal alpha-gamma prime line. The lower limit of the epsilon-phase can be fixed as 7.7 percent nitrogen - the point of intersection of the epsilon and gamma plus epsilon lines.

A similar series of experiments was carried out at 500° C using a high-nitrogen alloy as the starting material. In this case the equilibrium was thus approached from the high nitrogen side. The boundaries of the gamma prime phase determined from the results of these experiments are in good agreement with those mentioned above. This shows that this technique of determining the phase boundaries in the iron-nitrogen system gave reliable results.

IV. EXPERIMENTAL RESULTS AND DISCUSSION

The iron-nitrogen phase diagram was determined by analyzing the data* obtained by the controlled atmosphere nitrogenizing process, and the x-ray investigation of numerous iron-nitrogen alloys. Before presenting the phase diagram, however, it seems desirable to describe the various iron-nitrogen phases individually.

The iron-nitrogen phases detected in this investigation are described in order of increasing nitrogen concentration. The results of this investigation are also discussed in light of previous work summarized earlier.

A. Alpha-phase (Nitrogen-ferrite)

The alpha phase has a body-centered cubic structure, and is capable of containing a small amount of nitrogen in solution. This phase resembles the ferrite phase in the iron-carbon system and may thus be named nitrogen-ferrite. The lattice parameter of nitrogen-ferrite is affected only slightly by the presence of nitrogen. Experiments conducted to study the variation of lattice parameter with increasing nitrogen content showed a lack of consistent measurable change. The adoption of the back reflection x-ray techniques did not yield very reliable results. The x-ray method of phase boundary determinations was thus not applicable in this case.

---

* The detailed results of all nitriding experiments and x-ray structure determinations are presented in Appendix III.

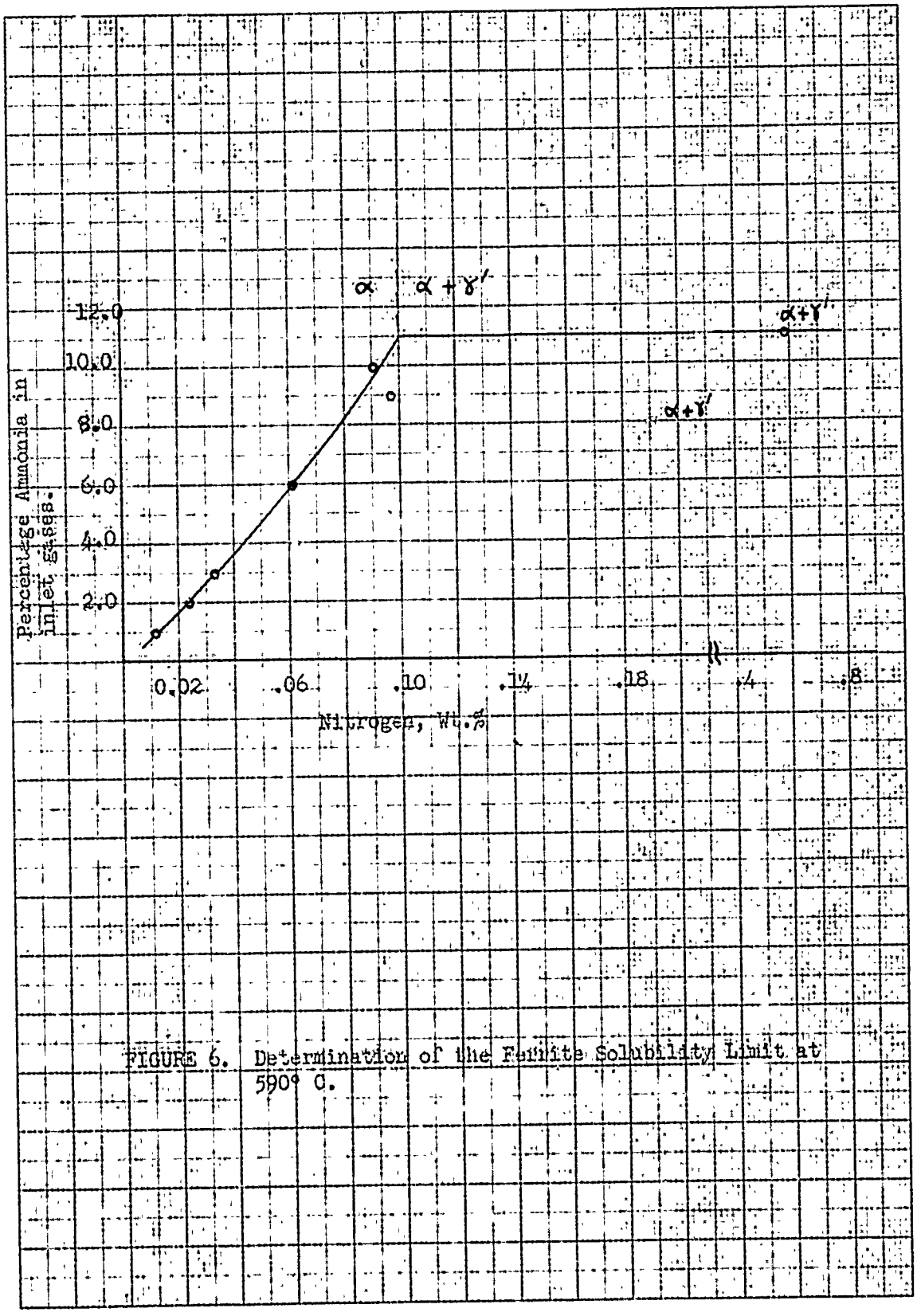

FIGURE 6. Determination of the Ferrite Solubility Limit at 590° C.

These results are in direct contradiction to the findings of Eisenhut and Kaupp[17] who found an appreciable increase of the ferrite cell dimensions with increasing nitrogen content, and used this behavior to determine the alpha solubility line. As already indicated in the preceding review of early work on the iron-nitrogen system, Hägg[18] did not notice any appreciable change in the ferrite cell dimensions. The results of this investigation confirm Hägg's findings.

The solubility of nitrogen in the alpha phase was therefore determined by the controlled atmosphere nitriding method. The results of a typical series of nitriding experiments at 590° C (the first eutectoid temperature) are plotted in Figure 6. It can be seen from this plot, that the solubility limit at 590° C is 0.10 percent nitrogen by weight. Table III lists the results of similar investigations at temperatures both below and above the eutectoid temperature. These are also plotted in Figure 7. The solubility limits determined by Dijkstra[31] are also shown for comparison. The agreement between the results obtained by Dijkstra's anelastic measurements and the controlled atmosphere nitriding method used in this investigation is quite good.

As shown in Figure 7, Dijkstra's curve crosses the solubility limit determined in this investigation. The differences between the two sets of values, though small, may be significant. Dijkstra's anelastic measurements were done on quenched samples. It is possible that a slight precipitation may have occurred in his

TABLE III

Solubility Limit of Nitrogen-ferrite (α)

Temperature ° C	Nitrogen Weight Percent
(910)	(0.00)
700	0.07
650	0.086
590	0.10
550	0.070
500	0.050
450	0.033

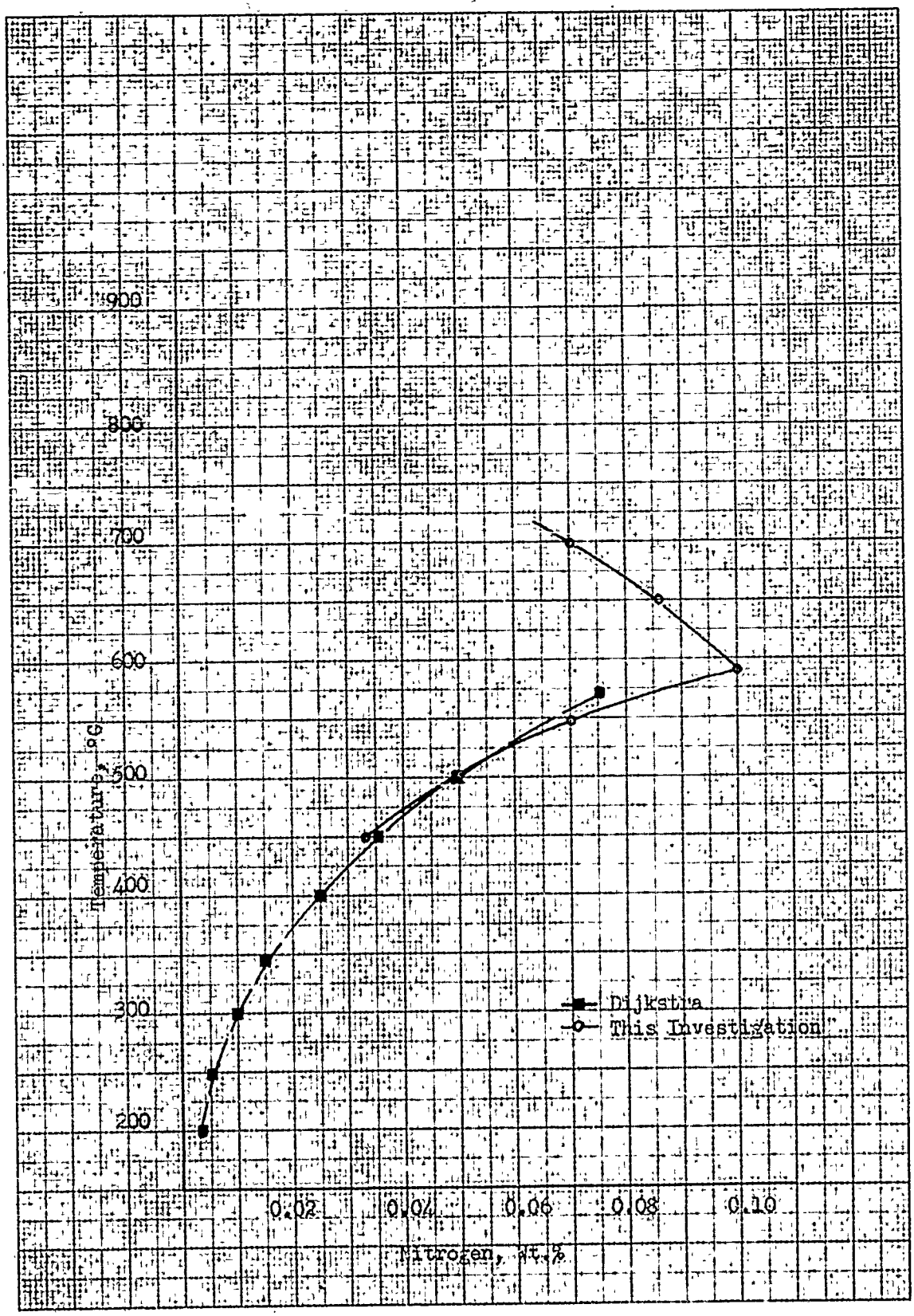

FIGURE 7. Solubility Limit of Nitrogen-Ferrite as a Function of Temperature.

samples quenched from above 500° C. This would account for his lower values for the solubility limits for the higher temperatures. On the other hand, the precipitation of the stable nitride (gamma prime) from the nitrogen-ferrite may be very sluggish in the lower temperature range and thus Dijkstra's values in this range may exceed the saturation limit. The method of controlled atmosphere nitrogenizing used in this investigation is more reliable since the measurements are carried out at temperature.

The solubility limit given in Figure 7 is notably lower than the one reported by Eisenhut and Kaupp, but as already pointed out, the latter is based on x-ray parameter measurements which appear to be questionable. Seferian's[30] results are of the same order of magnitude, but slightly larger than those shown in Figure 7.

B. Gamma-phase (Nitrogen-austenite)

The gamma phase, or nitrogen-austenite, as it may be labeled to distinguish it from the structurally similar austenite phase in the iron-carbon system, has a face-centered cubic arrangement of the iron atoms, and it contains nitrogen in solution.

Nitrogen austenite is stable above the eutectoid temperature of 590° C. When cooled from above this temperature it decomposes into a pearlitic structure if the cooling is sufficiently slow. To prevent this pearlite reaction, all samples prepared in this investigation were water quenched from the nitrogenizing temperature. In spite of this rapid cooling, it was not possible to

preserve the low-nitrogen samples in a completely austenitic condition, due to the formation of martensite during the quench. Samples containing more than 2.4 percent nitrogen by weight remained completely austenitic, whereby one may infer that the M_s temperature for iron-nitrogen alloys of these compositions is below room temperature. Samples containing less than 2.4 percent by weight had two structural components: austenite and martensite. It was safe to assume that compositions containing only austenite and martensite were completely austenitic at the nitriding temperature which was also the quenching temperature.

The lattice parameter of nitrogen austenite increases with increasing nitrogen content. Figure 8 indicates the results of x-ray diffraction measurements. The data of Eisenhut and Kaupp[17] are also given in the same figure. Their lattice parameter values lie consistently above those found in this investigation. Their values are, however, based on Debye-Scherrer film measurements, while the present values are based on the results obtained by using the Phragmen number 2 focusing camera, and the cosine^2 θ method of extrapolation.

The lattice parameter vs. nitrogen content line shown in Figure 8 was then used to determine the homogeneity limits of nitrogen-austenite field. The usual lattice parameter method was followed. Thus the higher limit of the gamma-phase filed was found to be 2.64, 2.80, 2.75 and 2.70 at 625, 650, 675 and 700^0 C respectively. These values are in good agreement with those reported by Eisenhut and Kaupp[17] and Lehrer[16].

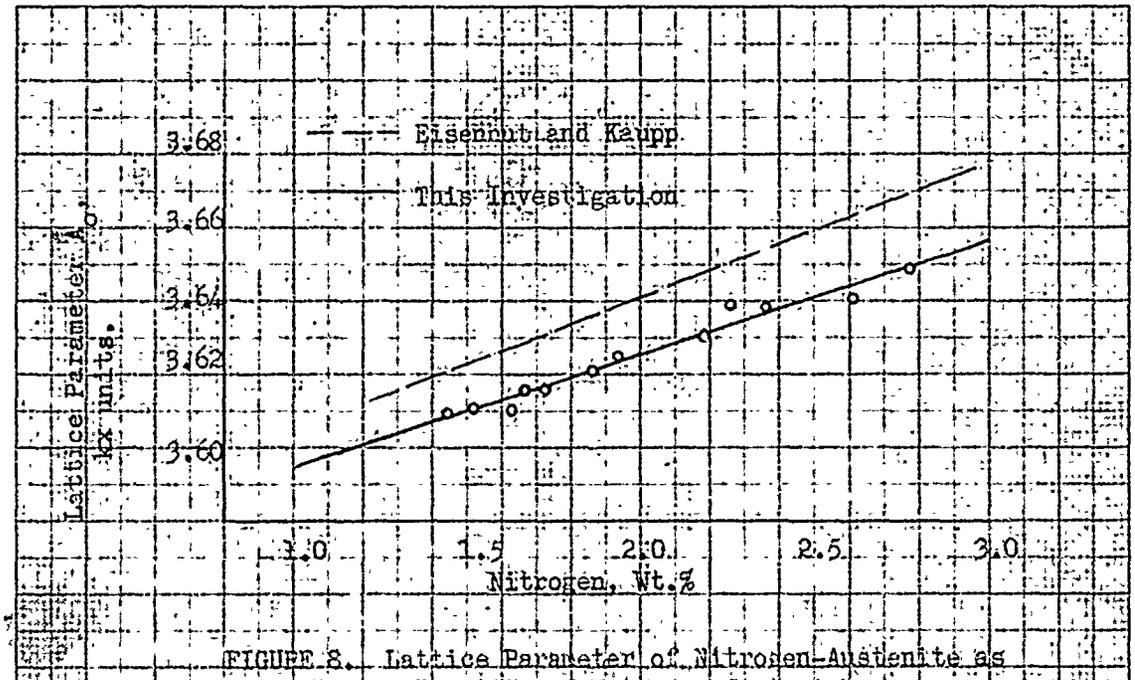

FIGURE 8. Lattice Parameter of Nitrogen-Austenite as a Function of Nitrogen Content.

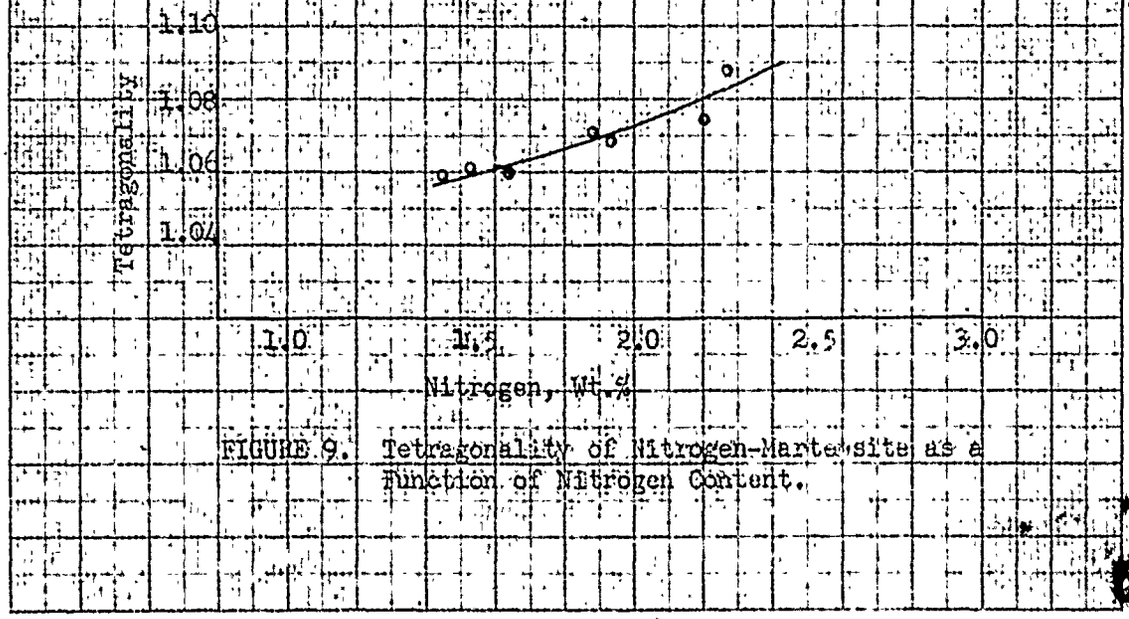

FIGURE 9. Tetragonality of Nitrogen-Martensite as a Function of Nitrogen Content.

TABLE IV

Homogeneity Limits of Nitrogen-austenite (γ)

Temperature °C	Lower Limit (Weight Percent Nitrogen)	Upper Limit (Weight Percent Nitrogen)	
910	(0.00) (α-γ)	-	
700	-	2.70	(γ-ε)
675	1.40 (α-γ)	2.75	(γ-ε)
650	1.64 (α-γ)	2.80	(γ-ε-γ')
625	-	2.64	(γ-γ')
590 (eutectoid temperature)		2.35	(α-γ-γ') by extrapolation

The lower limit of the nitrogen-austenite field could not be determined by x-ray methods, since the samples of this chemical composition contained only small amounts of retained austenite. The controlled atmosphere technique was, therefore, employed to secure these values. The results of these experiments indicate that the lower limit is 1.40 percent nitrogen by weight at 675° C. The lowest nitrogen content at which only austenite and martensite existed in a sample quenched from 650° C was 1.64 percent by weight. This value approximately defines the low nitrogen limit of the austenite region at 650° C. The line drawn through these two points coincides with the phase boundary reported by Eisenhut and Kaupp and by Lehrer.

C. Nitrogen-martensite

Nitrogen-austenite was found to transform into a body-centered tetragonal structure during cooling. Rapid quenching did not suppress this transformation. The transformation thus appears to be of a martensitic type, and the body-centered tetragonal structure is named nitrogen-martensite. Metallographic examination of massive samples quenched from the austenite field reveals that nitrogen-martensite has a characteristic needle-like shape, and it responds to tempering in a fashion similar to the iron-carbon martensite. Figure 10 illustrates the microstructure of a thin foil specimen containing about 2.0 percent nitrogen by weight.

The tetragonality of the nitrogen-martensite increases with increasing nitrogen content. Figure 9 summarizes the results of

Figure 10. Photomicrograph Showing Nitrogen-Martensite in a Matrix of Nitrogen-Austenite.

Nitrogenized at 700° C for 2 hours in a gas stream containing 7.0 percent ammonia. Nitrogen content about 2.0 percent by weight. Quenched from 700° C in ice water. No tempering. Picral Etch. Magnification X1,000.

some x-ray measurements in this respect. The values shown in this plot are not highly accurate, since the Debye-Scherrer method was used for the determinations.

Eisenhut and Kaupp[17] have reported the existence of tetragonal nitrogen-martensite, and this investigation confirms its existence.

D. Gamma-prime phase (Fe_4N)

The gamma-prime phase has a face-centered cubic structure, and it exists in a very limited range of composition.

An x-ray diffraction pattern of this phase with cobalt K radiation gave several faint lines in addition to those normally given by face-centered cubic structure. These lines appear to be superlattice reflections corresponding to the (100), (110), (210), (211), (221), (310), (320), and (321) planes. The relative intensities of these lines, and their spacings are in very good agreement with the recent work of Jack[36] on the structure of the gamma-prime phase. These results therefore confirm Jack's interpretation of the crystal structure of this phase.

The unit cell dimensions of this phase increase with increasing nitrogen content. The lattice parameter changed from 3.78_3 kx units at 5.29 percent nitrogen to 3.79_3 kx units at 5.71 percent nitrogen by weight. The variation of lattice parameter being very small, and the x-ray techniques used being incapable of much greater accuracy, this lattice parameter variation could not be used to determine the phase boundaries of the gamma-prime phase.

TABLE V

Homogeneity Limits of the Gamma-prime Phase (γ')

Temperature °C		Lower Limit (Weight Percent Nitrogen)	Upper Limit (Weight Percent Nitrogen)
650	(eutectoid temperature $\gamma - \varepsilon - \gamma'$)	5.30	-
625		-	5.6
600		5.30	-
590	(eutectoid temperature $\alpha - \gamma - \gamma'$)	5.30	-
550		5.45, 5.48	5.70, 5.80
500		5.45	5.75, 5.80
450		5.47	-

The homogeneity limits of the gamma-prime phase were therefore determined by the controlled atmosphere nitriding technique. The results are presented in Table V.

E. Epsilon phase (Fe_3N)

This phase has a hexagonal close packed structure and exists over a wide range of nitrogen concentrations.

The lattice parameters and the axial ratio c/a change appreciably as the nitrogen content of the epsilon phase varies. (Figure 11). The lattice parameters and the axial ratio do not change linearly with increasing nitrogen content, indicating that Vegard's Rule is not obeyed in this case. The best fit is obtained by curved lines, and these lines are extrapolated to lower nitrogen contents.

The lower homogeneity limits of the epsilon phase were determined by measuring the lattice parameters of the epsilon phase in the two-phase field and then finding the composition of the epsilon phase from the curves in Figure 11. The results are presented in Table VI and Figure 12.

It can be seen from Figure 12 that the epsilon-phase field extends above the gamma-prime-phase field. Several attempts were made to produce samples containing only the epsilon phase with nitrogen contents near its lower limit of homogeneity. However, the temperatures at which this phase is stable are quite high and the consequent erratic nature of the catalytic dissociation of ammonia prevented adequate control of the composition of the sample produced by

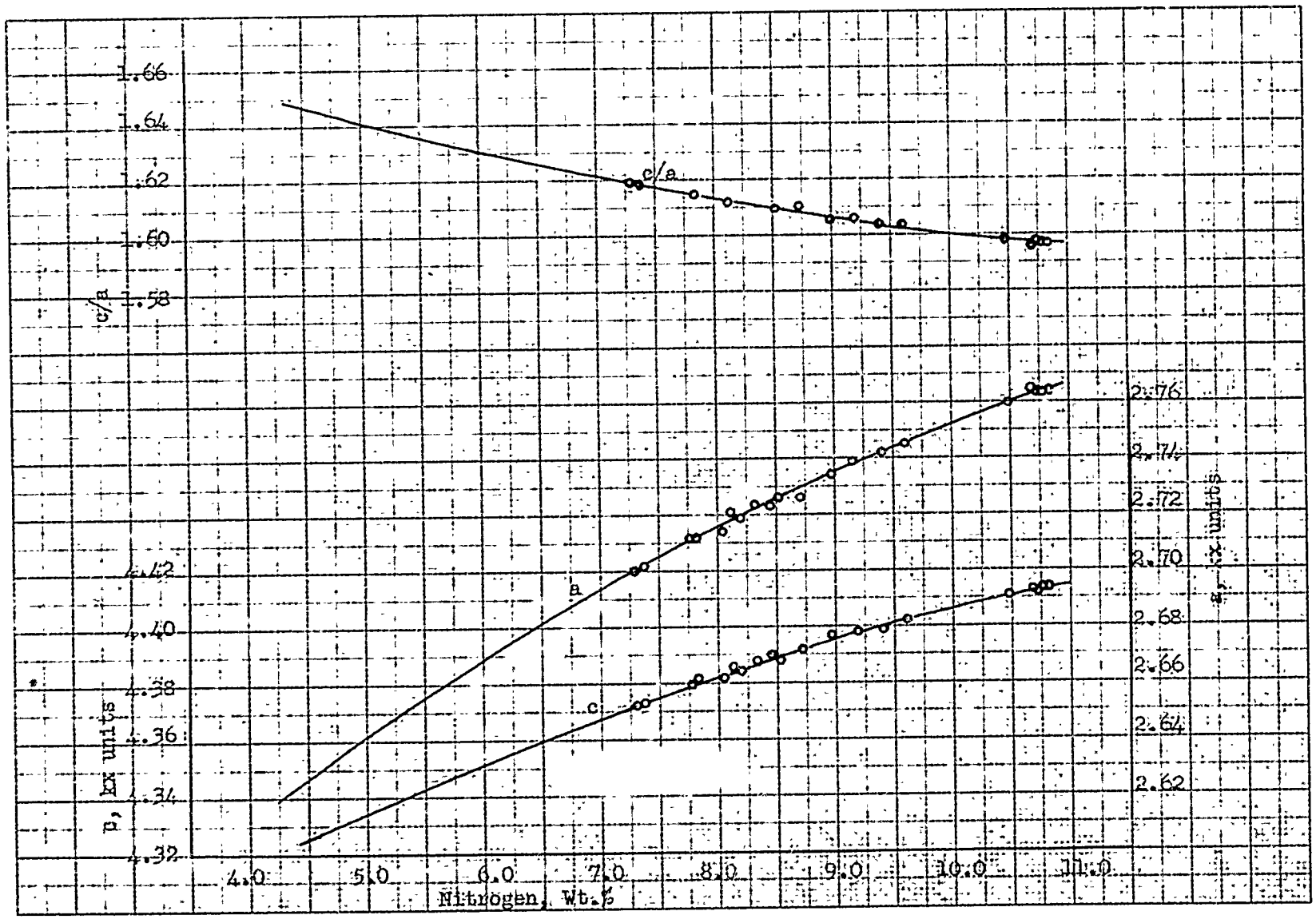

FIGURE 11. Lattice Parameters and Axial Ratio of the Epsilon Phase as Functions of Nitrogen Content.

TABLE VI

Homogeneity Limits of the Epsilon Phase

Temperature °C	Weight Percent Nitrogen		Phase Equilibrium
	X-ray Method	Controlled Atmosphere Nitrogenizing Method	
675	4.35	-	$\gamma - \varepsilon$
	5.0	-	$\varepsilon - \gamma'$
650	4.5	-	$\gamma - \varepsilon - \gamma'$
	6.2	-	$\gamma' - \varepsilon$
625	6.6	-	$\gamma' - \varepsilon$
550	7.35	-	$\gamma' - \varepsilon$
500	7.70, 7.75	7.70	$\gamma' - \varepsilon$
450	7.95	7.95	$\gamma' - \varepsilon$

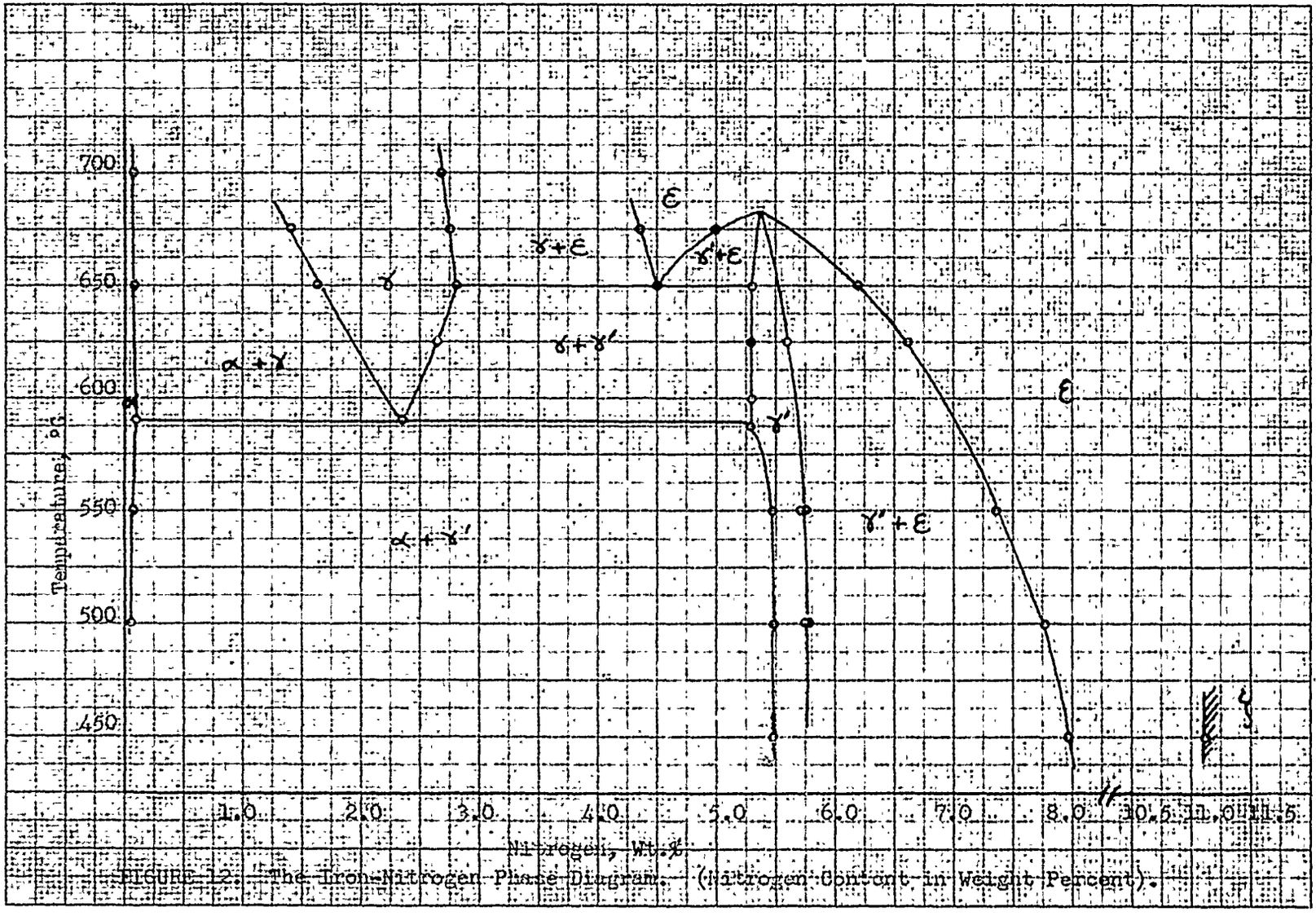

FIGURE 12. The Iron-Nitrogen Phase Diagram. (Nitrogen Content in Weight Percent).

nitrogenizing. As a result, no samples containing only the low nitrogen epsilon phase could be produced. An attempt was made to obtain such a sample by heating a high nitrogen epsilon phase to about 675° C and quenching it after its nitrogen content had approached the desired value. These attempts, however, proved futile due to a very rapid dissociation of the epsilon phase which could not be controlled. Due to the lack of a single phase parameter measurement in the low nitrogen region, the values in Table VI had to be based on the extrapolated lines shown in Figure 11.

The controlled atmosphere nitriding technique was also used to determine the lower limit of the epsilon phase at 450 and 500° C. The results obtained by this method are included in Table VI and are in good agreement with the results derived from lattice parameter measurements.

F. Zeta-phase (Fe_2N)

The zeta phase has an orthorhombic structure, the unit cell dimensions being approximately a = 2.75, b = 4.82 and c = 4.43 kx units respectively. This phase could be produced only by nitrogenizing at 450° C and existed at nitrogen concentrations above 11.1 percent by weight. Several attempts to approach this composition at 475 and 500° C were unsuccessful.

The x-ray technique used in this investigation was not accurate enough to warrant any interpretation of the atomic arrangement of this phase. The x-ray diffraction patterns obtained by using

cobalt K_α radiation were, however, in good agreement with the structure proposed by Jack[36].

The lower limit of the zeta phase was found to be 11.1 percent nitrogen at 450° C which is also in agreement with Jack's work.

It may be added that this investigation confirmed the existence of this orthorhombic phase originally proposed by Hägg[18], and recently reinvestigated by Jack.

G. The Iron-Nitrogen Phase Diagram

The various single phase regions hereto described individually are fitted together to form the constitution diagram shown in Figure 12.

The phase diagram shows the presence of two eutectoid reactions. The first eutectoid contains the alpha and gamma-prime phases, and the other reaction involves the decomposition of the epsilon phase into an eutectoid containing gamma and gamma-prime phases.

The first eutectoid has been suggested by several previous investigators[12,13,14,15,16,17,18,19,30]. No attempt was made in this investigation to determine the eutectoid temperature precisely. This was taken to be 590° C which is consistent with the most recent determinations by Lehrer[16] and Eisenhut and Kaupp[17]. Other determinations range from 580° C suggested by Fry[7,12] to 608° proposed by Bramley and Haywood[28].

The eutectoid composition, as determined by the intersection of the homogeneity limits of the austenite phase (Figure 12), is 2.35 percent nitrogen by weight. This value is in agreement with

the results of Eisenhut and Kaupp and Lehrer, but differs appreciably from the values ranging from 1.5 to 1.8 percent nitrogen suggested by Fry[12], Sawuer[13], Epstein and coworkers[14,15] and Hägg[18,19].

The present experimental evidence in favor of the proposed value of 2.35 percent nitrogen is, however, quite reliable and satisfactory.

This eutectoid eutectoid reaction can thus be stated as follows:

$$\text{At } 590^{\circ}\text{ C} \qquad \gamma_{2.35} \rightleftharpoons \alpha_{0.10} + \gamma'_{5.30}$$

The subscripts indicate the nitrogen content in weight percent.

The existence of the second eutectoid reaction shown in Figure 12 has been proposed earlier by Lehrer[16]. The temperature of this eutectoid reaction is fixed at 650° C. Iron-nitrogen alloys near the eutectoid region quenched from 650°±2° C contain either gamma + gamma prime or gamma + epsilon or gamma-prime + epsilon depending on the exact quenching temperature and composition of the alloy. These results show that the eutectoid temperature is 650° C. Lehrer[16] has also proposed the same temperature for this eutectoid reaction and Eisenhut and Kaupp[17] have proposed that a peritectoid reaction takes place at this temperature. Epstein and coworkers[14,15] have also reported the existence of thermal arrests at 660° C. The reaction temperature of 650° C is thus in good agreement with results of previous work.

Epstein and his coworkers like Eisenhut and Kaupp have suggested that a peritectoid transformation takes place at this temperature. Lehrer, however, has indicated an eutectoid reaction. Epstein and his coworkers have based their proposal on metallographic investigations in which they were unable to detect the presence of an eutectoid. The reliability of this negative reasoning may, however, be questioned. The inconsistency found between the experimental results of Eisenhut and Kaupp and their proposed peritectoid reaction has already been pointed out earlier. Their results show that their samples containing from 4.6 to 5.2 percent nitrogen by weight and quenched from above 650° C cor tained epsilon + gamma prime. If a peritectoid reaction were to occur at this temperature, such samples should not contain the gamma prime phase. Their experimental results which contradict the possibility of the peritectoid reaction can, however, be easily explained by the occurrence of an eutectoid transformation at 650° C as shown in Figure 12. The variation of the lattice constants of the epsilon phase plotted in Figure 11, and the values in the gamma prime plus low nitrogen epsilon-phase field demonstrate that the epsilon phase definitely exists at nitrogen concentrations less than 5.3 percent. The lattice constants of the epsilon phase have two different but constant values in the two two-phase fields; the low nitrogen epsilon + gamma-prime field, and the gamma-prime + high nitrogen epsilon field. Furthermore, an observation of the relative intensities of the strongest diffracted lines from the epsilon and gamma-prime phases showed

that the amount of the epsilon phase decreases gradually as the composition of the iron-nitrogen alloys quenched from slightly over 650° C increases. From 5.2 to 5.4 percent nitrogen, the x-ray diffraction patterns do not contain any lines belonging to the hexagonal epsilon phase. The epsilon phase reappears at increasing nitrogen content with alloys up to 5.98 percent nitrogen containing the gamma-prime phase in addition to the hexagonal phase. A similar variation is found at 660 and 675° C, the nitrogen concentrations, however, being slightly altered in accordance with the phase diagram given in Figure 12. The results of lattice parameter measurements, and observation of the intensities of the strongest diffraction lines of the gamma-prime and epsilon phases therefore confirms the existence of a eutectoid reaction at 650° C originally proposed by Lehrer[16].

The eutectoid composition was fixed at 4.5 percent nitrogen by weight by the lattice parameter measurements made in this investigation. This agrees with that inferred from the observations of the intensity of the strongest line of the epsilon phase. The value of 4.5 percent determined in this investigation is also in agreement with Lehrer's results.

The eutectoid reaction at 650° C is summarized by the relation

$$\text{At } 650^\circ \text{ C:} \qquad \varepsilon_{4.5} \rightleftharpoons \gamma_{2.80} + \gamma'_{5.30}$$

where the subscripts indicate the nonvariant compositions in weight percent nitrogen.

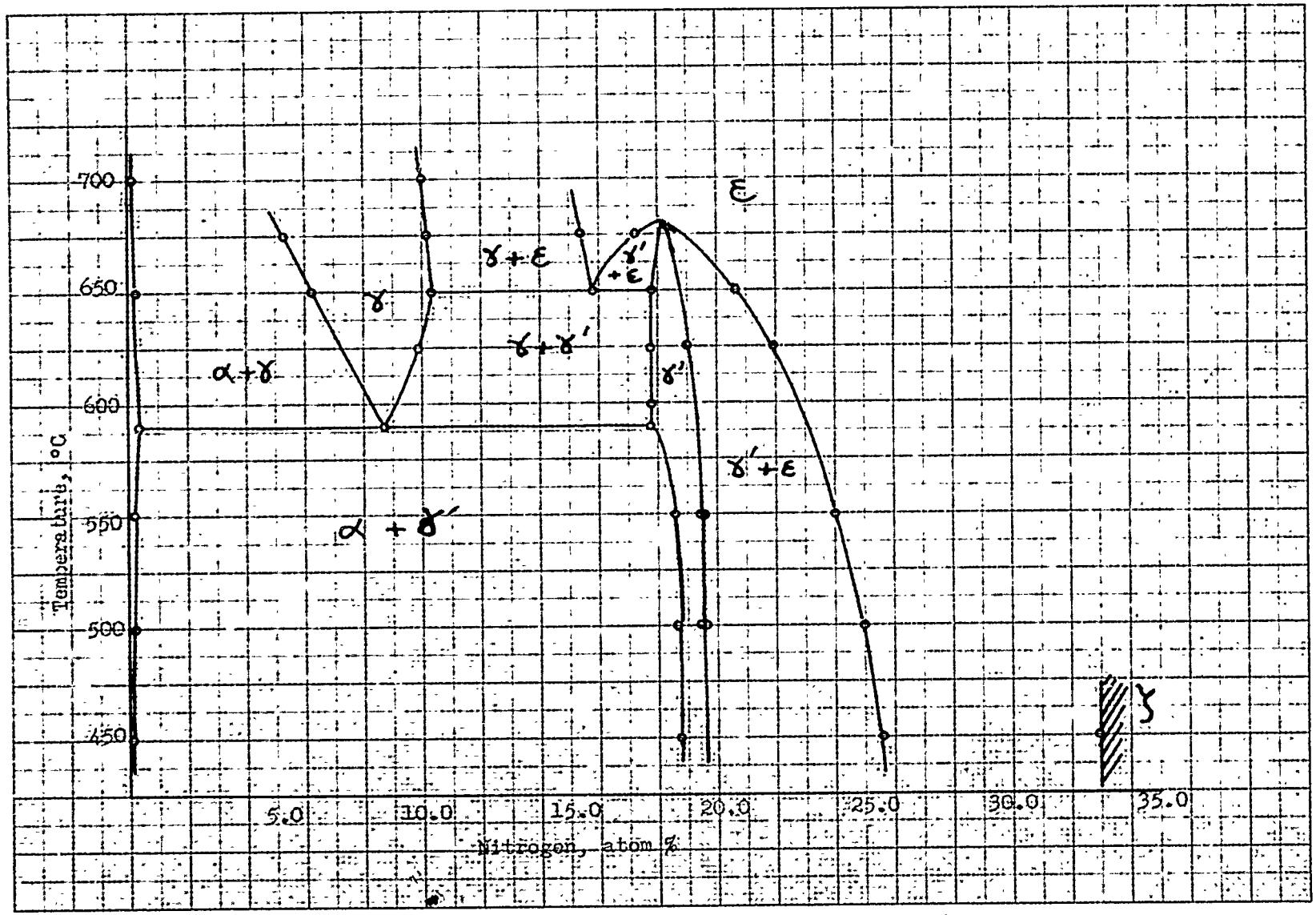

FIGURE 13. The Iron-Nitrogen Phase Diagram. (Nitrogen Content in Atom Percent).

The zeta phase, whose existence is confirmed by the results of this investigation, is shown to begin at 11.1 percent nitrogen. The exact shape of this phase boundary, and the upper limit of the zeta phase, is, however, unknown.

The iron-nitrogen phase diagram, redrawn to show the compositions in atomic percent nitrogen, is shown in Figure 13. The two eutectoid reactions are again summarized below with the subscripts showing the corresponding nonvariant compositions in atomic percent nitrogen.

At 590° C: $\gamma_{8.76} \rightleftharpoons \alpha_{0.398} + \gamma'_{17.8}$

At 650° C: $\varepsilon_{15.8} \rightleftharpoons \gamma_{10.3} + \gamma'_{17.8}$

In conclusion it is important to emphasize that the phase diagram determined in this investigation resembles that of Lehrer more closely than any other published diagrams. However, there are a number of differences in detail. For example, Lehrer was unable to measure the solubility limit in the alpha phase and thus accepted the higher value of 0.42 weight percent reported in the literature. The maximum solubility of nitrogen in nitrogen-ferrite is fixed at 0.10 (weight percent) by this investigation. The homogeneity limits of the gamma phase have been determined more accurately and the maximum solubility of nitrogen in the gamma phase is shown to decrease as the temperatures rise above 650° C. The epsilon-phase field has also been more thoroughly investigated and in particular the homogeneity limits near the eutectoid composition of 4.5 percent nitrogen

have been determined. The boundaries of the gamma-phase field fixed by this investigation are slightly lower than those proposed by Lehrer. Further, the presence of the eutectoid reaction at 650° C and the existence of the zeta phase are definitely confirmed.

V. THEORETICAL CALCULATIONS OF THE EQUILIBRIUM RELATIONSHIPS

The iron-nitrogen system is essentially different from the usual binary systems of metallurgical significance in that it contains a gaseous component. Due to this important factor, the equilibrium relationships in the iron-nitrogen system cannot be completely represented by the conventional two-dimensional phase diagram (Figures 12 and 13). In a metal-gas system, pressure is an important variable and its effect on the phase relations must be considered. A three-dimensional diagram with temperature, composition and pressure on the three axes is therefore necessary to show the effect of these three variables on the phase relationships in the iron-nitrogen system. In the following discussion, the fugacity of nitrogen is used as the third variable since it can be computed directly from the equilibrium constants of the phase reactions. To convert fugacity into pressure it is necessary to extrapolate the equation of state for nitrogen, but this is not attempted since the extrapolation is much too large to be justifiable.

The thermodynamic calculations carried out as a part of this investigation and the method of computing the fugacity axis of the three-dimensional equilibrium diagram are presented below.

No attempt was made to determine the equilibrium constants of the reactions involving the iron-nitrogen phases. The equilibrium constants have been measured by earlier investigators and since these are used freely in the following treatment, a brief

review of the literature is included here.

For the sake of uniformity, all the iron-nitrogen phases are referred to in the manner described in the previous chapter. The iron-nitrogen compound labelled Fe_4N in the literature is called the gamma-prime phase. Similarly, the compound Fe_3N (containing about 8 to 11 percent nitrogen by weight) is designated as the epsilon phase. The chemical reactions involving these compounds are also appropriately modified in the following discussion.

A. Thermodynamic Properties of the Iron-Nitrogen Phases

The specific heats of the gamma-prime (Fe_4N) and epsilon phases have been determined by Satoh[38]. His method of sample preparation and his treatment of experimental data are not very satisfactory. However, no other determination of the specific heats being available, his values are accepted with reservations.

The heats of formation of the gamma-prime and epsilon phases have been measured by Fowler and Hartog[39] and by Satoh[40]. Fowler and Hartog, however, employed erroneous data for the heats of solution of ferrous sulfate and ammonium sulfate and thus their values are not very reliable.

The equilibrium relationships between iron and the iron-nitrogen phases (gamma prime and epsilon) have been investigated by Noyes and Smith[41], by Emmett and his associates[32,42] and by Lehrer[43]. Noyes and Smith employed a static method of reaching equilibrium in the iron + iron-nitrogen phases + hydrogen + ammonia systems. They did not identify the exact nature of the

iron-nitrogen phases involved in their work. Emmett and his co-workers improved upon the experimental techniques used by Noyes and Smith. They adopted the dynamic method of reaching equilibrium, and studied the equilibrium relationships in the alpha + gamma-prime + ammonia + hydrogen and gamma-prime + epsilon + ammonia + hydrogen systems. Lehrer, who also used the dynamic method of equilibration, investigated the equilibria involving the gamma phase in addition to those studied by Emmett and his coworkers. Further, Lehrer's investigations covered the temperature range of 345 to 744° C, while Emmett and his coworkers limited their work to the range of 400 to 575° C. The results of these two independent investigations by Emmett and his coworkers[32,42], and by Lehrer[43] are in good agreement with each other, and thus appear to be quite reliable.

Kelley[44] has computed the thermodynamic functions of the gamma-prime and epsilon phases from the data of Satoh[38,40], Noyes and Smith[41], Emmett and his associates[32,42], and Lehrer[43]. Kelley's computations involve the questionable data of Satoh's[38] specific heat measurements. Therefore his equations cannot be used with certainty at temperatures beyond the range investigated by Lehrer - 345 to 744° C.

B. The Alpha-Gamma Equilibrium

Zener[45] has recently proposed a thermodynamic method* of

---

* A detailed derivation of the formulae suggested by Zener, and a criticism of the assumptions involved are presented in Appendix IV.

studying the phase relationships in medium alloy steels. Though his treatment was mainly concerned with iron-carbon-alloy systems, it can be applied to the iron-nitrogen system as the basis of his method is quite general.

The composition of the alpha and gamma phases in mutual equilibrium obey the fundamental laws of thermodynamics. Zener has suggested the following relationships:

$$\frac{C_j^{\alpha}}{C_j^{\gamma}} = \frac{\beta^{\alpha}}{\beta^{\gamma}} \cdot e^{\Delta F_j^{\circ}/RT} \qquad (6)$$

and

$$C_j^{\alpha} - C_j^{\gamma} = \Delta F_{Fe}^{\circ}/RT \qquad (7)$$

where:

C_j^{α} = Mol fraction of element j in the alpha phase

C_j^{γ} = Mol fraction of element j in the gamma phase

β^{α} = Ratio of interstitial positions to number of lattice atoms in the alpha phase.

β^{γ} = Ratio of interstitial positions to number of lattice atoms in the gamma phase.

ΔF_j° = Standard free energy change associated with the transfer of one mole of element j from the alpha to the gamma phase.

ΔF_{Fe}° = Standard free energy change associated with the transfer of one mole of iron from the alpha to the gamma phase.

R = Gas constant

T = Absolute temperature

The quantities β^{γ} and β^{α} can be easily evaluated for the iron-nitrogen system. In the face-centered cubic gamma phase, there are four atoms of iron and four possible interstitial positions (in the center of each edge, and the center of the cube) per unit cell, with the result that β^{γ} is unity. In the body-centered alpha phase, there are two atoms of iron and six possible interstitial positions (the center of each face and the center of each edge) per unit cell. Thus β^{α} is three.

Substituting these values for β^{γ} and β^{α} respectively, and solving the two equations (6 and 7) simultaneously, one obtains:

$$C_j^{\alpha} = \frac{\Delta F^{\circ}_{Fe}/RT}{1 - \frac{1}{3}\, e^{-\Delta F^{\circ}_j/RT}} \tag{8}$$

$$C_j^{\gamma} = \frac{\Delta F^{\circ}_{Fe}/RT}{1 - 3e^{\Delta F^{\circ}_j/RT}} \tag{9}$$

To solve for the compositions C_N^{α} and C_N^{γ} of the alpha and gamma phases in mutual equilibrium in the iron-nitrogen system, it is necessary to know the values of ΔF°_{Fe} and ΔF°_N.

ΔF°_N is computed from equation (6) and the compositions of the alpha and gamma phases at the eutectoid temperature. These are 0.10 and 2.35 percent nitrogen by weight as determined in this investigation. Then

At 590° C (863° K) $\quad C_N^{\alpha} = 0.003975$

$\qquad\qquad\qquad\quad C_N^{\gamma} = 0.08755$

and

$$\Delta F^{\circ}_N = R \times T \times \ln \frac{C_N^{\alpha}}{3\, C_N^{\gamma}}$$

or

$$\Delta F_N^o = -7186 \text{ calories per mole} \qquad (10)$$

ΔF_N^o is assumed to remain constant at temperatures between 1500 to 590° C. The value of ΔF_N^o given in equation (10) and the known values of ΔF_{Fe}^o [46] were used in equations (8) and (9) to compute the compositions of the alpha and gamma phases in mutual equilibrium. The results are presented in Table VII. Experimentally determined values are included in the same table for the sake of comparison.

Figure 14 shows the computed composition of the alpha and gamma phases in mutual equilibrium. The experimentally determined values are also shown in this plot. It can be seen from this diagram that there is good agreement between theory and experiment. However, the number of experimental points being limited, no definite conclusions can be drawn regarding the propriety of the assumptions involved in the theoretical calculations.

C. The Fugacities of Nitrogen at the Gamma Phase Boundaries

As already pointed out, it is quite important to study the effect of pressure on the phase relationships in the iron-nitrogen system. Instead of calculating the pressure component of the equilibrium diagram, the following treatment is based on the calculations of fugacity. Fugacity is expressed in the conventional units of number of atmospheres of nitrogen.

The calculation of fugacity in the gamma phase is based on the known solubility of nitrogen at atmospheric pressure, and the

TABLE VII

Alpha-Gamma Equilibrium

(Nitrogen, Weight Percent)

Temperature °C	Alpha Phase	Gamma Phase
	Calculated Experimental.	Calculated Experimental.
1500	+0.081	+0.21
1400	0.000	0.000
1350	-0.024	-0.075
1300	-0.038	-0.127
1250	-0.049	-0.180
1200	-0.053	-0.207
1150	-0.051	-0.217
1100	-0.043	-0.213
1050	-0.036	-0.190
1000	-0.024	-0.140
950	-0.011	-0.075
910	0.000	0.000
850	+0.020	+0.177
800	+0.037	+0.398
750	+0.059	+0.750
700	+0.074, 0.070	+1.17
675	+0.081	+1.41, 1.40
650	+0.088, 0.086	+1.67, 1.64
600	+0.098	+2.18
590(eutectoid) (temperature)	+0.10, 0.10	+2.35, 2.35

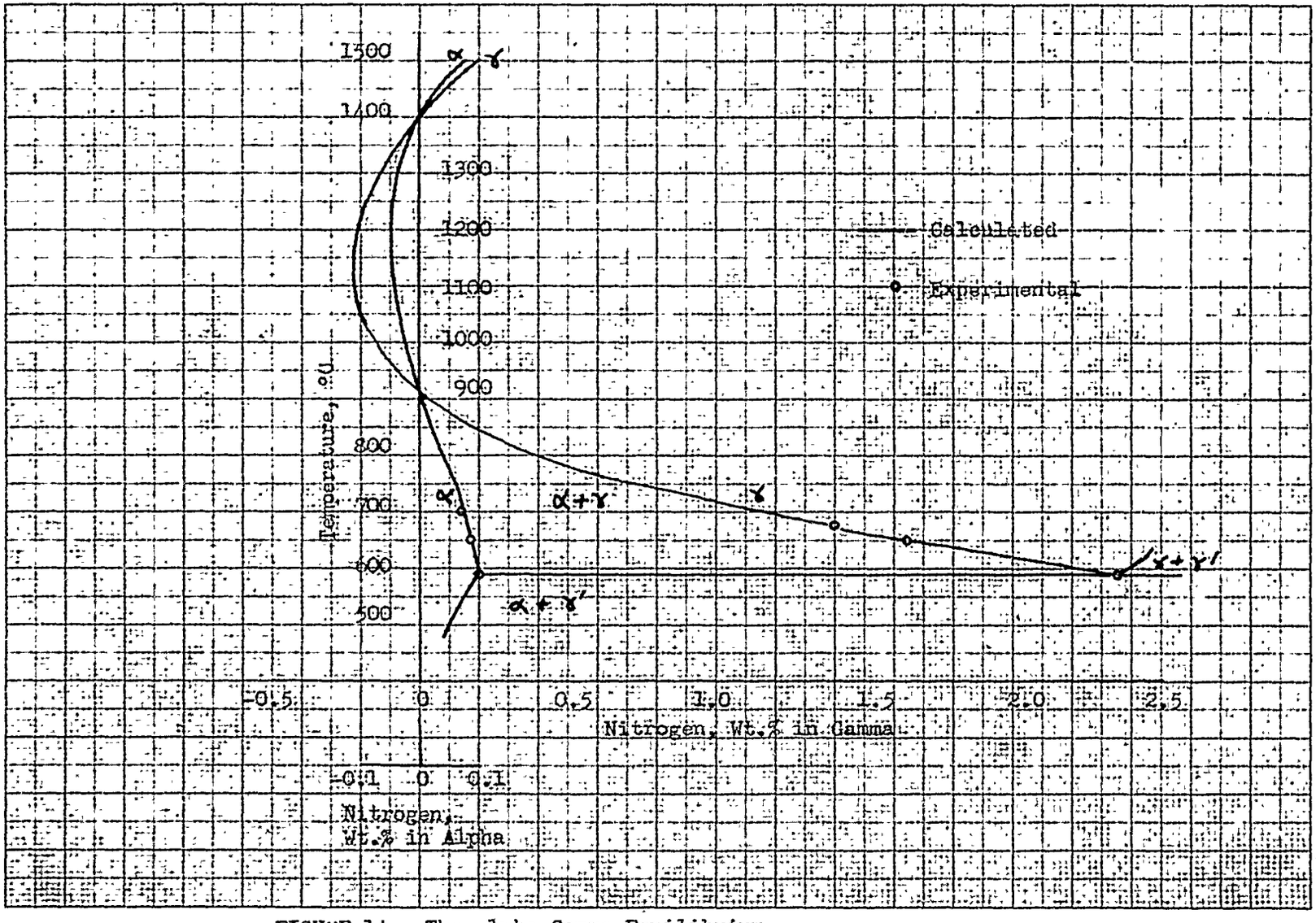

FIGURE 14. The Alpha-Gamma Equilibrium.

homogeneity limits of the austenite field determined in this investigation.

The solubility of nitrogen in pure iron has been measured by Iwase[47], Hayasi[48], Sieverts and his coworkers[49,50], and by Martin[51]. The experimental methods used by Iwase and Hayasi were not very good, and their results are therefore of questionable value. Sieverts and his coworkers, and Martin used the conventional Sievert's type of apparatus for measuring the solubility of nitrogen, and the results of these investigations are in fair agreement. Martin's experimental techniques were superior to those used by Sieverts and therefore his results are used in the following calculations.

Figure 15 shows the solubility of nitrogen in gamma iron under atmospheric pressure of nitrogen, based on Martin's data. The solubility at temperatures from 590° C to 900° C is determined by extrapolating Martin's data. Table VIII shows the results of this extrapolation.

The solution of nitrogen in gamma iron obeys Sievert's Law,

$$\text{Weight percent nitrogen in austenite} = K_T^{\gamma}\sqrt{p_{N_2}} \qquad (11)$$

where K_T^{γ} is the solubility in weight percent at atmospheric pressure of nitrogen, and p_{N_2} is the pressure of nitrogen in atmospheres. The use of fugacity (f_{N_2}) instead of pressure (p_{N_2}) enables one to use this relationship to high values of fugacity where nitrogen would ordinarily deviate from the ideal gas law. It is further assumed the activity of nitrogen dissolved in the austenite phase can be correctly represented by its weight percent.

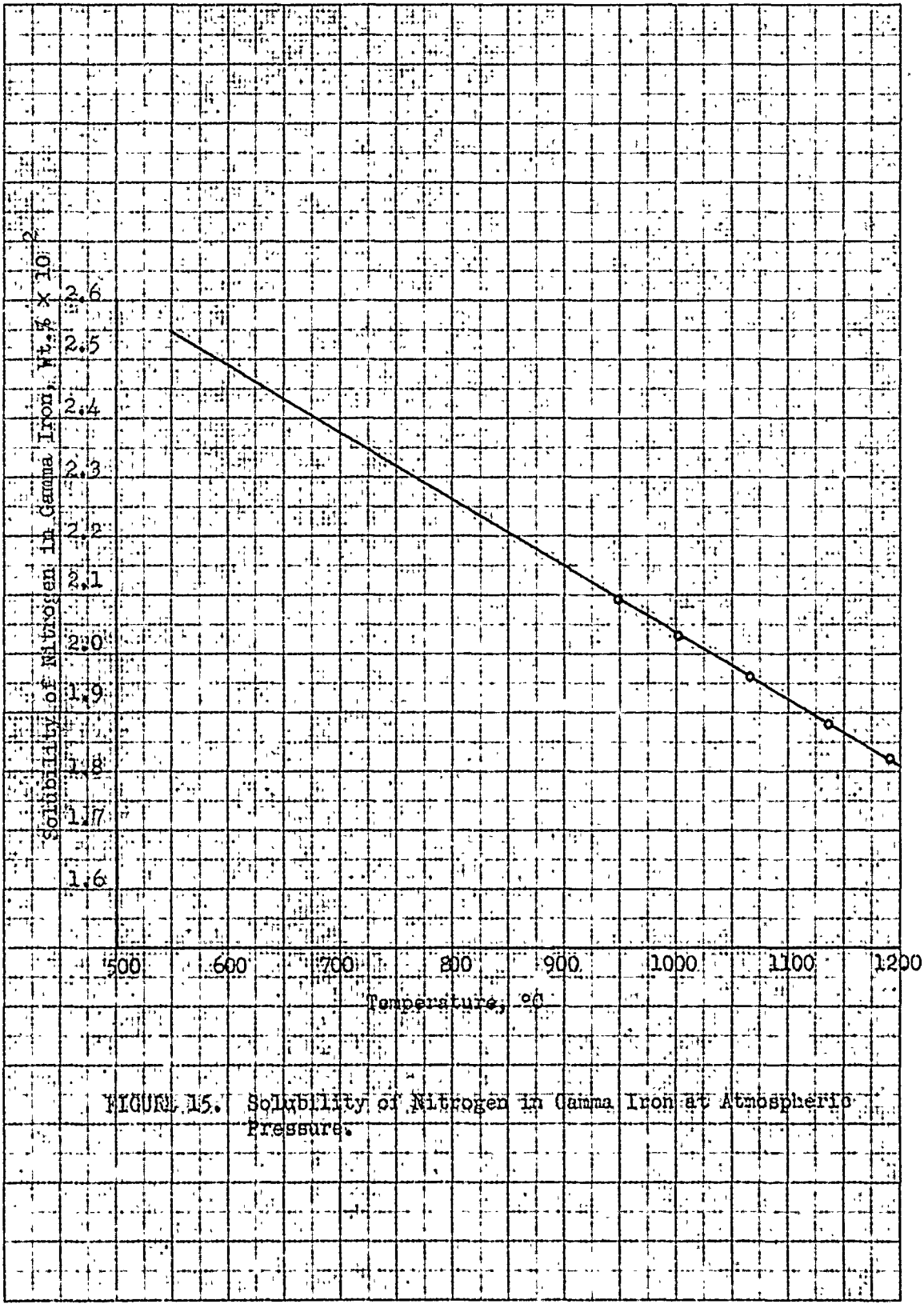

FIGURE 15. Solubility of Nitrogen in Gamma Iron at Atmospheric Pressure.

TABLE VIII

Solubility of Nitrogen in Gamma Iron

Under Atmospheric Pressure

Temperature °C	Solubility or K_T^{γ} (Nitrogen, Weight Percent)
1191	1.82×10^{-2} (Martin)
1135	1.88×10^{-2} (Martin)
1065	1.96×10^{-2} (Martin)
1000	2.03×10^{-2} (Martin)
946	2.09×10^{-2} (Martin)
900	$2.14_3 \times 10^{-2}$ (Extrapolated)
850	$2.20_0 \times 10^{-2}$ (Extrapolated)
800	$2.25_6 \times 10^{-2}$ (Extrapolated)
750	$2.31_1 \times 10^{-2}$ (Extrapolated)
700	$2.36_9 \times 10^{-2}$ (Extrapolated)
675	$2.39_7 \times 10^{-2}$ (Extrapolated)
650	$2.42_6 \times 10^{-2}$ (Extrapolated)
625	$2.45_1 \times 10^{-2}$ (Extrapolated)
590	$2.49_2 \times 10^{-2}$ (Extrapolated)

Since K_T^{γ} is equal to the solubility of nitrogen at atmospheric pressure (fugacity of one atmosphere), the solubilities listed in Table VIII represent the values of K_T^{γ}.

Now the fugacity of nitrogen can be computed from the relationship

$$f_{N_2} = \left(\frac{\text{weight percent nitrogen}}{K_T^{\gamma}}\right)^2 \qquad (12)$$

Table IX shows the values of the fugacity of nitrogen corresponding to the homogeneity limits of the austenite field. The upper homogeneity limits of the gamma field were based on experimental data obtained in this investigation. The compositions at the lower limit of the austenite field were obtained by applying Zener's method discussed earlier, together with the present experimental data.

D. The Fugacity of Nitrogen at the Alpha Phase Boundary

Above the eutectoid temperature (590° C), the alpha phase exists in equilibrium with the gamma phase. The fugacity of nitrogen at the solubility limit of the alpha phase is therefore equal to that calculated for the lower limit of the austenite field at the same temperature. This is shown in Table IX.

Below the eutectoid temperature the alpha phase exists in equilibrium with the gamma prime phase. The fugacity of nitrogen corresponding to the ferrite solubility limit can therefore be calculated from the equilibrium constant of the reaction.

$$\gamma' = \alpha + N_2 \text{ (gas)} \qquad (13)$$

TABLE IX

Fugacity of Nitrogen at the Phase Boundaries in the Iron-Nitrogen System

Temperature °C	Fugacity of Nitrogen, in Atmospheres Phase Equilibria					
	$\alpha+\gamma'$	$\alpha+\gamma$	$\gamma+\gamma'$	$\gamma+\varepsilon$ low nitrogen	$\gamma'+\varepsilon$ low nitrogen	$\gamma'+\varepsilon$ high nitrogen
850		64.7				
800		311.2				
750		1053				
700		2439		12990		
675		3411		13160	26540	34570
650		4682	13320	13320	13320	42360
				($\gamma-\varepsilon-\gamma'$ eutectoid)		
625		6067	11600			52550
590	8479*	9100*	9100*			42230
	($\alpha-\gamma-\gamma'$ eutectoid)					
550	6668					40930
500	4893					35920
450	3553					28920

* The value of 9100 is based on the extrapolation of Martin's[51] data, and is discarded in favor of the value of 8479 based on equilibrium measurements. Rounding off the last two figures, the fugacity of nitrogen at the $\alpha-\gamma-\gamma'$ eutectoid temperature is taken to be 8500 atmospheres.

The equilibrium constant, K_1, of this reaction is

$$K_1 = \frac{a_\alpha \times f_{N_2}}{a_{\gamma'}} \qquad (14)$$

where a_α and $a_{\gamma'}$ are the activities of alpha and gamma-prime phases respectively. Assuming that the alpha phase is almost pure iron and that the gamma-prime phase is pure, the following simplified relationship is obtained.

$$K_1 = f_{N_2} = e^{-\Delta F_1^\circ/RT} \qquad (15)$$

The standard free energy change, F°, of reaction (13) obtained from Kelley's[44] work is as follows:

$$\Delta F^\circ = 7720 + 32.56T \log T - 17.86 \times 10^{-3} T^2 - 107.10T \qquad (16)$$

The fugacity of nitrogen is obtained by solving equation (15) and (16). The values thus obtained correspond to the fugacity of nitrogen at the solubility limit of nitrogen-ferrite and the corresponding lower limit of the gamma-prime phase (Table IX).

The calculation of the fugacity of nitrogen at the eutectoid temperature is quite important. The value based on the alpha-gamma-prime equilibrium is 8479 atmospheres, which compares favorably with the value of 9100 atmospheres obtained from the solubility relationships in the austenite field. The first value is more accurate, since it is based on reliable equilibrium data, while the latter involves an extrapolation of Martin's[51] results. Rounding off the last two digits, the fugacity of nitrogen at the eutectoid temperature (590° C) is taken to be 8500 atmospheres.

E. The Solubility of Nitrogen in Ferrite

The fugacity of nitrogen at the ferrite solubility limit listed in Table IX can be used to calculate the solubility of nitrogen in alpha iron at atmospheric pressure. The relationship

$$\text{Weight percent nitrogen in alpha iron} = K_T \times \sqrt{f_{N_2}} \qquad (17)$$

expresses the Sieverts Law for the alpha phase. As already pointed out K_T is equal to the solubility of nitrogen at a temperature T under one atmosphere pressure of nitrogen. Equation (17) may be rewritten as follows:

$$K_T = \frac{\text{Weight percent nitrogen in alpha iron}}{\sqrt{f_{N_2}}} \qquad (18)$$

The solubility of nitrogen in alpha iron was calculated from the ferrite solubility limit and the corresponding values of f_{N_2}. The results are listed in Table X, converted to the more conventional units of milligrams of nitrogen per hundred grams of iron.

The solubility of nitrogen in alpha iron has been measured by Iwase[47], Hayasi[48] and by Sieverts and his associates[49]. The results of these investigators are included in Table X for the sake of comparison. It can be seen from Table X that the theoretically calculated values shown in the last column are consistent with the experimental determinations considering the uncertainty of the latter.

TABLE X

Solubility of Nitrogen in Alpha Iron at One Atmosphere of Pressure

Temperature ° C	Solubility in Mg. of Nitrogen/100 gms. of Fe Experimentally Determined			
	Iwase	Hayasi	Sieverts and his coworkers	Calculated in this investigation
890	-	-	1.15 - 18.4	-
880	-	<0.04	0.92 - 2.69	-
852	2.2	-	-	-
850	-	-	0.35 - 2.27	2.48_5
800	-	-	0.10 - 2.00	2.09_2
770	-	0	-	-
750	-	-	0.07 - 0.48	1.78_6
722	2.1	-	-	-
700	-	-	-	1.49_8
675	-	-	-	1.37_0
650	-	-	-	1.27_2
625	-	-	-	1.19_4
622	1.3	-	-	-
590	-	-	-	1.08_6
550	-	-	-	0.85_7
500	-	-	-	0.71_5
450	-	-	-	0.55_4

F. The Fugacity of Nitrogen at the Epsilon Phase Boundary

The epsilon phase exists in equilibrium with nitrogen-austenite at temperatures above 650° C. Thus the fugacity of nitrogen at the epsilon phase boundary is the same as that at the upper homogeneity limit of the gamma phase. Table IX shows the values of the fugacity of nitrogen at the gamma-epsilon phase boundary.

The calculation of the fugacity of nitrogen at the gamma-prime epsilon boundary is based on the following reaction

$$\varepsilon = \alpha + 2N_2 \text{ (gas)} \qquad (19)$$

The equilibrium constant, K_2, for this reaction is

$$K_2 = \frac{a_\alpha \times f_{N_2}^2}{a_\varepsilon} \qquad (20)$$

where a_α and a_ε are the activities of the alpha and epsilon phases respectively. Assuming that the alpha phase is almost pure iron, and that the activity of the epsilon phase at the phase boundary is unity, the following equation is obtained

$$K_2 = f_{N_2}^2 \qquad (21)$$

In order to calculate K_2, the reaction (19) may be split up into the following reactions.

$$\varepsilon + 3H_2(\text{gas}) = \gamma' + 2NH_3(\text{gas}) \quad --K_3 \qquad (22)$$

$$2NH\ (\text{gas}) = 3H_2(\text{gas}) + N_2(\text{gas}) \quad --K_4 \qquad (23)$$

and

$$\gamma' = \alpha + N_2(\text{gas}) \quad --K_1$$

where the last reaction is the same as that expressed by equation (13).

It is evident that the equilibrium constants of these reactions are related to K_2 as follows

$$K_2 = K_3 \times K_4 \times K_1 \tag{24}$$

The equilibrium constant $K_3 = (p^2_{NH_3}/p^3_{H_2})$ has been determined by Lehrer[43]. The value of K_4 can be evaluated by using the relationship

$$K_4 = e^{-\Delta F^\circ_4/RT} \tag{25}$$

where ΔF°_4 is the standard free energy change for the reaction (23). Kelley[44] has given the following equation for computing ΔF°_4.

$$\Delta F^\circ_4 = 19120 - 27.92T \log T + 4.38 \times 10^{-3} T^2 - 0.398 \times 10^5 T^{-1} + 30.78T \tag{26}$$

The method of calculating the value of K_1 has been described previously.

The values of K_3, K_4 and K_1 thus obtained are used in computing the fugacity of nitrogen at the epsilon-gamma-prime phase boundary. The results of these calculations are shown in Table IX.

G. The Fugacity-Temperature-Concentration Diagram

The true equilibrium relationships in the iron-nitrogen system can be shown in a three-dimensional fugacity-temperature-concentration diagram. Since this three-dimensional diagram is, however, quite complicated, no attempt is made to show it in perspective. Instead, several two-dimensional sections are presented.

It is important to note that the vapor pressure of iron is extremely small in comparison with that of nitrogen and it is

therefore neglected in calculating the effect of fugacity on the iron-nitrogen system.

Figure 16 shows the projection of the three-dimensional equilibrium diagram on the temperature-fugacity plane. This projection contains two quadruple points, 1 and 2. At the point 1 four phases exist in equilibrium: alpha, gamma, gamma-prime, and nitrogen gas. The point 2 represents a similar situation where gamma, gamma-prime, epsilon and nitrogen gas exist in equilibrium. It is possible to look upon point 3 as a degenerate quadruple point, which is due to the fact that the gamma-prime and epsilon phases have the same composition at this point. Due to this degeneracy there are only three three-phase lines meeting at this point.

Isothermal sections through the temperature-fugacity-concentration diagram are shown in Figure 17. These sections are drawn at 500, 590, 625, 650 and 675° C respectively* and are self-explanatory. The fugacity-concentration relationships in the alpha and gamma phase are based on the square root law of Sieverts. Table XI lists the nitrogen content of the alpha and gamma phases as a function of temperature and fugacity. These values are used in the isothermal sections in Figure 17. In drawing these sections, it is assumed that the concentration of the solid phases in mutual equilibrium (where no gas is present) is not changed by an increase in

---

* The sections are chosen below the lower eutectoid, at the lower eutectoid, between the lower and upper eutectoids, at the upper eutectoid, and above the upper eutectoid.

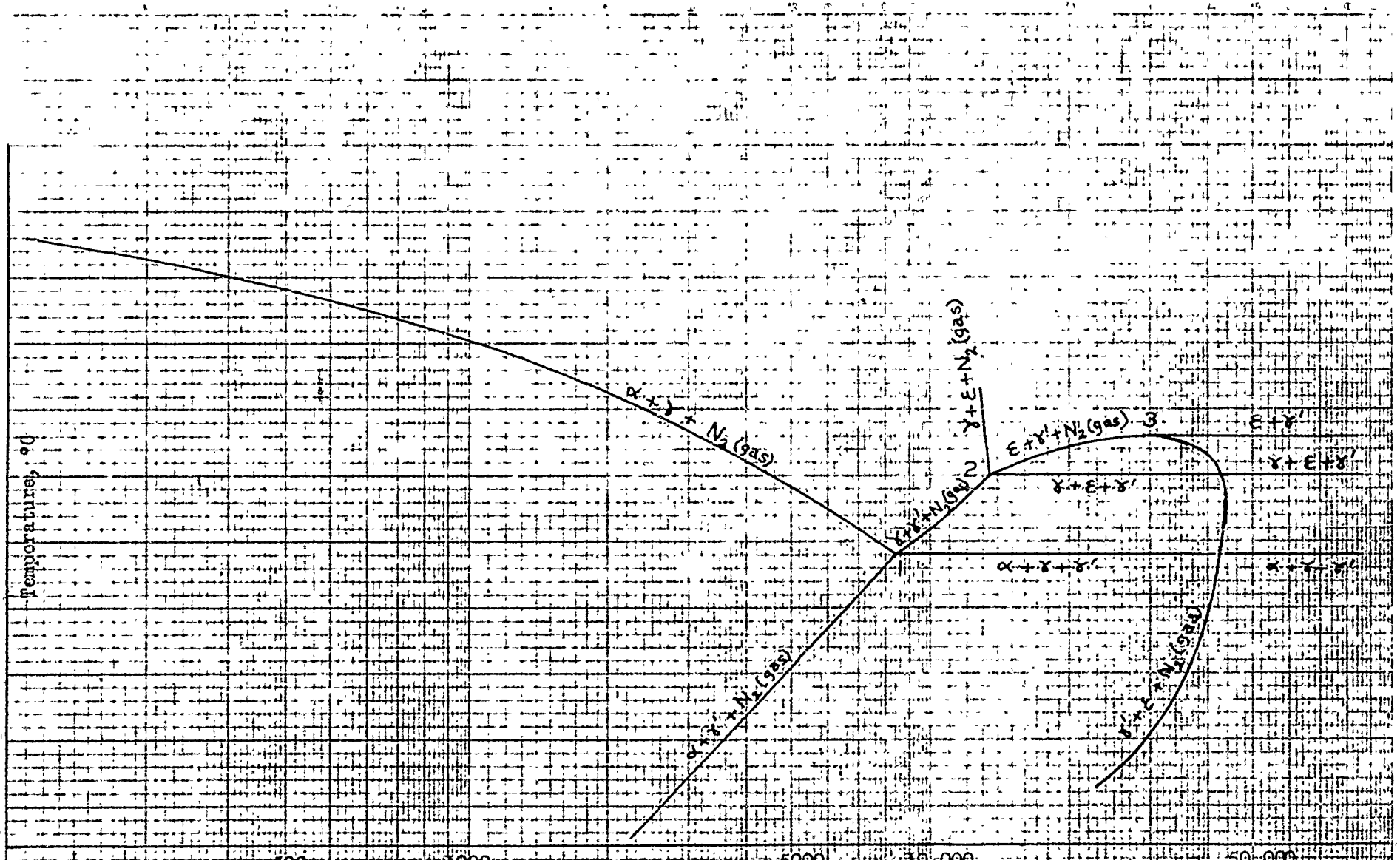

FIGURE 16. Projection of the Temperature-Fugacity-Concentration Diagram of the Iron-Nitrogen System on the Temperature-Fugacity Plane.

TABLE XI

The Composition of the Alpha and Gamma Phases as Affected by Temperature and Fugacity

Fugacity of Nitrogen in Atmospheres	Temperature °C 800	700	675	650	625	590	550	500	450
	(Nitrogen, Weight Percent)								
100	0.02 (α)	0.015 (α)	0.014 (α)	0.013 (α)	0.012 (α)	0.011 (α)	0.009 (α)	0.007 (α)	0.006 (α)
311.2	0.037 (α)	-	-	-	-	-	-	-	-
	0.398 (γ)	-	-	-	-	-	-	-	-
400	0.451 (γ)	0.030 (α)	0.027 (α)	0.025 (α)	0.024 (α)	0.022 (α)	0.017 (α)	0.014 (α)	0.011 (α)
900	0.677 (γ)	0.045 (α)	0.041 (α)	0.038 (α)	0.036 (α)	0.033 (α)	0.026 (α)	0.021 (α)	0.017 (α)
2439	-	0.074 (α)	-	-	-	-	-	-	-
	-	1.17 (γ)	-	-	-	-	-	-	-
2500	1.13 (γ)	1.18 (γ)	0.069 (α)	0.064 (α)	0.060 (α)	0.054 (α)	0.042 (α)	0.036 (α)	0.028 (α)
3411	-	-	0.080 (α)	-	-	-	-	-	-
	-	-	1.40 (γ)	-	-	-	-	-	-
3553	-	-	-	-	-	-	-	-	0.033 (α) (γ')
3600	1.35 (γ)	1.42 (γ)	1.44 (γ)	0.076 (α)	0.072 (α)	0.065 (α)	0.051 (α)	0.043 (α)	
4682	-	-	-	0.087 (α)	-	-	-	-	-
	-	-	-	1.66 (γ)	-	-	-	-	-
4893	-	-	-	-	-	-	-	0.050 (α) (γ')	
4900	1.58 (γ)	1.66 (γ)	1.68 (γ)	1.70 (γ)	0.084 (α)	0.076 (α)	0.060 (α)		
6067	-	-	-	-	0.093 (γ)	-	-		

Fugacity of Nitrogen in Atmospheres	Temperature °C 800	700	675	650	625	590	550	500	450
	(Nitrogen, Weight Percent)								
	-	-	-	-	1.91(٢)	-	-	-	
6400	1.80(٢)	1.90(٢)	1.92(٢)	1.94(٢)	1.96(٢)	0.087(٤)	0.068(٤)	-	
6668	-	-	-	-	-	-	0.070(٤) (٢')		
8100	2.03(٢)	2.13(٢)	2.16(٢)	2.18(٢)	2.21(٢)	0.098(٤)			
8500	-	-	-	-	-	0.100(٤)			
	-	-	-	-	-	2.35(٢)			
	-	-	-	-	-	(٢')			
9025	2.14(٢)	2.25(٢)	2.28(٢)	2.30(٢)	2.33(٢)				
10000	2.26(٢)	2.37(٢)	2.40(٢)	2.43(٢)	2.45(٢)				
11025	2.37(٢)	2.49(٢)	2.52(٢)	2.55(٢)	2.58(٢)				
11600	-	-	-	-	2.64(٢)				
	-	-	-	-	(٢')				
12100	2.48(٢)	2.61(٢)	2.64(٢)	2.67(٢)					
12990	-	2.70(٢)	-	-					
	-	(٣)	-	-					
13160	-	-	2.75(٢)	-					
	-	-	(٣)	-					
13320	-	-	-	2.80(٢)					
	-	-	-	(٢+٢')					

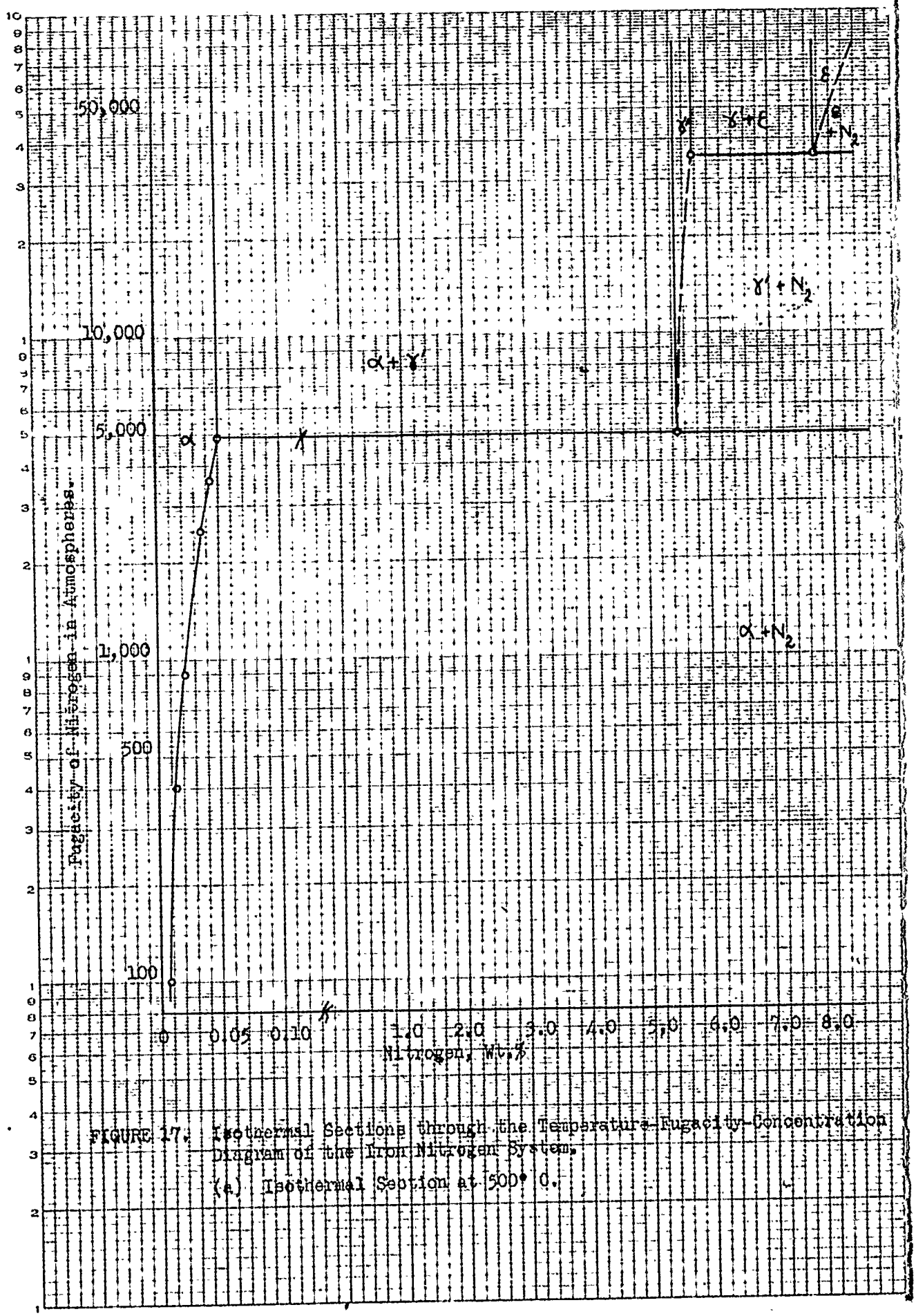

FIGURE 17. Isothermal Sections through the Temperature-Fugacity-Concentration Diagram of the Iron-Nitrogen System.

(a) Isothermal Section at 500° C.

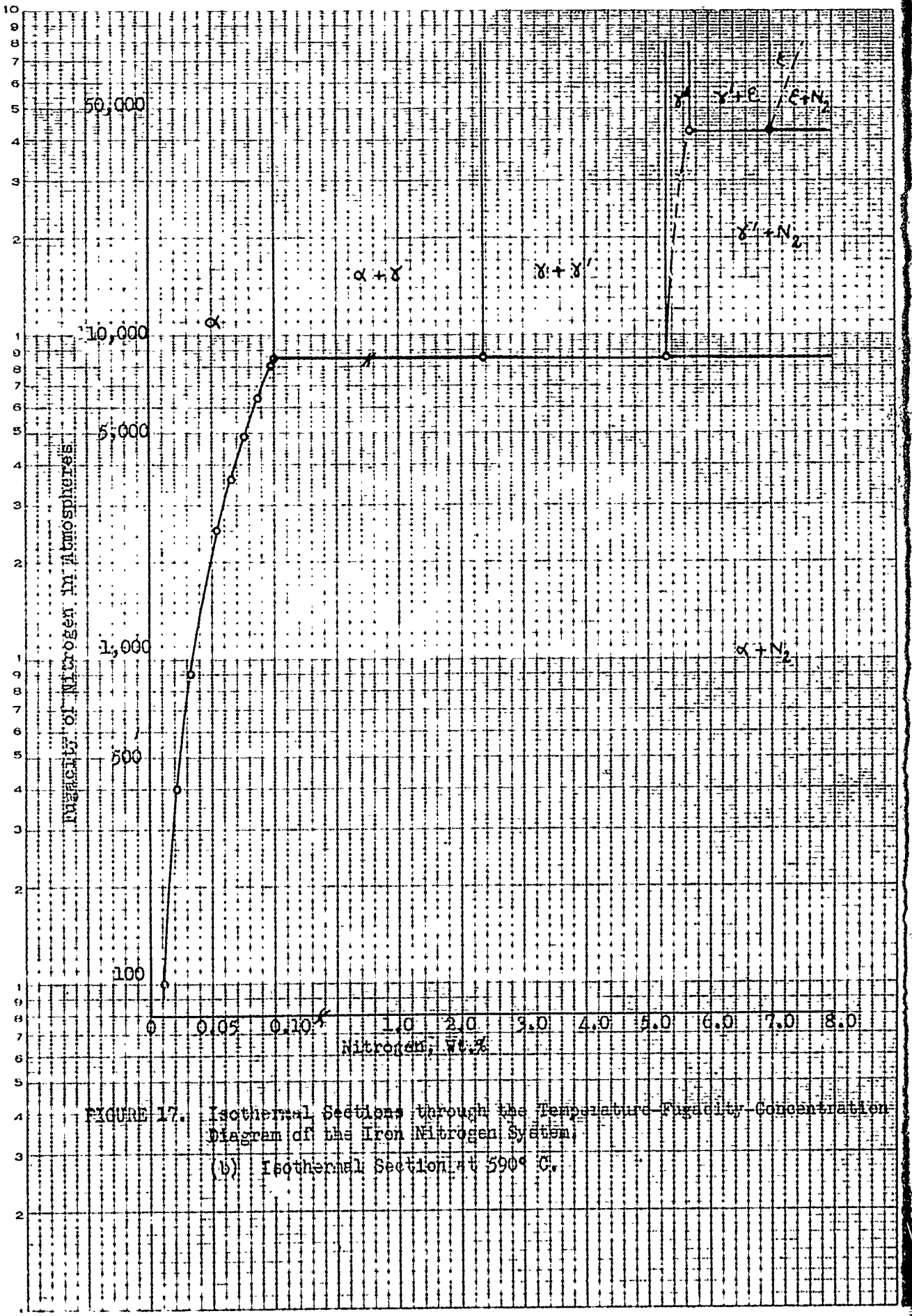

FIGURE 17. Isothermal Sections through the Temperature-Fugacity-Concentration Diagram of the Iron Nitrogen System.
(b) Isothermal Section at 590° C.

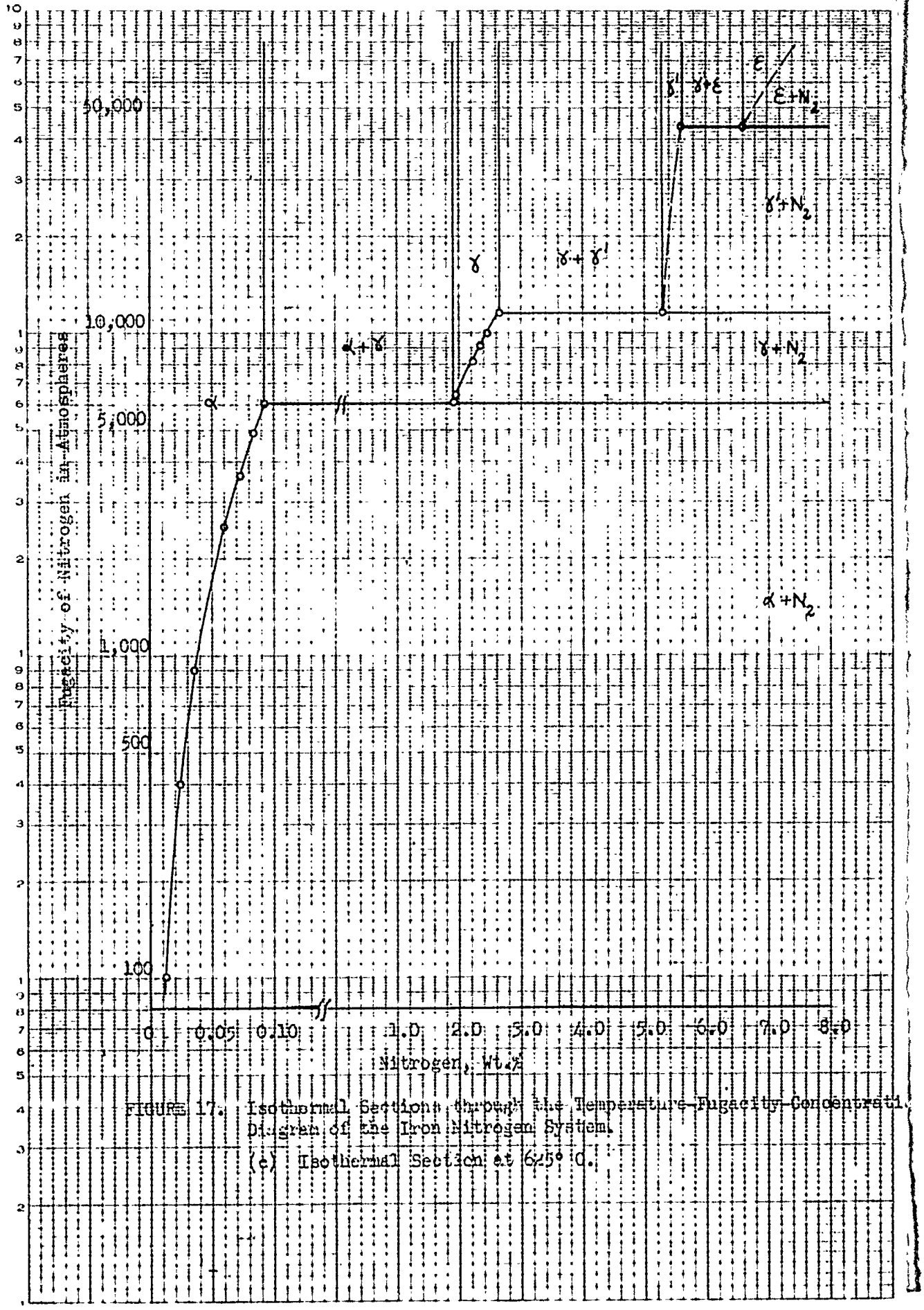

FIGURE 17. Isothermal Sections through the Temperature-Fugacity-Concentration Diagram of the Iron Nitrogen System.

(c) Isothermal Section at 625° C.

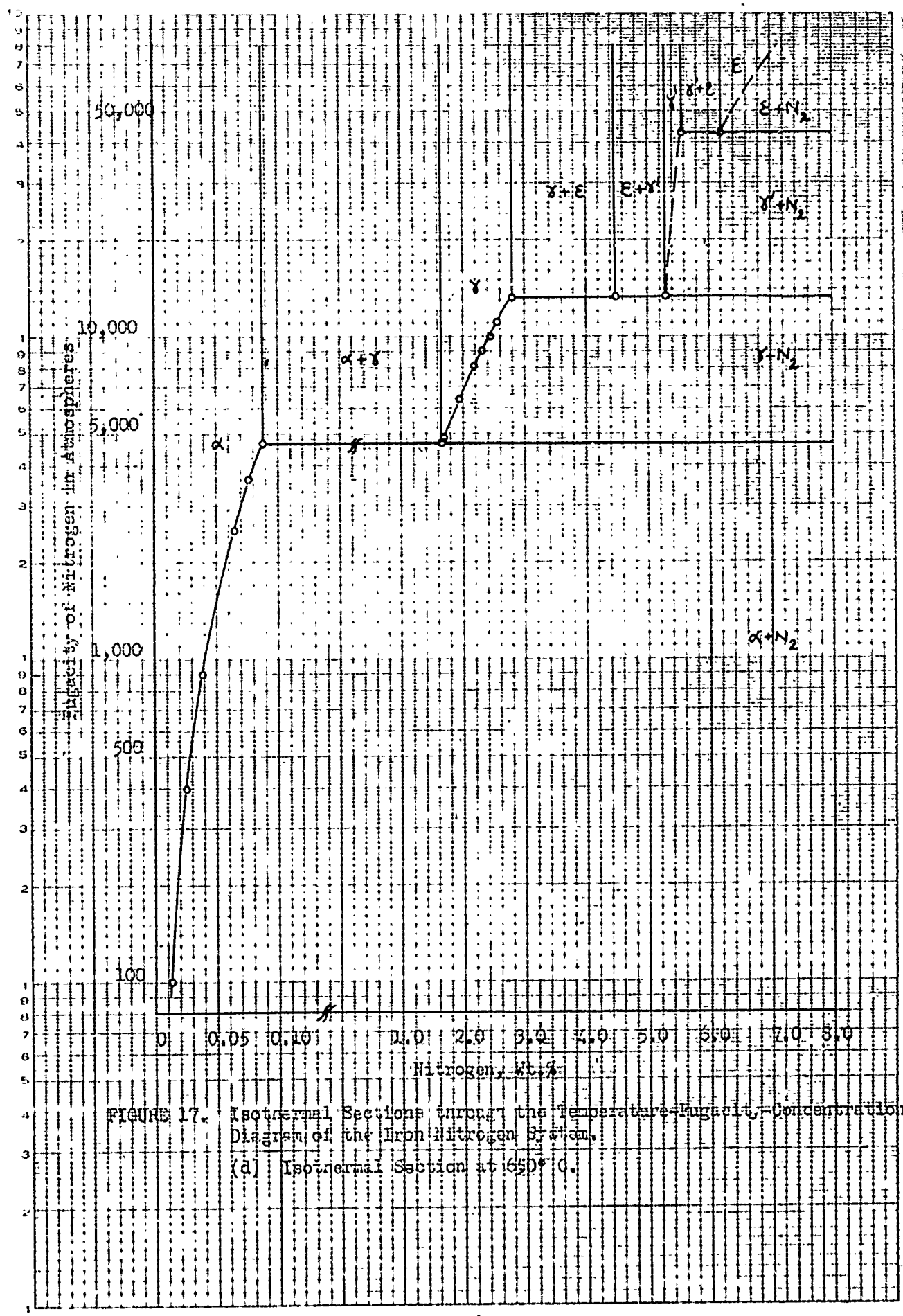

FIGURE 17. Isothermal Sections through the Temperature-Fugacity-Concentration Diagram of the Iron Nitrogen System.
(a) Isothermal Section at 650° C.

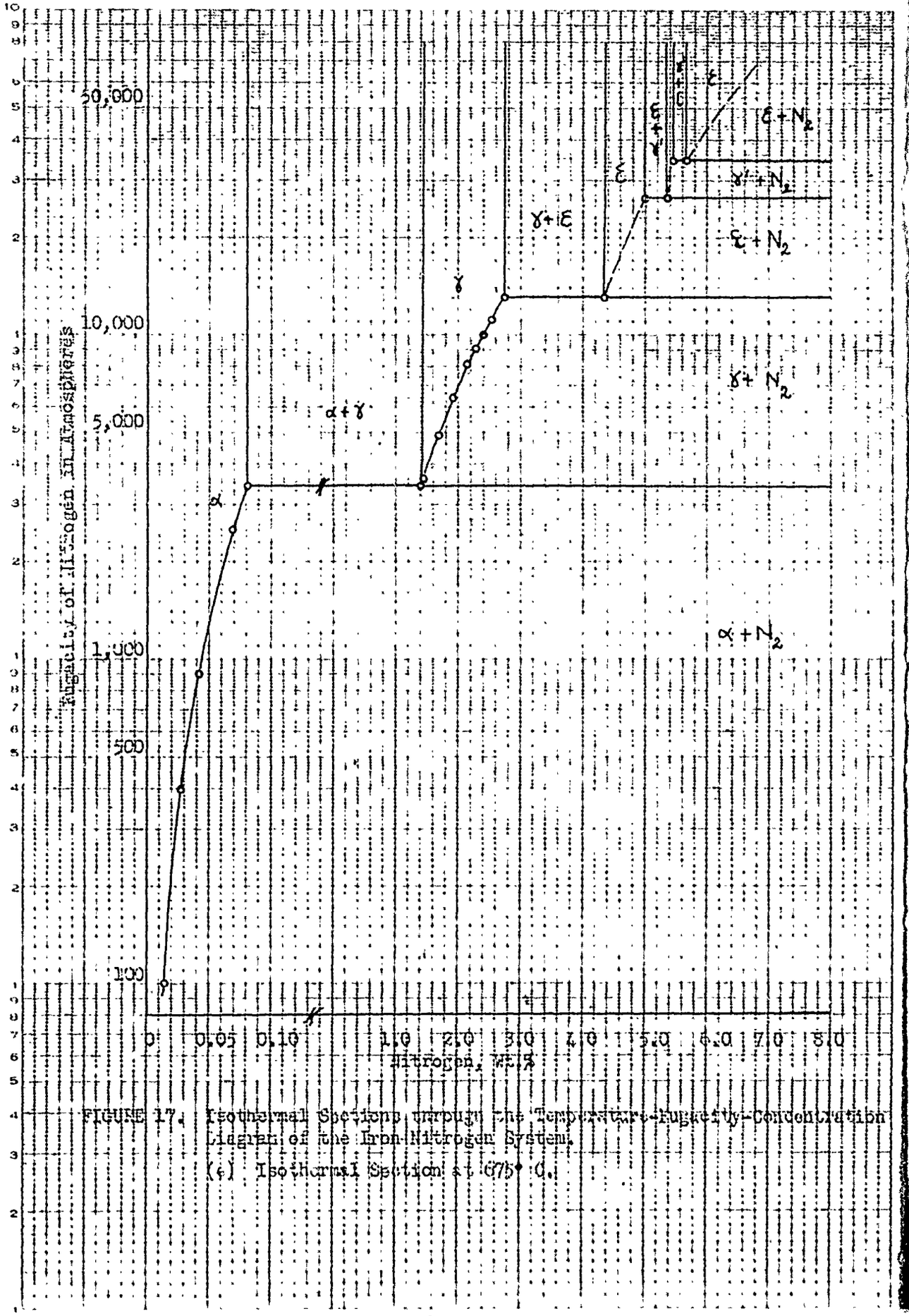

FIGURE 17. Isothermal Sections through the Temperature-Pressure-Composition Diagram of the Iron-Nitrogen System.
(c) Isothermal Section at 675° C.

the fugacity. The equilibrium relationship between nitrogen gas and the gamma-prime and epsilon phases are not known, and thus the boundaries between these phases are represented by dashed lines.

Figure 18 shows several iso-fugacity sections through the three-dimensional equilibrium diagram. These are constructed by combining the diagrams shown in Figures 16 and 17. Figure 18(a) shows a section at a fugacity of 1000 atmospheres of nitrogen, where one three-phase equilibrium is indicated among the phases alpha, gamma and nitrogen gas. A section at 5000 atmospheres (Figure 18(b)) contains two three-phase equilibria: alpha + gamma + nitrogen gas; and alpha + gamma prime + nitrogen gas. The temperatures of these three-phase reactions change progressively with increasing fugacity, until they coincide (Figure 18(c)) to give a four-phase equilibrium at a fugacity of 8500 atmospheres of nitrogen, which represents the quadruple point 1 in Figure 16. Figure 18(d), representing an iso-fugacity section at 10,000 atmospheres of nitrogen, shows two three-phase reactions: alpha - gamma - gamma prime and gamma - gamma prime - nitrogen gas. The low nitrogen epsilon phase appears in Figure 18(e), which is an iso-fugacity section through the quadruple point 2 in Figure 16. This section exhibits four-fold equilibrium among the gamma, epsilon, gamma-prime and gas (nitrogen) phases. The three-phase equilibrium among the epsilon, gamma-prime and nitrogen gas occurs at progressively higher temperatures as the fugacity is increased (20,000 atmosphere section in Figure (f)). The highest

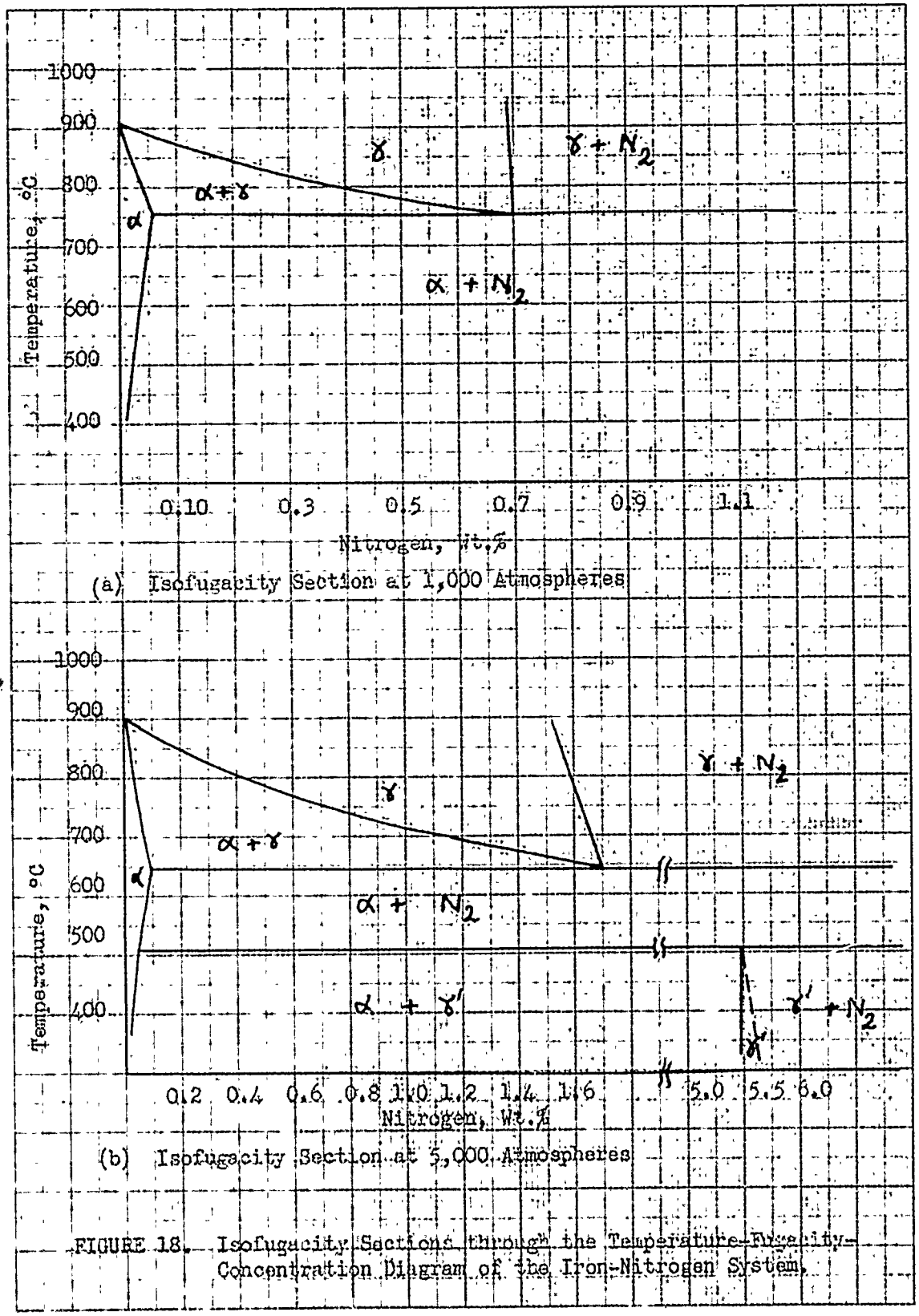

FIGURE 18. Isofugacity Sections through the Temperature-Fugacity-Concentration Diagram of the Iron-Nitrogen System.

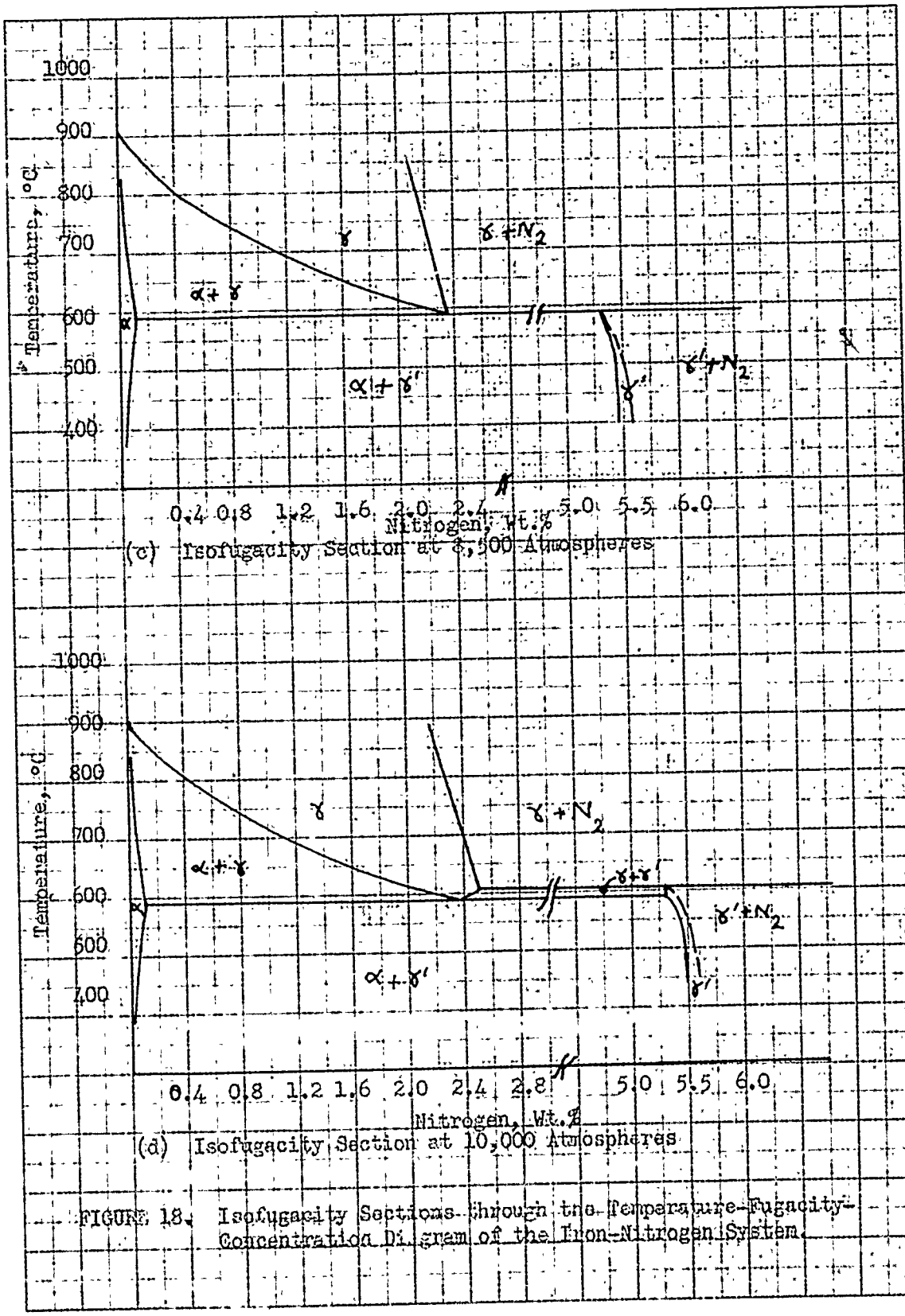

(c) Isofugacity Section at 8,500 Atmospheres

(d) Isofugacity Section at 10,000 Atmospheres

FIGURE 18. Isofugacity Sections through the Temperature-Fugacity-Concentration Diagram of the Iron-Nitrogen System.

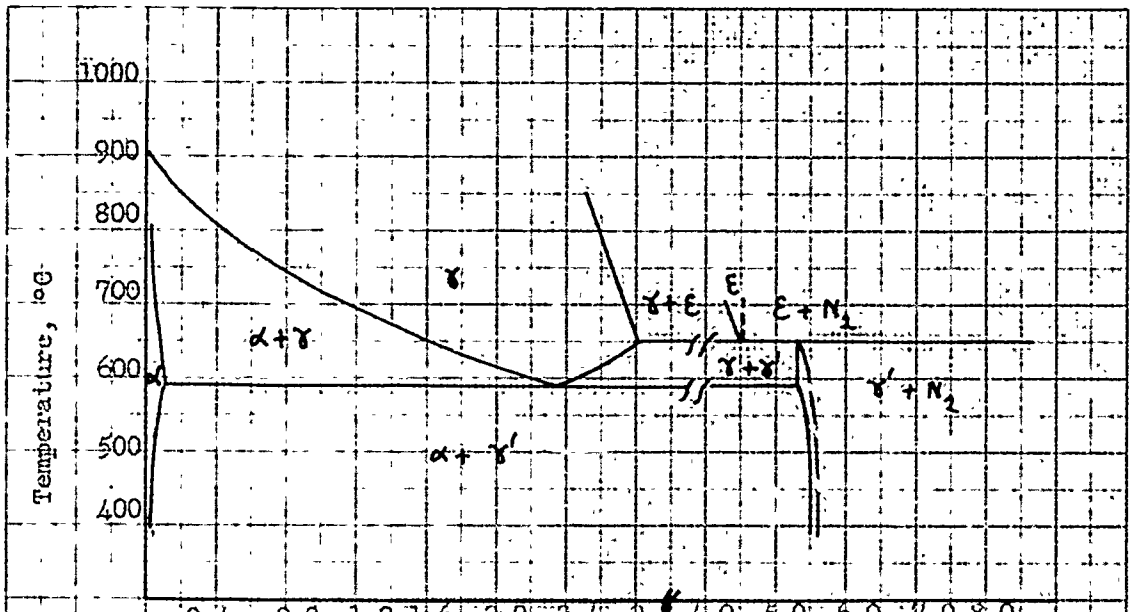

(e) Isofugacity Section at 13,320 Atmospheres.

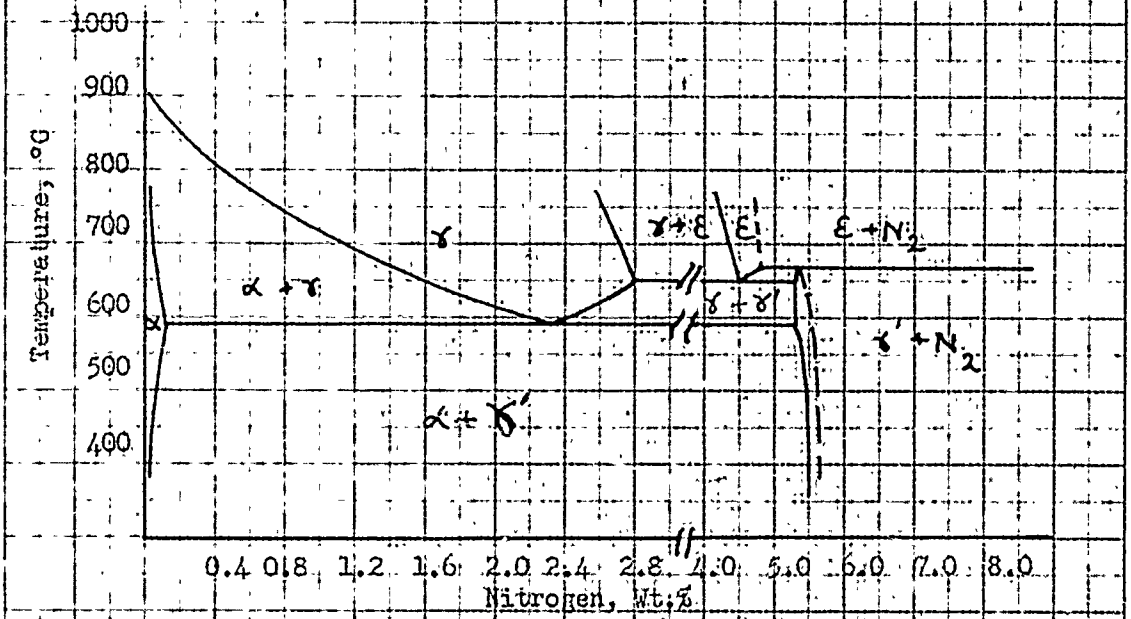

(f) Isofugacity Section at 20,000 Atmospheres.

FIGURE 18. Isofugacity Sections through the Temperature-Fugacity-Concentration Diagram of the Iron-Nitrogen System.

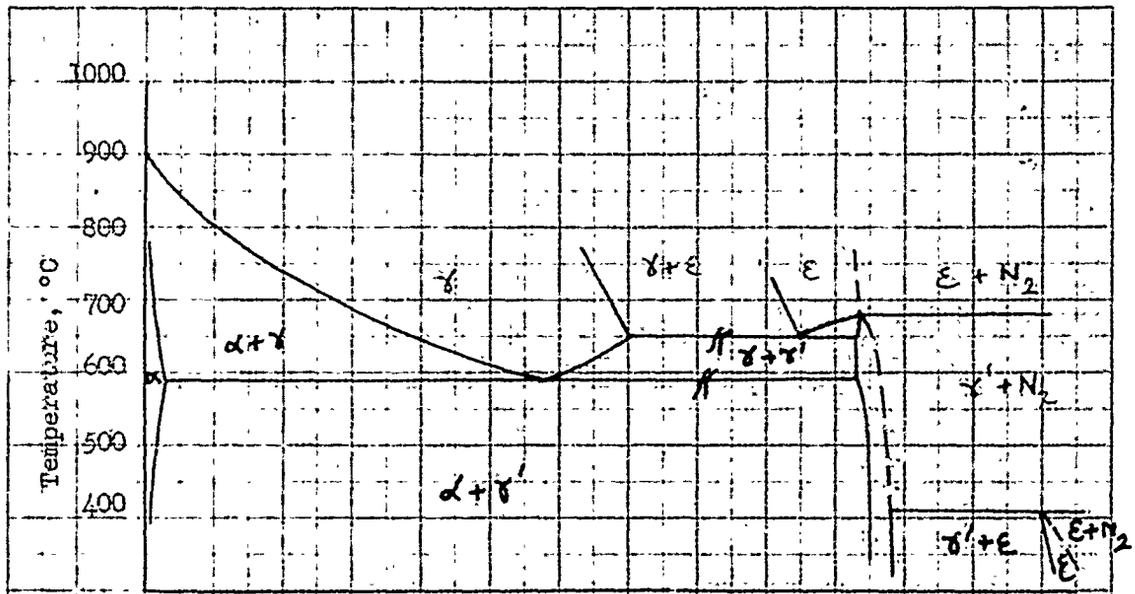

(g) Isofugacity Section at 30,000 Atmospheres.

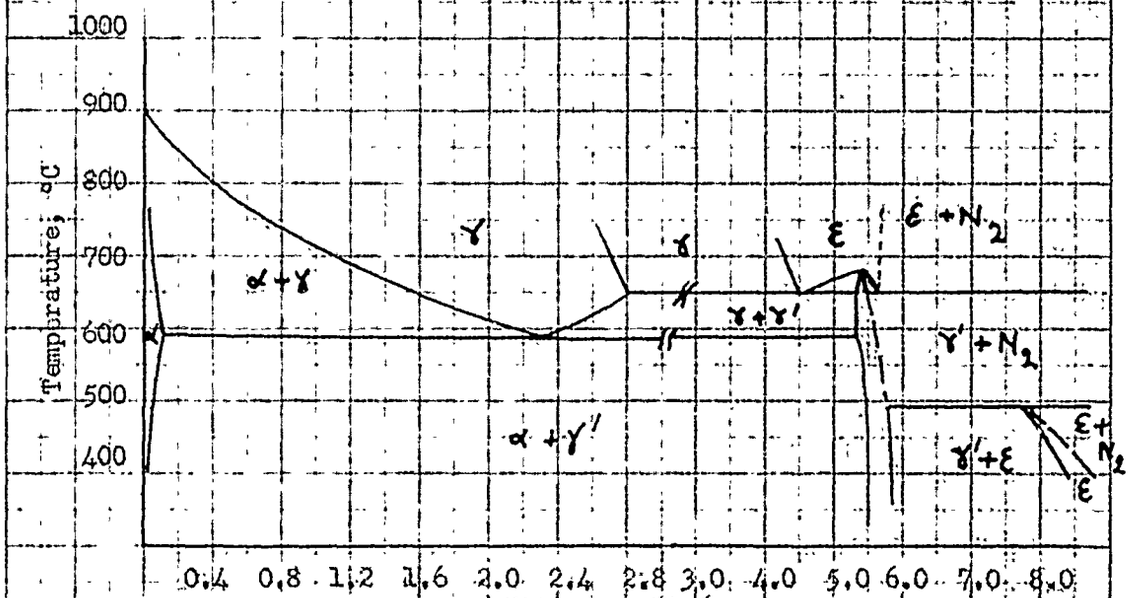

(h) Isofugacity Section at 35,000 Atmospheres

FIGURE 18. Isofugacity Sections through the Temperature-Fugacity-Concentration Diagram of the Iron-Nitrogen System.

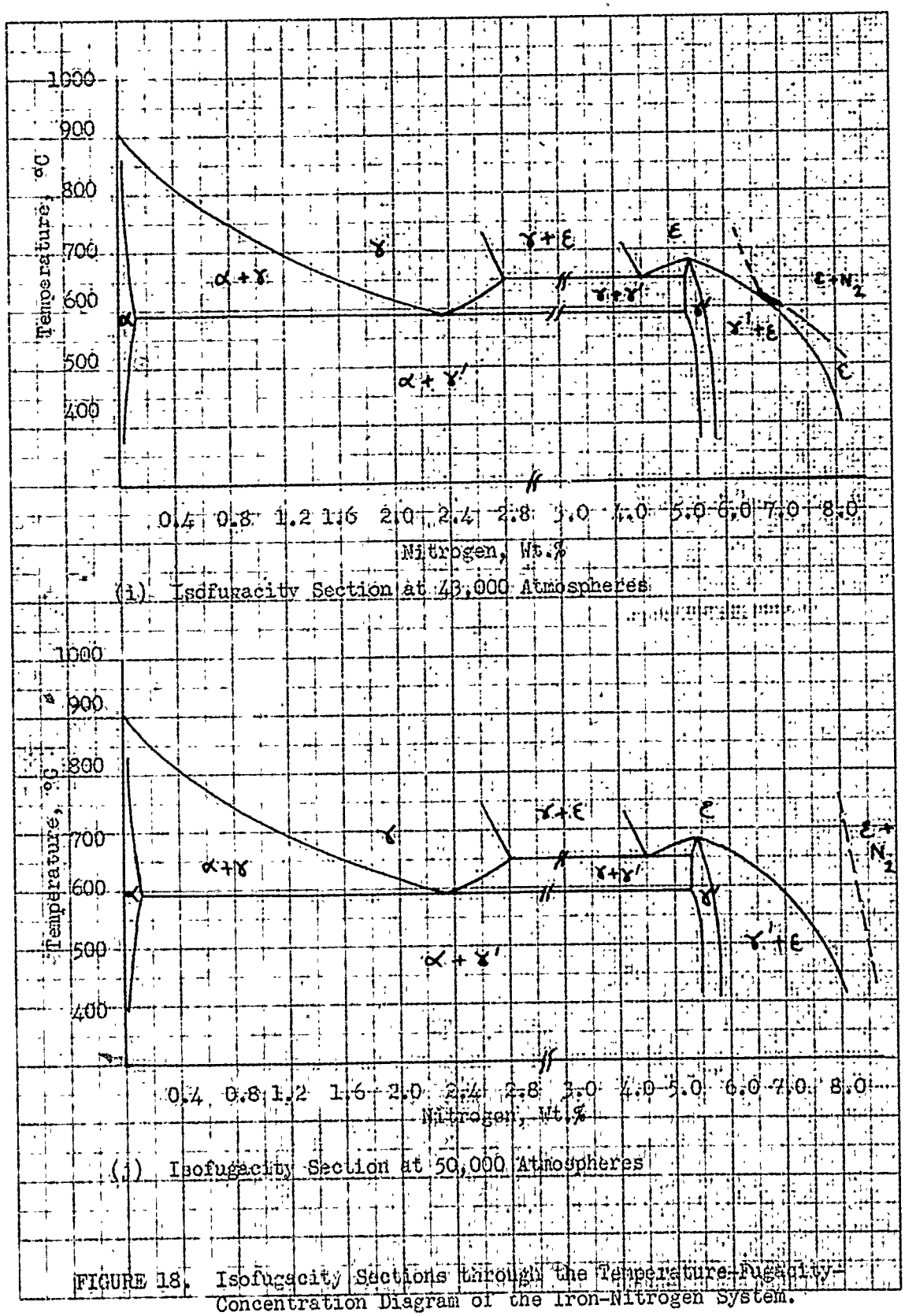

FIGURE 18. Isofugacity Sections through the Temperature-Fugacity-Concentration Diagram of the Iron-Nitrogen System.

temperature is 680° C and is uniquely defined by the degenerate quadruple point 3 in Figure 16. This is shown by the section (Figure 18(g)) at 30,000 atmospheres, where a high-nitrogen epsilon phase also comes into the picture at lower temperatures. The next section (Figure 18(H)), 35,000 atmospheres, shows the two epsilon regions approaching each other, finally meeting at about 43,000 atmospheres, (Figure 18(i)). The section at 50,000 atmospheres (Figure 18(j)) shows only one merged epsilon-phase field.

VI. CONCLUSIONS

1. A method for the determination of the phase boundaries in the iron-nitrogen system was developed. This method depends on the relationship between the nitrogenizing power of an ammonia-hydrogen gas mixture and the nitrogen concentration in the iron-nitrogen alloy produced by nitrogenizing.

2. The following iron-nitrogen phases were found to exist in the temperature range of 450 to 675° C.

Phase	Structure	Remarks
α	B.C.C.; a_o = 2.86 kx units	Maximum solubility 0.10 percent nitrogen at 590° C
γ	F.C.C.; a_o = 3.61_0 kx units at 1.45 percent nitrogen to 3.64_8 kx units at 2.79 percent nitrogen	Maximum solubility 2.80 percent nitrogen at 650° C
γ'	F.C.C.; a_o = 3.78_3 to 3.79_3 kx units	Homogeneity limit 5.30 to 5.75 percent nitrogen
Martensite	B.C.T. c/a = 1.01 to 1.09	
ε	H.C.P.; c = 4.37_3 to 4.414 and a = 2.70_2 to 2.76_4 kx units.	Very wide range of homogeneity, 4.35 to 11.0 percent nitrogen by weight
ζ	Orthorhombic a = 2.75, b = 4.82 c = 4.43 kx units	Lower homogeneity limit 11.1 percent nitrogen at 450° C

3. The phase boundaries of the alpha, gamma, gamma-prime and epsilon phases were determined to give the iron-nitrogen phase diagram in the temperature range of 450 to 700° C.

4. Two eutectoid reactions were found to exist in the phase diagram:

At 590° C $\quad \gamma_{2.35} \rightleftharpoons \alpha_{0.10} + \gamma'_{5.30}$

At 650° C $\quad \varepsilon_{4.5} \rightleftharpoons \gamma_{2.80} + \gamma'_{5.30}$

The subscripts show the nonvariant composition in nitrogen, weight percent.

5. The alpha-gamma phase boundaries computed by Zener's method are in good agreement with experiments.

6. The solubility of nitrogen in alpha iron under atmospheric pressure of nitrogen was computed.

7. The effect of the fugacity of nitrogen on the phase relationships in the iron-nitrogen system was calculated. Several iso-fugacity and isothermal sections are presented.

Appendix I

DETERMINATION OF NITROGEN IN IRON-NITROGEN ALLOYS

The micro-Kjeldahl method was used to determine the nitrogen content of the iron-nitrogen alloys studied in this work. This method was chosen after a considerable amount of preliminary investigations in which the vacuum-fusion technique was also emplcyed for nitrogen determination. The latter required complicated apparatus, and great care in handling. The micro-Kjeldahl technique was relatively faster and gave reproducible results. The micro-Kjeldahl determinations were made at the Watertown Arsenal Laboratories and the vacuum-fusion analyses were conducted in the analytical laboratory of the Metallurgy Department of the Massachusetts Institute of Technology.

Since the micro-Kejldahl technique was used almost exclusively in this investigation, a brief description of the apparatus and procedure and the results of some trial determinations are presented below.

The micro-Kjeldahl method used for nitrogen determinations is a modification of the original Allen[52] method. It is a distillation technique and it determines the nitrogen soluble in either acid or alkali. The sample is dissolved in an acid and the nitrogen is fixed as the ammonium salt of the acid. The solution is then made alkaline and the nitrogen is distilled off in the form of ammonia. The original Allen method has been greatly modified and

improved by the introduction of the micro-distillation apparatus described by Beeghley[53].

The Apparatus

A standard micro-Kjeldahl apparatus was used. It was constructed of Pyrex glass with standard-taper ground glass joints. The steam distillation apparatus used has been described by Beeghly[52]. The steam generating flask had a capacity of 500 ml. A West-type condenser cooled the distillate which was received in 50 ml. Nessler tubes, or a beaker depending on the nitrogen content of the sample analyzed. A series of samples could be distilled without interrupting the steam flow by merely interchanging the distillation flasks. This change could be made in a matter of seconds.

A Coleman Photoelectric Spectrophotometer was used for low nitrogen samples. It was set at 410 Mu, and a band width of 30 Mu was employed.

Reagents

Sulfuric Acid: C. P., concentrated

Sulfuric Acid: C. P., 1-4, (1 part by volume C. P. concentrated acid, 4 parts by volume distilled water).

Sodium Hydoxide: Prepared by dissolving 600 grams of sodium hydroxide, C. P., in 1100 ml. of water, digesting it overnight with Devarda's alloy and then rapidly boiling out approximately 100 ml. of water in order to eliminate any traces of ammonia present in the reagent.

Nessler's Reagent: Dissolve 50 grams of potassium iodide, C. P., in a minimum quantity of cold water. Add a saturated solution of mercuric chloride, C. P., until a slight but permanent precipitate persists. Add 400 ml. of a clarified 50 percent solution of potassium hydroxide, C. P., dilute to one liter, let settle, and decant.

Procedure

The sample to be analyzed was weighed out (0.1 gram) and transferred to a 100 ml. semi-micro-Kjeldahl digestion flask and dissolved in 10 ml. of dilute sulfuric acid (1-4). The digestion was carried out by heating to a completely clear solution. The digestion flask was then connected to the steam distillation apparatus and 25 ml. of nitrogen-free sodium hydroxide was introduced through the stoppered thistle tube. The delivery end of the condenser tube was submerged in a measured volume of standard sulfuric acid (approximately 0.025 Normal) and the distillation was continued until about 125 to 150 ml. of distillate was collected in the beaker. The excess standard sulfuric acid in the beaker was then titrated with standard sodium hycroxide (approximately 0.025 Normal, standardized against Bureau of Standards acid potassium phthalate) using methyl red as indicator. The nitrogen content of the sample was then calculated from the sodium hydroxide equivalent of the sulfuric acid which was neutralized by the ammonium hydroxide produced by the chemical reaction with the sample.

When the sample contained less than 0.1 percent nitrogen the titration technique was not very reliable. In these cases the

spectrophotometer method was used. A duplicate sample (0.1 gram) was digested and the distillate collected as before. The distillate was then Nesslerized, and its transmittance was determined with the spectrophotometer. The nitrogen content was then read off from a standard calibration curve of log transmittance vs. nitrogen concentration.

A blank determination was frequently made with the reagents used in the test and the results obtained by the titration or transmittance method were corrected for the nitrogen content of the blank.

Nitrogen-free water required in this method was prepared by treating 4 liters of distilled water with 2 grams of sodium hydroxide and 2 grams of Devarda's alloy, digesting the solution for 8 hours on a warm plate, digesting overnight cold, boiling down to three liters and finally distilling. Fifty ml. portions of the distillate were periodically tested for nitrogen with Nessler's reagent. When the Nessler test showed that nitrogen was absent, the remainder of the distillate was collected for use

All the analytical work was carried out in an ammonia free room to minimize errors.

Test Experiments and Discussion

The reproducibility of the micro-Kjeldahl method was tested by analyzing a large number of iron-nitrogen alloys. Each sample was analyzed five times and the nitrogen content of the samples

varied from 0.001 to 11.00 percent. The results of these test experiments are summarized in Table XII.

The micro-Kjeldahl method was compared with the vacuum-fusion method by analyzing some iron-nitrogen alloys by both the methods and comparing the results. The results are shown in Table XIII.

The results presented in Tables XII and XIII show that the micro-Kjeldahl technique is quite reproducible and it agrees with the vacuum-fusion method.

TABLE XII

Reproducibility of the Micro-Kjeldahl Method

Sample No.	Nitrogen, Weight Percent (Micro-Kjeldahl Method) (1)	(2)	(3)	(4)	(5)
312-H[X]	0.009	0.009	0.009	0.008	0.0075
61-W[X]	0.014	0.013	0.0115	0.0115	0.012
36-H[X]	0.033	0.035	0.0362	0.035	0.0355
305-H[X]	0.110	0.112	0.110	0.114	0.112
88-A[X]	0.377	0.386	0.394	0.386	0.352
7-H[X]	0.737	0.737	0.772	0.763	0.763
321-H[X]	1.029	1.012	1.029	1.020	1.020
62-H[X]	1.475	1.458	1.475	1.458	1.475
61-H[X]	2.024	2.058	2.075	2.075	2.058
121-H[X]	2.555	2.555	2.555	2.521	2.504
32-A[X]	3.353	3.70	3.353	3.387	3.387
84-H[X]	4.905	4.820	4.853	4.870	4.870
77-W[X]	5.128	5.128	5.145	5.128	5.145
83-H[X]	5.488	5.505	5.488	5.454	5.505
68-H[X]	6.174	6.157	6.174	6.157	6.174
10-A[X]	6.526	6.474	6.526	6.491	6.560
102-H[X]	7.125	7.109	7.092	7.057	7.109
99-H[X]	7.657	7.657	7.649	7.640	7.632
104-H[X]	8.163	8.146	8.180	8.180	8.163
105-H[X]	8.678	8.643	8.609	8.643	8.643
35-A[X]	9.140	9.107	9.227	9.174	9.192
25-A[X]	9.878	9.775	9.844	9.878	9.878
12-A[X]	10.290	10.290	10.256	10.324	10.256
7-A[X]	10.701	10.667	10.701	10.667	10.684

TABLE XIII

Comparison of the Vacuum-Fusion and Micro-Kjeldahl Methods

Sample No.	Nitrogen, Weight Percent: Vacuum Fusion	Micro-Kjeldahl
3-A	0.0021, 0.0024	0.0015, 0.0016
1-A	0.0018, 0.0019, 0.0020	0.0022
60-W	0.012	0.014, 0.021
61-W	0.014	0.014, 0.021
58-W	0.042, 0.044	0.035, 0.035
52-W	1.11, 1.19	1.115, 1.214
32-A	3.43, 3.52	3.36, 3.43
108-H	5.18, 5.19	5.12
83-H	5.31, 5.36	5.30
93-H	5.18, 5.68	5.50
94-H	5.55, 5.62	5.52
68-H	6.16, 6.18	6.16
64-A	6.27	6.15, 6.22
63-A	7.87	7.77, 7.79
39-A	9.35, 9.42	9.33, 9.43
36-A	9.90, 9.97	9.83, 9.90
21-A	10.01, 10.15	10.00, 10.00
25-A	10.01, 10.15	10.04, 10.10
28-A	9.92, 9.98	10.04, 10.10
20-A	10.20, 10.31	10.22, 10.25

Sample No.	Nitrogen, Weight Percent	
	Vacuum Fusion	Micro-Kjeldahl
22-A	10.55, 10.55	10.43, 10.50
11-A	10.32, 10.53	10.46, 10.50
19-A	10.65, 10.67	10.63, 10.67
30-A	10.55, 10.79	10.70, 10.70
58-A	10.67, 10.78, 10.82	10.67, 10.79
14-A	10.75, 10.87, 10.92	10.78, 10.78
18-A	10.78, 10.80, 10.92	10.82, 10.82

Appendix II

SUMMARY OF PRELIMINARY NITROGENIZING EXPERIMENTS

A considerable amount of preliminary work was necessary to study the variables of the nitrogenizing process. The results of this investigation are summarized below.

Pure ammonia was used in all the initial nitriding runs. Ammonia was passed over a sample of carbonyl iron powder and the exit gases were analyzed by a dissociation pipette. The dissociation measurements made in this way were only approximate. Table XIV includes the results of a series of nitrogenizing experiments conducted in this manner. The samples were allowed to cool in an ammonia atmosphere in all these runs.

It can be seen from the data presented in Table XIV that almost all the samples had about 10 percent nitrogen in spite of the fact that the ammonia dissociation varied from 0 to 100 percent, with increasing nitriding temperature. It thus appeared that considerable nitrogen pick-up occurred during cooling. Some experiments were therefore carried out to test this hypothesis. Table XV shows the results of these experiments.

An examination of the results summarized in Table XV shows that the nitrogen content of the sample either increased or decreased depending upon whether the sample cooled in an ammonia or nitrogen atmosphere. Water quenched samples, prepared under identical conditions, however, had the same nitrogen content. Water

TABLE XIV

Results of Preliminary Nitrogenizing Experiments

Material: Carbonyl Iron Powder

Conditions: Constant Flow Rate of Ammonia
Duration at Temperature, 6 Hours
Cooling in an Ammonia Atmosphere

Run No.	Sample Number	Temperature ° C	Dissociation Reading	Nitrogen Weight Percent
42	32-A	270	0	3.36, 3.43
20	10-A	325	0 - 5	6.58, 6.65
41	31-A	410	7	10.75
28	18-A	420	6	10.82, 10.82
21	11-A	425	5 - 6	10.32, 10.53
5	7-A	450	-	11.00, 11.09
29	19-A	450	10 - 30	10.63, 10.67
22	12-A	500	25 - 30	10.60, 10.70
30	20-A	500	40 - 55	10.31, 10.31
23	13-A	600	75 - 85	10.03, 10.07
31	21-A	600	80 - 85	10.01, 10.15
35	25-A	620	95 - 98	10.01, 10.15
43	33-A	650	95 - 100	10.88, 10.95
34	24-A	670	100	10.78, 10.78
32	22-A	720	100	10.55, 10.55
24	14-A	725	100	10.08, 10.25

TABLE XV

Influence of Cooling Atmosphere on the Nitrogen Content of Nitrogenized Samples

Material: Carbonyl Iron Powder

Inlet Gas: Pure Ammonia at Constant Flow Rate

Nitrogenizing Temperature °C	Sample Number	Dissociation Reading	Cooling Condition	Nitrogen Weight Percent
625	66-A	70	NH_3, furnace cooled	10.79
"	66-W	70	Water quenched	5.47
"	67-A	70	N_2, furnace cooled	5.58
"	67-W	70	Water quenched	5.46
"	68-A	70	N_2, at increased rate, cooled in furnace	5.67
"	68-W	70	Water quenched	5.49
700	52-A	85	N_2, furnace cooled	0.08
"	52-W	85	Water quenched	1.17
"	55-A	75	N_2, furnace cooled	0.06
"	55-W	75	Water quenched	3.56
900	58-A	100	NH_3, furnace cooled	10.73
"	58-W	100	Water quenched	0.035

quenching was therefore adopted as the standard cooling procedure throughout the investigation.

Another important issue studied in this preliminary work was the effect of progressive dissociation of ammonia in the gas stream as it flowed along the length of the sample. To determine the magnitude of this effect, a series of experiments were conducted in which the nitrogenized specimens were water quenched and trisected. The sections numbered -1, -2, and -3 respectively in Table XVI represent positions progressively farther down stream relative to the inlet. The results of these runs summarized in Table XVI warrent the conclusion that the variation in the nitrogen concentration of a specimen, owing to a difference in position relative to the gas inlet, was negligible in comparison with analytical variations.

TABLE XVI

Variation of the Nitrogen Content of a Sample Due to a Difference in Position Relative to the Nitriding Gas Stream

Material: Carbonyl Iron Powder

Inlet Gas: Pure Ammonia at Constant Flow Rate

Nitrogenizing Temperature °C	Sample Number	Nitrogen Weight Percent
650	111-1-W	0.14
	-2-W	0.14
	-3-W	0.14
650	103-1-W	5.09 - 5.19
	-2-W	5.15 - 5.15
	-3-W	5.15 - 5.20
650	105-1-W	5.55 - 5.58
	-2-W	5.55 - 5.55
	-3-W	5.44 - 5.55
700	107-1-W	0.053
	-2-W	0.035
	-3-W	0.05
700	110-1-W	0.05
	-2-W	0.05
	-3-W	0.04

Appendix III

EXPERIMENTAL RESULTS

The results obtained from the controlled atmosphere nitrogenizing experiments are presented in the following pages. The starting material in all these experiments was carbonyl iron powder which was previously decarburized by a wet hydrogen treatment, except in cases where a high nitrogen alloy was used to approach the phase boundary from the high nitrogen side. Specific mention is made of the latter cases in the following tables.

The results of x-ray parameter measurements on the various iron-nitrogen phases are also included here.

TABLE XVII

Results of Controlled Atmosphere Nitrogenizing

Experiments at 450° C

Sample Number	Percent Ammonia in Inlet Gas	Nitrogen, Weight Percent, in Water-quenched Sample	Phases Present
		Series A	
361-H	1	0.0455	$\alpha + \gamma'$
362-H	2	0.027	α
363-H	3	0.0465	$\alpha + \gamma'$
364-H	4	0.0215	α
365-H	5	0.0230	α
366-H	6	0.0250	α
367-H	7	0.0125	α
368-H	8	0.0440	$\alpha' + \gamma'$
369-H	9	0.054	$\alpha + \gamma'$
370-H	10	0.089	$\alpha + \gamma'$
		Series B	
600-H	2.0	5.50	γ'
601-H	4.0	7.97	ε
602-H	6.0	7.91	$\varepsilon + \gamma'_{tr.}$
603-H	8.0	8.98	ε
604-H	10.0	8.05	ε
605-H	12.0	8.59	ε

TABLE XVII, Con't.

Sample Number	Percent Ammonia in Inlet Gas	Nitrogen, Weight Percent, in Water-quenched Sample	Phases Present
		Series C	
630-H	20.0	0.187	$\alpha + \gamma'$
631-H	25.0	0.237	$\alpha + \gamma'$
632-H	30.0	5.32	$\alpha_{tr.} + \gamma'$
633-H	35.0	5.47	γ'
634-H	40.0	5.48	γ'
635-H	45.0	5.41	$\alpha_{tr.} + \gamma'$
636-H	50.0	5.36	$\alpha_{tr.} + \gamma'$
637-H	55.0	5.505	γ'
638-H	60.0	5.49	γ'

TABLE XVIII

Results of Controlled Atmosphere Nitrogenizing

Experiments at 500° C

Sample Number	Percent Ammonia in Inlet Gas	Nitrogen, Weight Percent, in Water-quenched Sample	Phases Present
86-H	10.0	0.055	$\alpha + \gamma'_{tr}$
87-H	12.5	0.046	α
88-H	15.0	0.060	α
89-H	17.5	1.04	$\alpha + \gamma'$
90-H	20.0	0.275	$\alpha + \gamma'$
91-H	22.5	5.53	γ'
92-H	25.0	5.50	γ'
93-H	27.5	5.52	γ'
94-H	30.0	5.52	γ'
95-H	32.5	6.11	$\gamma' + \varepsilon_{tr}$
96-H	35.0	5.37	γ'
97-H	37.5	5.56	γ'
98-H	40.0	5.60	γ'
99-H	42.5	7.59	$\gamma' + \varepsilon$
100-H	45.0	5.43	γ'
101-H	47.5	5.71	γ'
102-H	50.0	7.02	$\gamma' + \varepsilon$
103-H	52.5	7.83	ε
104-H	55.0	8.17	ε

TABLE XVIII, Con't.

Sample Number	Percent Ammonia in Inlet Gas	Nitrogen, Weight Percent, in Water-quenched Sample	Phases Present
105-H	57.5	8.66	ε
106-H	60.0	8.33	ε
107-H	62.5	8.72	ε
	Series B		
500-H	2.0	5.50	γ'
501-H	4.0	5.54	γ'
502-H	6.0	5.49	γ'
503-H	8.0	6.51	$\gamma'+\varepsilon$
504-H	10.0	6.11	$\gamma'+\varepsilon$
505-H	12.0	6.56	$\gamma'+\varepsilon$
	Series C		
506$^{\times}$-H	20	5.55	γ'
507$^{\times}$-H	25	5.49	γ'
508$^{\times}$-H	30	5.51	γ'
509$^{\times}$-H	35	5.50	γ'
510$^{\times}$-H	40	5.56	γ'
511$^{\times}$-H	45	5.58	γ'
512$^{\times}$-H	50	5.62	γ'
513$^{\times}$-H	55	5.64	γ'
514$^{\times}$-H	60	7.20	$\gamma'+\varepsilon$

TABLE XVIII, Con't.

Sample Number	Percent Ammonia in Inlet Gas	Nitrogen, Weight Percent, in Water-quenched Sample	Phases Present
515-H	65	7.36	$\gamma' + \varepsilon$
516-H	70	6.85	$\gamma' + \varepsilon$
517-H	75	7.55	$\gamma' + \varepsilon$
518-H	80	7.76	ε
519-H	85	8.12	ε
520-H	90	8.515	ε
		Series D	
525-H	1.0	0.013	α
526-H	2.0	0.100	$\alpha + \gamma'_{tr}$
527-H	3.0	0.0255	α
528-H	4.0	0.053	α
529-H	5.0	0.0335	α
530-H	6.0	0.0445	α
531-H	7.0	0.101	$\alpha + \gamma'_{tr}$
532-H	8.0	0.051	α

TABLE XIX

Results of Controlled Atmosphere Nitrogenizing

Experiments at 550° C

Sample Number	Percent Ammonia in Inlet Gas	Nitrogen, Weight Percent, in Water-quenched Sample	Phases Present
		Series A	
20-H	2.0	0.030	α
26-H	10.0	0.059	α
22-H	12.0	0.069	α
24-H	14.0	0.062	α
27-H	15.0	5.36 - 5.38	γ'
	(Starting Material Contained 8.0 Percent Nitrogen)		
		Series B	
36-H	2.0	0.033 - 0.035	α
37-H	4.0	0.0335 - 0.034	α
38-H	6.0	5.64	γ'
39-H	8.0	0.079 - 0.081	$\alpha + \gamma'_{tr}$
40-H	10.0	5.65	γ'
		Series C	
53-H	2.0	0.021	α
54-H	4.0	0.023	α
55-H	6.0	0.035	α
56-H	8.0	0.032	α
57-H	10.0	0.044	α

TABLE XIX, Con't.

Sample Number	Percent Ammonia in Inlet Gas	Nitrogen, Weight Percent, in Water-quenched Sample	Phases Present
58-H	12.0	0.100	$\alpha+\gamma'$
59-H	14.0	0.38	$\alpha+\gamma'$
	Series D		
	(Starting material contained 8.0 percent nitrogen)		
125-H	1.0	0.042	α
126-H	2.0	0.109	$\alpha+\gamma'$
127-H	3.0	5.48	γ'
128-H	4.0	5.53	γ'
129-H	6.0	5.61	γ'
130-H	7.5	5.70	γ'
	Series E		
560-H	15.0	0.71	$\alpha+\gamma'$
606-H	16.0	5.30	γ'
607-H	17.0	5.45	γ'
608-H	18.0	5.49	γ'
609-H	19.0	5.46	γ'

TABLE XX

Results of Controlled Atmosphere Nitrogenizing

Experiments at 590° C

Sample Number	Percent Ammonia in Inlet Gas	Nitrogen, Weight Percent, in Water-Quenched Sample	Phases Present
280-H	1.0	0.012	α
281-H	2.0	0.024	α
282-H	3.0	0.034	α
283-H	4.0	0.062	α
284-H	5.0	0.097	α
285-H	6.0	0.062	α
286-H	7.0	0.59	$\alpha + \gamma'$
287-H	8.0	0.17	$\alpha + \gamma'_{tr}$
288-H	9.0	0.097	α
289-H	10.0	0.090	α
290-H	11.0	0.485	$\alpha + \gamma'$
291-H	12.0	2.06	$\alpha + \gamma'$
292-H	13.0	5.27	γ'
293-H	14.0	5.56	γ'
294-H	15.0	5.48	γ'

TABLE XXI

Results of Controlled Atmosphere Nitrogenizing

Experiments at 600° C

Sample Number	Percent Ammonia in Inlet Gas	Nitrogen, Weight Percent, in Water-quenched Sample	Phases Present
		Series A	
201-H	10.0	0.035	$\alpha + \gamma'$
202-H	12.5	5.50	γ'
203-H	15.0	5.30	γ'
204-H	17.5	5.33	γ'
205-H	20.0	5.26	γ'
206-H	22.5	5.43	γ'
207-H	25.0	5.57	γ'
208-H	27.5	5.52	γ'
		Series B	
350-H	2.0	0.087	α
351-H	4.0	5.35	γ'
352-H	6.0	5.43	γ'
353-H	8.0	5.59	γ'

TABLE XXII

Results of Controlled Atmosphere Nitrogenizing

Experiments at 650° C

Sample Number	Percent Ammonia in Inlet Gas	Nitrogen, Weight Percent, in Water-quenched Sample	Phases Present
		Series A	
45-H	2	0.010	α
46-H	4	0.063	α
47-H	6	0.59	α + Martensite
48-H	8	1.04	α + Martensite
49-H	10	2.70	γ
50-H	12	5.30	γ'
51-H	14	5.22	$\gamma+\gamma'$
52-H	16	5.34	γ'
		Series B	
421-H	2	0.0285	α
422-H	4	0.0565	α
423-H	6	0.297	α + Martensite
427-H	14	2.27	γ
428-H	16	3.26	$\gamma+\varepsilon$
429-H	18	5.20	$\gamma'+\varepsilon$
431-H	22	5.28	γ'
432-H	24	5.36	γ'

TABLE XXIII

Results of Controlled Atmosphere Nitrogenizing

Experiments at 675 and 700° C

Sample Number	Percent Ammonia in Inlet Gas	Nitrogen, Weight Percent, in Water-quenched Sample	Phases Present
		675° C	
563-H	6.0	0.047	α
564-H	8.0	1.88	γ + Martensite
565-H	10.0	1.45	γ + Martensite
566-H	12.0	1.53	γ + Martensite
567-H	14.0	1.68	γ + Martensite
		700° C	
301-H	12.5	0.013	α
302-H	15.0	0.425	α + Martensite
303-H	17.5	0.029	α
304-H	20.0	0.050	α
305-H	22.5	0.105	α + Martensite
306-H	25	0.070	α
307-H	27.5	0.12	α + Martensite

TABLE XXIV

Lattice Parameter of Nitrogen-Austenite

Temperature ° C	Sample Number	Nitrogen, Weight Percent, in Water-quenched Sample	Phases Present	a_o kx units
625	161-H	1.73	$\gamma + M$	3.61_5
	181-H	2.79	γ	3.64_8
	186-H	4.13	$\gamma + \gamma'$	3.64_5
	164-H	4.63	$\gamma + \gamma'$	3.64_4
	170-H	5.41	$\gamma + \gamma'$	3.64_2
650	425-H	1.64	$\gamma + M$	3.61_0
	424-H	1.95	$\gamma + M$	3.62_5
	426-H	2.20	$\gamma + M$	3.63_0
	427-H	2.27	$\gamma + M$	3.63_9
	434-H	2.62	$\gamma + M_{tr}$	3.64_0
	428-H	3.26	$\gamma + \varepsilon$	3.64_9
	430-H	3.46	$\gamma + \gamma'$	3.65_1
675	565-H	1.45	$\gamma + M$	3.61_0
	566-H	1.53	$\gamma + M$	3.61_1
	567-H	1.68	$\gamma + M$	3.61_5
	564-H	1.88	$\gamma + M$	3.62_2
	568-H	2.39	$\gamma + M$	3.63_8
	572-H	2.795	$\gamma + \varepsilon_{tr}$	3.64_8
	584-H	3.46	$\gamma + \varepsilon$	3.64_7
700	55-W	3.54	$\gamma + \varepsilon$	3.64_6

TABLE XXV

Tetragonality of Nitrogen-Martensite

Sample Number	Nitrogen, Weight Percent, in Water-quenched Sample	Phases Present	Tetragonality c/a
565-H	1.45	$\gamma + M$	1.05_9
566-H	1.53	$\gamma + M$	1.06_1
425-H	1.64	$\gamma + M$	1.06_0
564-H	1.88	$\gamma + M$	1.07_2
424-H	1.95	$\gamma + M$	1.06_9
426-H	2.20	$\gamma + M$	1.07_4
427-H	2.27	$\gamma + M$	1.08_8

TABLE XXVI

Lattice Parameters of the Epsilon Phase

Temperature ° C	Sample Number	Nitrogen, Weight Percent, in Water-quenched Sample	Phases Present	c kx units	a kx units
450	602-H	7.91	$\gamma'_{tr}+\varepsilon$	4.38_0	2.71_4
	601-H	7.97	ε	4.38_2	2.71_4
	604-H	8.05	ε	4.38_2	2.71_4
	605-H	8.59	ε	4.39_0	2.72_8
	603-H	8.98	ε	4.39_5	2.73_4
500	504-H	6.11	$\gamma'+\varepsilon$	4.37_8	2.71_0
	514-H	6.47	$\gamma'+\varepsilon$	4.37_9	2.71_2
	503-H	6.51	$\gamma'+\varepsilon$	4.38_0	2.71_0
	505-H	6.56	$\gamma'+\varepsilon$	4.37_9	2.71_1
	516-H	7.36	$\gamma'+\varepsilon$	4.37_7	2.71_0
	521-H	7.50	$\gamma'+\varepsilon$	4.37_8	2.71_2
	517-H	7.55	$\gamma'+\varepsilon$	4.37_9	2.71_0
	518-H	7.76	ε	4.38_0	2.71_2
	519-H	8.12	ε	4.38_6	2.71_9
	106-H	8.33	ε	4.38_8	2.72_4
	145-H	8.45	ε	4.39_0	2.72_3
	540-H	8.51	ε	4.38_8	2.72_6
	149-H	8.55	ε	4.38_9	2.72_7
	107-H	8.72	ε	4.39_2	2.72_6
	522-H	8.98	ε	4.39_7	2.73_4

TABLE XXVI, Con't.

Temperature ° C	Sample Number	Nitrogen, Weight Percent, in Water-quenched Sample	Phases Present	c kx units	a kx units
550	405-H	6.09	$\gamma' + \varepsilon$	4.37_2	4.69_8
	410-H	6.41	$\gamma' + \varepsilon$	4.37_2	2.70_1
	406-H	6.49	$\gamma' + \varepsilon$	4.37_0	2.70_2
	413-H	6.84	$\gamma' + \varepsilon$	4.37_1	2.69_9
	411-H	6.99	$\gamma' + \varepsilon$	4.37_3	2.70_2
	408-H	7.11	$\gamma' + \varepsilon$	4.37_1	2.70_1
	412-H	7.30	$\gamma'_a + \varepsilon$	4.37_2	2.70_0
	409-H	7.38	ε	4.37_3	2.70_2
625	167-H	5.72	$\gamma' + \varepsilon$	4.36_4	2.68_4
	168-H	5.77	$\gamma' + \varepsilon$	4.36_2	2.68_6
650	428-H	3.26	$\gamma + \varepsilon$	4.32_5	2.62_6
	442-H	4.60_5	$\gamma' + \varepsilon$	4.33_0	2.62_5
	441-H	4.67	$\gamma' + \varepsilon$	4.32_4	2.62_8
	443-H	4.86	$\gamma' + \varepsilon$	4.32_1	2.62_6
	437-H	5.07	$\gamma' + \varepsilon$	4.32_7	2.62_5
	447-H	5.11	$\gamma' + \varepsilon$	4.32_9	2.62_3
	440-H	5.19	$\gamma' + \varepsilon$	4.32_3	2.62_7
	445-H	5.19	$\gamma' + \varepsilon$	4.32_5	2.62_4
	429-H	5.20	$\gamma' + \varepsilon$	4.32_7	2.62_5
	446-H	5.40	$\gamma' + \varepsilon$	4.32_3	2.62_8
	444-H	5.98	$\gamma' + \varepsilon$	4.36_6	2.67_5

TABLE XXVI, Con't.

Temperature ° C	Sample Number	Nitrogen, Weight Percent, in Water-quenched Sample	Phases Present	c kx units	a kx units
675	572-H	2.795	$\gamma+\varepsilon$	4.32_2	2.62_4
	584-H	3.46	$\gamma+\varepsilon$	4.32_0	2.62_1
	583-H	4.93	$\gamma'_{tr}+\varepsilon$	4.33_2	2.63_9
	581-H	4.94_5	$\gamma'_{tr}+\varepsilon$	4.33_4	2.64_3
	582-H	5.13	$\gamma'+\varepsilon$	4.33_3	2.64_0

Special High-Nitrogen Epsilon Phases Produced for Calibration

808-H	9.19	ε	4.39_8	2.73_9
805-H	9.40	ε	4.39_9	2.74_2
806-H	9.60	ε	4.40_2	2.74_5
11-A	10.48	ε	4.41_1	2.76_0
15-A	10.74	ε	4.41_2	2.76_4
14-A	10.78	ε	4.41_4	2.76_4
18-A	10.82	ε	4.41_4	2.76_4

Appendix IV

ZENER'S METHOD OF CALCULATING THE FERRITE-AUSTENITE PHASE BOUNDARIES

Since Zener's[45] method of calculating the ferrite-austenite equilibrium was applied to the iron-nitrogen system, a detailed derivation of his formulae is presented below.

The following notation is used

M = total number of lattice atoms

N_j = number of lattice atoms of type j

$X_j = N_j/M$ = lattice fraction of j atoms

m = total number of interstitial atoms

n_j = number of interstitial atoms of type j

$x_j = n_j/M$ = number of interstitial atoms of type j per lattice site

β = ratio of the number of possible interstitial positions to the number of lattice sites.

C_j = mol fraction of element j

The equilibrium condition of any system can be evaluated in terms of the free energy of the system where F the free energy is expressed by

$$F = H - TS \qquad \text{(i)}$$

H and S are the heat content and entropy of the system respectively.

The entropy S of a system can be evaluated from the principles of statistical mechanics and the relationship

$$S = k \ln W \qquad \text{(ii)}$$

where k is the Boltzman's constant, and W is the number of possible arrangements having the same macroscopic properties. In alloy systems, the entropy term may be divided into two parts.

$$S = S_p + S_a \qquad \text{(iii)}$$

S_a and S_p represent the entropy due to atomic oscillations, et cetera, and the entropy due to the positions of the atoms respectively. The positional entropy S_p may be further subdivided as follows:

$$S_p = S_{pl} + S_{pi} \qquad \text{(iv)}$$

where S_{pl} and S_{pi} are the contributions of the lattice and interstitial atoms respectively.

The term W can be computed by the methods of statistical mechanics as follows:

$$W_{pl} = \frac{M!}{\pi_j N_j!} \qquad \text{(v)}$$

and

$$W_{pi} = \frac{(\beta M)!}{(\beta M - m)! \pi_j n_j!} \qquad \text{(vi)}$$

Using the relationship (v), the term S_{pl} can be evaluated in the following way.

$$S_{pl} = k \ln \frac{M!}{N_1! N_2! \cdots}$$

or

$$\delta S_{pl} = k \delta \ln \frac{M_1}{N_1! N_2! \cdots}$$

By using Sterling's approximation,

$$\delta S_{pl} = k \left[\ln M \delta M - \ln N_1 \delta N_1 - \ln N_2 \delta N_2 \cdots \right]$$

But, $$\delta M = \delta N_1 + \delta N_2 \cdots$$

Therefore $$\delta S_{pL} = k\left[\ln M\delta N_1 + \ln M\delta N_2 \cdots - \ln N_1\delta N_1 - \ln N_2\delta N_2\right]$$

$$= k\left[\ln \frac{M}{N_1}\delta N_1 + \ln \frac{M}{N_2}\delta N_2 \cdots\right]$$

$$= -k\left[\ln \frac{N_1}{M}\delta N_1 + \ln \frac{N_2}{M}\delta N_2 \cdots\right]$$

But,

$$\frac{N_1}{M} = X_1 \quad ; \quad \frac{N_2}{M} = X_2 \quad \cdots$$

Thus $$\delta S_{pL} = -k\left[\ln X_1\delta N_1 - \ln X_2\delta N_2 \cdots\right]$$

or $$\delta S_{pL} = -k\sum_j \ln X_j\,\delta N_j \qquad \text{(vii)}$$

Similarly the term S_{pi} can be evaluated by using the equations (ii) and (vi).

$$\delta S_{pi} = k \ln\left[\frac{(\beta M)!}{(\beta M - m)!\,\Pi_j\, n_j!}\right]$$

Considering only small changes, and employing Sterling's approximations as before,

$$\delta S_{pi} = k\left[\ln(\beta M)\delta(\beta M) - \ln(\beta M - m)\delta(\beta M - m) - \sum_j (\ln n_j)\,\delta n_j\right]$$

The following relations are then used.

$$M = \sum N_j \quad ; \quad m = \sum n_j$$

or $$\delta M = \sum \delta N_j \quad ; \quad \delta m = \sum \delta n_j$$

and $$\delta(\beta M) = \beta \sum \delta N_j$$

If in addition to the above, $\beta M \gg n_j$, then

$$\delta S_{pi} = \left\{\begin{array}{l} \delta(\beta M)\left[\ln(\beta M) - \ln(\beta M - m)\right] - \ln(\beta M - m)\delta m \\ -\sum (\ln n_j)\,\delta n_j \end{array}\right\}$$

Now, $$\frac{\beta M}{\beta M - m} = \frac{1}{1 - m/\beta M}$$

Therefore,
$$\delta S_{pi} = -k\left[\delta(\beta M)\ln\left(1-\frac{m}{\beta M}\right) - \ln(\beta M - m)\delta m - \sum(\ln n_j)\delta n_j\right]$$

or
$$\delta S_{pi} = -k\left[\beta\sum \delta N_j \cdot \ln\left(1-\frac{m}{\beta M}\right) + \sum \ln\left(\frac{n_j}{\beta M - m}\right)\delta n_j\right] \qquad \text{(viii)}$$

Combining the equations (vii) and (viii)
$$\delta S_p = -k\left[\sum_j \ln X_j \delta N_j + \beta\sum \delta N_j \cdot \ln\left(1-\frac{m}{\beta M}\right) + \sum \ln\left(\frac{n_j}{\beta M - m}\right)\delta n_j\right] \qquad \text{(ix)}$$

The equation (ix) is the one derived by Zener. It may, however, be expressed in a slightly different manner as follows:

$$\delta S_p = -R\left\{\begin{array}{l}\sum \ln X_l \delta n_l + \ln(1 - X_i/\beta)\beta\sum \delta n_l \\ + \sum \ln\left(\frac{X_i/\beta}{1 - X_i/\beta}\right)\delta n_i\end{array}\right\} \qquad \text{(x)}$$

where X_1 and X_i are the lattice fractions of the substitutional and interstitial atoms respectively, and δn_1 and δn_i their respective infinitismal increments.

The equation (x) can be used to derive the partial molal entropies of the substitutional or interstitial atoms. This depends on the definition of partial molal entropy $\bar{S}_1$ for a component 1,

$$\bar{S}_j = \left(\frac{\delta S}{\delta n_1}\right)_{T, P, n_2, n_3 \cdots}$$

Using this defining relationship, $\bar{S}_1$ for lattice atoms can be evaluated as follows.

$$\bar{S}_l = \bar{S}_l^{\circ} - R \ln X_l + \beta R \ln(1 - \Sigma X_i/\beta) \qquad \text{(xi)}$$

$\bar{S}_i^\circ$ in the above equation includes S_a and is the partial molal entropy in a standard state. By neglecting the third term $\beta R \ln(1 - \Sigma X_i/\beta)$ which would be small for small values of X_i, the above equation can be simplified as follows:

$$\bar{S}_i = \bar{S}_i^\circ - R \ln X_i \qquad \text{(xii)}$$

The term $\bar{S}_i$ for the interstitial atoms can be similarly shown to be equal to

$$\bar{S}_i = \bar{S}_i^\circ - R \ln\left(\frac{X_i/\beta}{1 - X_i/\beta}\right) \qquad \text{(xiii)}$$

where $\bar{S}_i^\circ$ is the partial molal entropy in the standard state.

It can be seen that the equation (xiii) represents a more general solution of which equation (xii) is a special case as in this case $(1 - X_i/\beta)$ would be negligible and again β for a substitutional atom is unity. Thus

$$\bar{S}_j = \bar{S}_j^\circ - R \ln\left(\frac{X_j/\beta}{1 - X_j/\beta}\right) \qquad \text{(xiv)}$$

Now the equation (i) can be expressed in terms of partial molal quantities and combined with a similar relationship for the standard state as follows

$$\bar{F}_j - \bar{F}_j^\circ = \bar{H}_j - \bar{H}_j^\circ - T\bar{S}_j + T\bar{S}_j^\circ$$

At this stage Zener makes the assumption that

$$\bar{H}_j - \bar{H}_j^\circ = 0 \qquad \text{(xv)}$$

This means that

$$\bar{F}_j - \bar{F}_j^\circ = T\bar{S}_j^\circ - T\bar{S}_j$$

or substituting the values for $\bar{S}_j$ and $\bar{S}_j^\circ$ from equation (xiv)

$$\bar{F}_j - \bar{F}_j^\circ = RT \ln \left(\frac{X_j/\beta}{1 - X_j/\beta} \right) \qquad \text{(xvi)}$$

or

$$\bar{F}_j - \bar{F}_j^\circ = RT \ln \left(\frac{X_j}{\beta - X_j} \right) \qquad \text{(xvii)}$$

The assumption in equation (xv) gives a very simple expression for $\bar{F}_j - \bar{F}_j^\circ$ and thus simplifies the treatment of the subject. This assumption restricts the generality of Zener's equation. It is, however, assumed that the formulae can be applied to the iron-nitrogen system.

Continuing the development of Zener's theory, the equation (xvii) can be simplified as follows, if X_j is negligible in comparison with β.

$$\bar{F}_j - \bar{F}_j^\circ = RT \ln X_j/\beta \qquad \text{(xviii)}$$

Since X_j is the lattice fraction of an element j, it is equal to the mole fraction of C_j if the number of interstitial atoms is small. Therefore

$$\bar{F}_j - \bar{F}_j^\circ = RT \ln C_j/\beta \qquad \text{(xix)}$$

This equation can be applied for the α and γ phases (in iron alloy systems).

$$\bar{F}_j^\alpha - \bar{F}_j^{\circ\alpha} = RT \ln C_j^\alpha/\beta^\alpha$$

$$\bar{F}_j^\gamma - \bar{F}_j^{\circ\gamma} = RT \ln C_j^\gamma/\beta^\gamma$$

By subtracting the latter from the former

$$\left(\bar{F}_j^\alpha - \bar{F}_j^\gamma\right) - \left(\bar{F}_j^{\circ\alpha} - \bar{F}_j^{\circ\gamma}\right) = RT \ln \left\{ \frac{C_j^\alpha}{C_j^\gamma} \cdot \frac{\beta^\gamma}{\beta^\alpha} \right\} \qquad \text{(xx)}$$

When the two phases α and γ are in equilibrium, the component j has the same chemical potential (or partial molal free energy) in both these phases. Thus

$$\bar{F}_j^{\alpha} - \bar{F}_j^{\gamma} = 0$$

Therefore

$$\Delta F_j^{\circ} = \bar{F}_j^{\circ\gamma} - \bar{F}_j^{\circ\alpha} = RT \ln \frac{C_j^{\alpha} \beta^{\gamma}}{C_j^{\gamma} \beta^{\alpha}} \qquad \text{(xxi)}$$

By using this equation it is possible to calculate the distribution of the component j in the α and γ phases at a temperature T, if the quantity ΔF_j° is know or vice versa.

The differential form of equation (xix) can be applied to iron as follows. The β term drops out in this relationship since iron is a substitutional atom.

$$d\bar{F}_{Fe} = RT \frac{dC_{Fe}}{C_{Fe}}$$

Now $dC_{Fe} = -\Sigma' C_j$ where the symbol Σ' denotes a summation over all components except iron. Substituting this value in the above differential equation and considering C_{Fe} to be approximately unity, the following relationship is obtained.

$$d\bar{F}_{Fe} = -RT \Sigma' dC_j$$

In a binary system (like iron-nitrogen) $\Sigma' dC_j = dC_j$, and

$$d\bar{F}_{Fe} = -RT\, dC_j$$

Integrating the above relationship between any given state and the standard state (which is pure iron in this case) one arrives at the solution

$$\bar{F}_{Fe} - \bar{F}_{Fe}^{\circ} = -RTC_j \qquad \text{(xxii)}$$

The equation (xxii) can be applied to the α and γ phases, and considering only equilibrium conditions where $(\bar{F}^{\gamma}_{Fe} - \bar{F}^{\alpha}_{Fe})$ is zero, the following equation is derived

$$\Delta F^{\circ}_{Fe} - \bar{F}^{\circ\gamma}_{Fe} - \bar{F}^{\circ\alpha}_{Fe} = RT\left(C_j^{\alpha} - C_j^{\gamma}\right) \qquad \text{(xxiii)}$$

The equations (xxi) and (xxiii) can be solved simultaneously for C_j and C_j. Thus,

$$C_j^{\alpha} = \frac{-\Delta F^{\circ}_{Fe}/RT}{1 - \frac{\beta^{\gamma}}{\beta^{\alpha}} \cdot e^{-\Delta F^{\circ}_j/RT}} \qquad \text{(xxiv)}$$

and

$$C_j^{\gamma} = \frac{+\Delta F^{\circ}_{Fe}/RT}{1 - \frac{\beta^{\alpha}}{\beta^{\gamma}} \cdot e^{\Delta F^{\circ}_j/RT}} \qquad \text{(xxv)}$$

In these equations ΔF°_{Fe} represents the free energy change associated with the transfer of one mole of iron from the α to the γ phase. The corresponding quantity ΔF°_j represents the standard free energy change associated with the transfer of the element j from the α to the γ phase.

In closing this theoretical discussion of Zener's method, it is important to re-emphasize that the formulae can be correctly applied to the solutions which satisfy the relationship $\bar{H}_j - \bar{H}^{\circ}_j = 0$.

BIBLIOGRAPHY

1. Warren, H. N.: Chemical News, 55, 155 (1887).
2. Braune, H.: Stahl u. Eisen, 25, 1, 195 (1905).
3. Braune, H.: Rev. de Metallurgie, 2, 497 (1905).
4. Braune, H.: Jernkontorets Ann., 59, 636 (1905).
5. Strauss, B.: Stahl u. Eisen, 34, 1814 (1914).
6. Strauss, B.: Iron Age, 97, 432 (1916).
7. Fry, A.: Kruppsche Monatshefte, 4, 137 (1923).
8. Cowan, R. J. and Brice, J. T.: Trans. A. S. M., 26, 766 (1938).
9. Annonymous: "Sauvuer Medalist, Adolph W. Machlet", Metals Progress, 40, 46 (1941).
10. Tofaute, W. and Schottky, H.: Archiv. Eisenhuttenwesen, 14, 71 (1940).
11. Andrew, J. H.: Iron and Steel Inst., Carnegie Scholarship mem., 3, 236 (1911).
12. Fry, A.: Stahl u. Eisen, 43, 1271 (1923).
13. Swayer, C. B.: Trans. A. I. M. E., 69, 798 (1923).
14. Epstein, S., Cross, H. C., Groesbeck, E. C., and Wymore, I. J.: Bur. of Standards J. of Research, 3, No. 6, 1005 (1929).
15. Epstein, S.: Trans. A. S. S. T., 16, 19 (1929).
16. Lehrer, E.: Zeit. Elektrochemie, 37, 460 (1930).
17. Eisenhut, O. and Kaupp, E.: Zeit. Elektrochemie, 37, 392 (1930).
18. Hägg, G.: Nova Acta Regia, Soc. Sci. Upsaliensis, Series 4, 7, No. 1. (1929).
19. Hägg, G.: Z. phys. Chemie, 8, 455 (1930).
20. Palatnik, L.: Tech. Phys. U. S. S. R., 2, 598 (1935).
21. Remsen: J. Amer. Chem. Soc., 4, 134 (1881).

22. Bucher: J. Ind. Eng. Chem., 9, 233 (1917).

23. Fowler, G. I.: Chemical News, 63, 152 (1894).

24. Stahlschmidt: Pogg. Ann., 125, 37 (1865).

25. Harbord and Twynam: J. Iron and Steel Inst., 50, No. 2, 161 (1896).

26. Tschischewski, N.: J. Iron and Steel Insti., 92, II, 47 (1905).

27. Comstock, G. F. and Ruder, W. E.: Chem. and Met. Eng., 22, No. 9, 399 (1920).

28. Bramley, A. and Haywood, F. W.: Iron and Steel Inst., Carnegie Scholarship Mem., 17, 67 (1928).

29. Norton, J. T.: ScD. Thesis, M. I. T. "The Influence of Aluminum on the Iron-Nitrogen Phase Diagram" (1933).

30. Portevin, A. M. and Seferian, D.: Iron and Steel Inst., Symposium on the Welding of Iron and Steel, 2, 483 (1936).

31. Dijkstra, L. J.: J. of Metals, T. P. 2540, 1, No. 3, 252 (1949).

32. Brunauer, S., Jefferson, M. E., Emmett, P. H. and Hendricks, S. B.: J. Amer. Chem. Soc., 53, 1778 (1931).

33. Osawa, G. and Iwaizumi, S.: Zeit. Krist., 69, 26 (1928).

34. Brill, R.: Zeit. Krist., 68, 379 (1928).

35. Hendricks, S. B. and Kosting, P. R.: Zeit. Krist., 74, 511 (1930).

36. Jack, H. K.: Proc. Royal Soc., A, 195, 34 (1948).

37. Barrett, C. S.: "Structure of Metals", McGraw Hill Book Company (1943).

38. Satoh, S.: Sci. Papers Inst. Phys. Chem. Res. Tokyo, 28, 135 (1935).

39. Fowler and Hartog: J. Chem. Soc., 79, 299 (1906).

40. Satoh, S.: Sci. Papers Inst. Phys. Chem. Res. Tokyo, 28, 271 (1936).

41. Noyes and Smith: J. Amer. Chem. Soc., 43, 475 (1921).

42. Emmett, P. H., Hendricks, S. B. and Brunauer, S.: J. Amer. Chem. Soc., 52, 1456 (1930).

43. Lehrer, E.: Zeit. Elektrochemie, 37, 460 (1930).

44. Kelley, K. K.: U. S. Bur. of Mines Bull. 407. (1937).

45. Zener, C.: Trans. A. I. M. E., 167, 513 (1946).

46. Chipman, J.: Private communication.

47. Iwase, K.: Sci. Rep. Tohoku Univ., 15, 531 (1936).

48. Hayasi, I.: Tetsu-to-Hagane, 26, 101 (1940), Chem. Abstracts 34, 4713.

49. Sieverts: Zeit. phys. Chemie, 155(A), 299 (1931).

50. Sieverts: Zapf and Moritz, Zeit. phys. Chemie, 183(A), 19 (1938-39).

51. Martin, E.: Archiv. Eisenhüttenwesen, 3, 407 (1929-30).

52. Allen, A. H.: J. Iron and Steel Inst., 8, 181 (1880).

53. Beeghley, H. F.: Ind. Eng. Chem., Analytical Ed., 14, 137 (1942).

BIOGRAPHICAL NOTE

The author was born in Bombay, India on August 5, 1923. After passing the matriculation examination of Bombay University, he entered Elphinstone College, Bombay and received the diploma of I.Sc. in 1941. He then entered the Benares Hindu University from which he received the degree of Bachelor of Science in Metallurgy in 1945.

During the summers of 1942, 1943 and 1944 he worked as a trainee in the Mukund Iron and Steel Works, Bombay, The Indian Copper Corporation, Ghatsila, and the Tata Iron and Steel Company.

He came to the United States in February 1946 and entered the Graduate School of the Massachusetts Institute of Technology to pursue a course of study leading to the degree of Doctor of Science in Metallurgy. In October 1946, he was appointed Research Assistant in Metallurgy at the Massachusetts Institute of Technology.

The author is the recipient of the Hadfield Medal of the Mining, Metallurgical and Geological Institute of India.

He is a student member of the American Institute of Mining and Metallurgical Engineers and the American Society for Metals, and a member of the Sigma Xi.

ABSTRACT

The binary iron-nitrogen system constitutes the basis of the more complicated alloys of commercial importance which are used in the nitriding process. Several attempts have been made to determine the iron-nitrogen phase diagram. The results of the previous investigators differ considerably from one another, and thus it was deemed necessary to redetermine the phase diagram.

Iron-nitrogen alloys were prepared by nitrogenizing carbonyl iron powder, previously decarburized by a wet hydrogen treatment. The nitrogenizing gas was a mixture of ammonia and hydrogen.

Two experimental techniques were employed to determine the phase boundaries: (1) A controlled atmosphere nitriding technique, and (2) X-ray diffraction studies on the iron-nitrogen alloys produced by the above.

While the x-ray method is commonly used in phase-boundary determinations, the controlled atmosphere nitrogenizing technique represents an additional tool of special value in determining the iron-nitrogen phase diagram. This method consists, in principle, of nitrogenizing iron in a gas phase of controlled "nitroding power" and then co-relating the nitriding power of the gas phase with the nitrogen content of the iron-nitrogen alloy produced. It is founded on the thermodynamic principles which govern the distribution of nitrogen between the gas and solid phases. This method has a distinct advantage over the other methods

of phase-boundary determination in that it reports the conditions existing at temperature, and is applicable to complex diagrams involving small solubilities.

The nitrogen content of the iron-nitrogen alloys was determined by the micro-Kjeldahl method. This method of chemical analysis was tested for reproducibility, compared with vacuum-fusion analysis, and was found to be quite accurate.

The results of x-ray investigation showed the presence of six iron-nitrogen phases:

(1) Alpha phase with a body-centered cubic structure (a_o = 2.86 kx units).

(2) Gamma-phase with a face-centered cubic structure. The lattice parameter varies from 3.61_0 to 3.64_8 kx units as the nitrogen content changes from 1.45 to 2.79 per-cent by weight.

(3) Nitrogen-martensite with a body-centered tetragonal structure. The tetragonality increases with increasing nitrogen content.

(4) Gamma -prime phase with a face-centered cubic structure containing about 5.5 percent nitrogen. The lattice parameter varies slightly with increasing nitrogen content.

(5) Epsilon phase, hexagonal close-packed structure. The lattice parameters and axial ratio change appreciably with increasing nitrogen content. The nitrogen content of this phase varies from 4.35 to 11.0 percent by weight.

(6) Zeta phase, orthorhombic structure. a - 2.75, b - 4.82, c - 4.42 kx units. The lower limit of this phase is 11.1 percent.

The phase boundaries of these phases were determined in the temperature range of 450 to 700° C. The results obtained by the x-ray method and the controlled atmosphere nitrogenizing technique were in good agreement with each other. The phase diagram constructed by combining the single-phase fields exhibits two eutectoid reactions

At 590° C: $\gamma_{2.35} \rightleftharpoons \alpha_{0.10} + \gamma'_{5.30}$

At 650° C: $\varepsilon_{4.5} \rightleftharpoons \gamma_{2.80} + \gamma'_{5.30}$

The subscripts indicate the nonvariant compositions of the phases in weight percent nitrogen.

The boundaries of the alpha + gamma field were omputed by Zener's method, and the results of these theoretical calculations were in good agreement with experimental determinations.

The solubility of nitrogen in alpha iron under atmospheric pressure of nitrogen was calculated and was found to be consistent with the experimental results of other investigators.

The effect of fugacity on the equilibrium relationships in the iron-nitrogen system was calculated by combining the results of this investigation with available thermodynamic data on the iron-nitrogen system. The results of these calculations were used in constructing several iso-fugacity and isothermal sections through the temperature-fugacity-concentration diagram of the iron-nitrogen system. The sections illustrate the equilibrium relationships in the iron-nitrogen system.